Geological Society of America Special Papers

Strike-slip tectonics and seismicity along the northern Caribbean plate boundary from Cuba to Hispaniola

E. Calais, J. Perrot and B. Mercier de Lépinay

Geological Society of America Special Papers 1998;326;125-169
doi: 10.1130/0-8137-2326-4.125

Geological Society of America
Special Paper 326
1998

Strike-slip tectonics and seismicity along the northern Caribbean plate boundary from Cuba to Hispaniola

E. Calais, J. Perrot, and B. Mercier de Lépinay
CNRS, UMR Géosciences Azur, 250 rue Albert Einstein, Valbonne 06560, France

ABSTRACT

We present a compilation of marine geophysical data (Seabeam bathymetry, side-scan sonar, seismic-reflection profiles) collected along the northern Caribbean plate boundary from the southern margin of Cuba to the northern margin of Hispaniola. We compare the structural observations with the seismicity to quantify the kinematic regime along the plate boundary. The marine data show a narrow zone of active deformation extending along a major left-lateral strike-slip fault, the Oriente fault. The most prominent structural feature is the Santiago deformed belt, a transpressive deformation area that extends along the southern Cuban margin and displays active folding and reverse faulting. Dextral offsets in the Oriente fault trace create tensional strain and local pull-apart basins. The earthquake distribution and source parameters are well correlated with the active tectonic structures. They show a combination of north-south compression and left-lateral shear starting at about 78°W long. and continuing all the way to the east along the southern Cuban margin. Our results indicate the existence of a small convergence component added to the mostly strike-slip displacement between the Caribbean and North America plates. This convergence component is responsible for large-scale transpressive structures such as the Santiago deformed belt and is compatible with local tensional structures due to the geometry of the main fault trace. On the basis of instrumental and historical seismicity records, we compute a seismic slip rate of 13–15 mm/yr along the northern Caribbean plate boundary. This result agrees well with the 12 ± 3 mm/yr NUVEL-1 estimate and could indicate that most of the stress along the plate boundary is released seismically.

INTRODUCTION

The Caribbean domain and Central America form a small lithospheric plate between North and South America (Fig. 1), which was first identified by Molnar and Sykes (1969) on the basis of seismicity. Although the North and South America plates show little relative motion, the Caribbean plate is moving eastward relative to them at a rate of 12 ± 3 mm/yr (DeMets et al., 1990). This displacement occurs along two major strike-slip fault zones: the Bocono and El Pilar faults along its southern boundary, and the Polochic-Motagua, Swan, and Oriente faults along its northern boundary. The Caribbean plate is bounded to the east by the Lesser Antilles subduction zone, and to the west by the Central America subduction zone. Despite this apparently well-constrained kinematic framework, the current motion of the Caribbean plate is one of the more poorly known among all major plates. The Caribbean plate does not have any active spreading centers, except a short segment of spreading ridge in the Cayman trough. Moreover, most of its northern transform boundary is located at sea, and detailed mapping of its trace has been undertaken only recently.

We present in this chapter a synthesis of the active tectonic structures along the northern Caribbean plate boundary from Cuba to Hispaniola, identified from marine geophysical data

Calais, E., Perrot, J., and Mercier de Lépinay, B., 1998, Strike-slip tectonics and seismicity along the northern Caribbean plate boundary from Cuba to Hispaniola, *in* Dolan, J. F., and Mann, P., eds., Active Strike-Slip and Collisional Tectonics of the Northern Caribbean Plate Boundary Zone: Boulder, Colorado, Geological Society of America Special Paper 326.

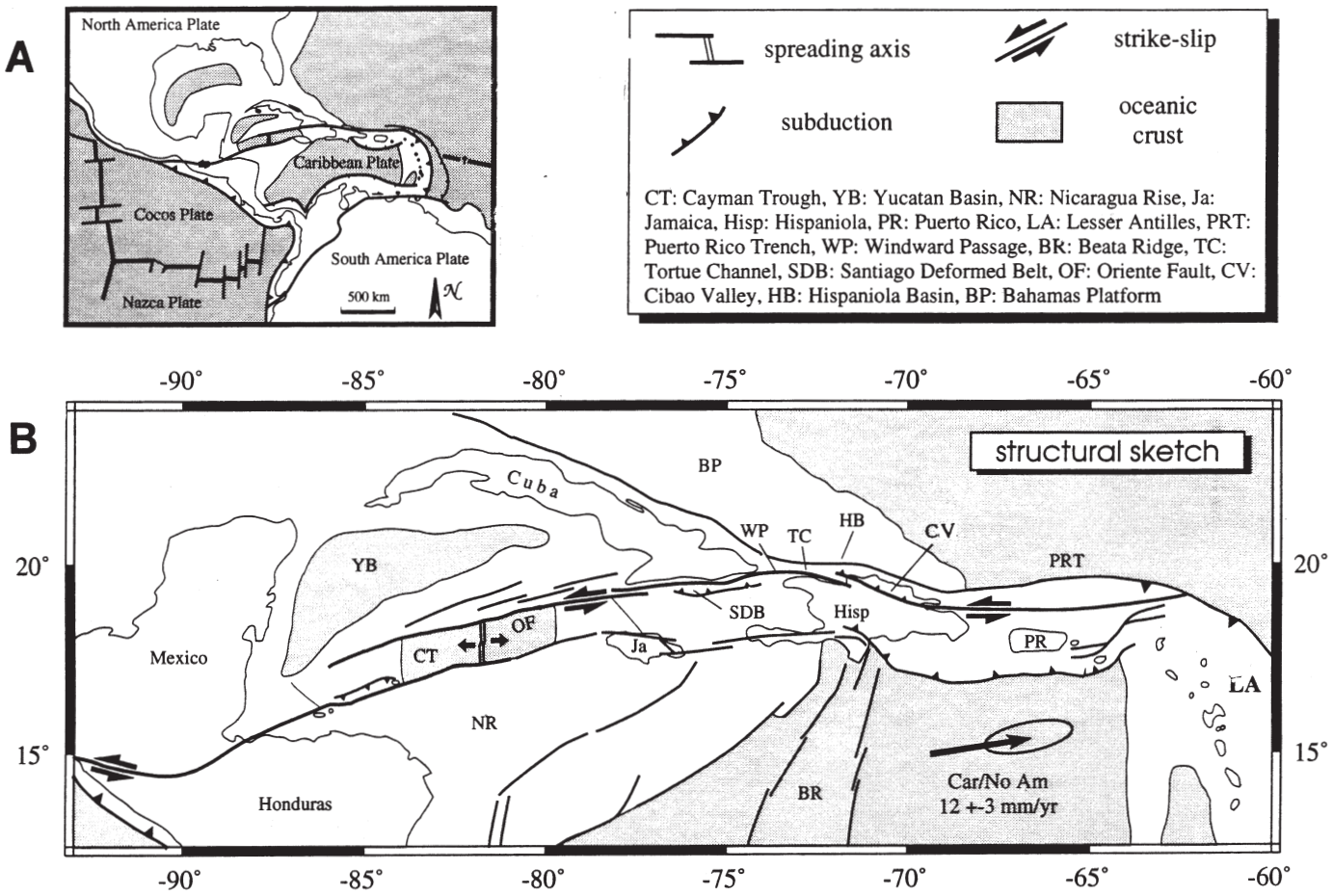

Figure 1. (A) Kinematic framework of the Caribbean plate. (B) Major active faults along the northern Caribbean plate boundary.

(seabeam bathymetry, seismic reflection, side-scan sonar) and teleseismic data. This comprehensive data set allows us to image in great detail the present-day trace of the plate boundary and its associated structures and to characterize the deformation regime along it.

THE NORTHERN CARIBBEAN PLATE BOUNDARY, GEOLOGICAL SETTING

The northern boundary of the Caribbean plate consists of two major strike-slip systems, the Swan and the Oriente fault zones (Fig. 1). The Swan fault is the marine extension of the Polochic-Motagua fault zone of Central America. It is connected to the Oriente fault by the mid-Cayman spreading center, a short oceanic spreading ridge that has been generating the oceanic crust of the Cayman trough since late Eocene (Rosencrantz et al., 1988). The Oriente fault follows the southern Cuban margin and the northern coast of Hispaniola. It continues onland into northern Dominican Republic (Mann et al., this volume) and merges farther east with the Puerto Rico subduction trench (Dolan et al., this volume).

From the mid-Cayman spreading center to the western end of the Cuban margin, the geometry of the Oriente fault is poorly known. It has been thought to follow the foot of the southern escarpment of the Cayman ridge, as shown by some seismic reflection profiles (Goreau, 1983) and by recent seismicity (Fig. 2). Further east, the plate boundary trace continues along the southern margin of Cuba where it corresponds to a prominent topographic scarp, the Oriente Wall. This scarp extends from the summits of the Sierra Maestra of Cuba (2,000 m) into a deep (6,500 m) and narrow east-west–trending marine basin, the Oriente Deep (Case and Holcombe, 1980; Mercier de Lépinay et al., 1989). The Oriente Deep was first interpreted as an active pull-apart basin (Mann and Burke, 1984) on the basis of its topography and its close spatial association with the Oriente transform zone. However, seismic reflection, magnetism, and gravity profiles led Goreau (1983) to the conclusion that the southern Cuban margin is structurally complex and shows mainly compressive tectonics. He described folds and north-dipping reverse faults affecting the sediments of the Oriente Deep, and he noticed a high negative gravimetric anomaly parallel to the Deep, slightly shifted to the north. On the basis of

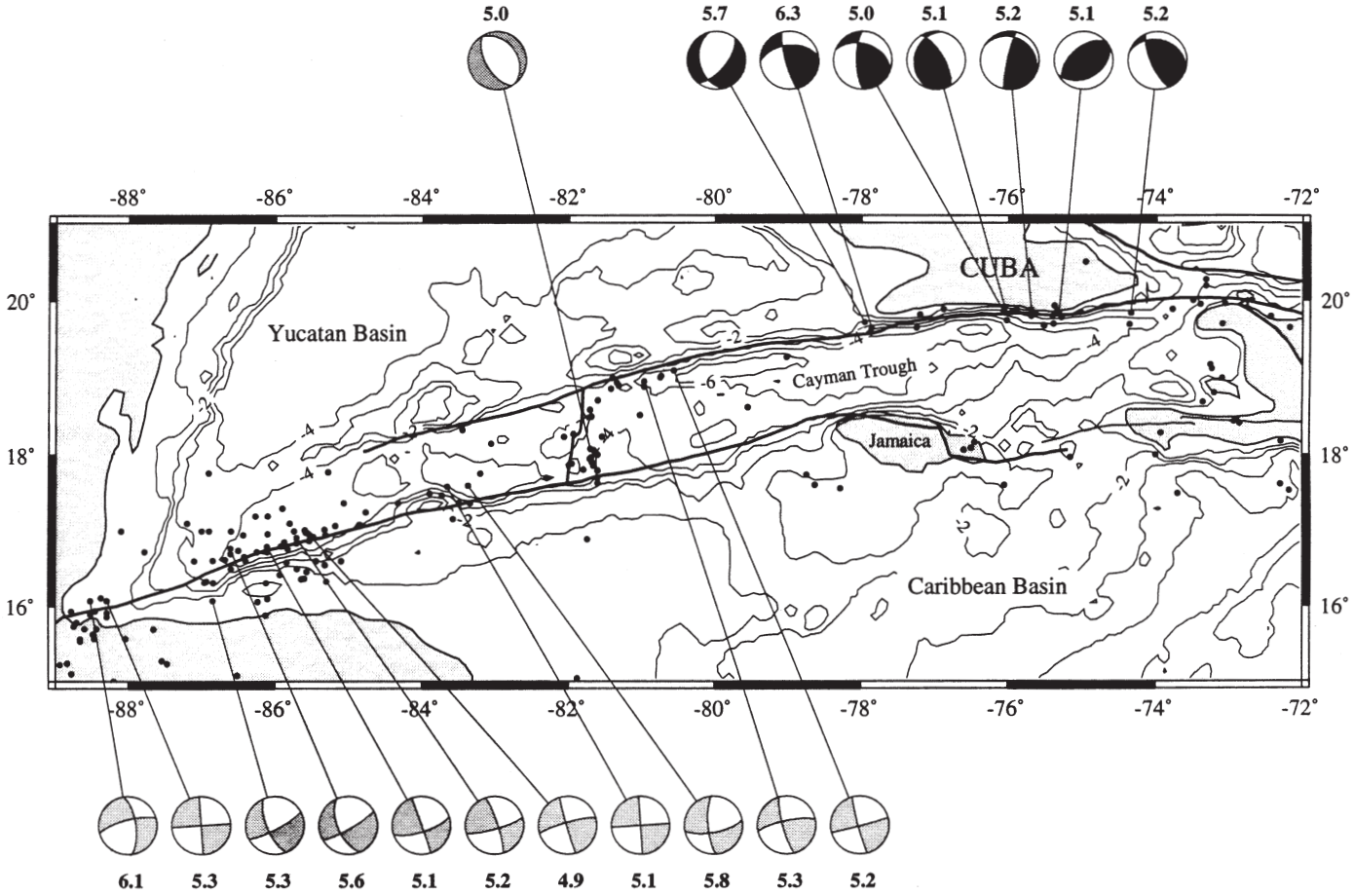

Figure 2. Seismicity (black dots, ISC catalog, 1960–1993, Ms > 3.5) and earthquake focal mechanisms (CMT catalog, 1977–1993) in the Cayman trough and along the southern Cuban margin. Bathymetry labeled in thousand meters.

these observations, he compared this area to a subduction zone and proposed the existence of a major south-verging thrust parallel to the southern Cuban margin.

East of the Cuban margin, the plate boundary trace crosses the Windward Passage, a 90-km-wide strait between the southeastern Cuban coast and the northwestern peninsula of Haiti. Prior to our investigations, few data were available in the Windward Passage. On the basis of two single channel seismic lines, Goreau (1983) defined the main morphostructural units of the Windward Passage, namely, the Windward Passage Sill and the Windward Passage Deep. Two additional multichannel seismic lines (written communication, R/V *F. H. Moore*, University of Texas at Austin, cruise CT2, 1989) led Mann and Burke (1984) to interpret the Windward Passage Deep as an active pull-apart basin. They also postulated the Tortue channel (Fig. 1) to be the eastward prolongation of the Oriente fault, although other authors claimed that it was connected with the western end of the North America plate subduction under Puerto Rico and Hispaniola (Mascle and Letouzey, 1990).

THE PLATE BOUNDARY TRACE AND ITS ASSOCIATED STRUCTURES

Figure 3 displays a tectonic map of the active structures in the study area, established from a morphostructural analysis of Seabeam bathymetry, 50 single channel seismic lines, and a full high-resolution side-scan sonar coverage in the Windward Passage area. Figure 4 shows the location of some of the figures referenced in this chapter. We identify four major structural domains and describe them from west to east in the following sections.

The Cabo Cruz basin

In the western part of the study area, the plate boundary trace is divided into two parallel faults that trend N80°E. These faults bound the northern and southern margin of a rectilinear depression, the Cabo Cruz basin (Fig. 5). This basin is internally divided into a series of oblique horsts and grabens delimited by normal faults trending N45° to 50°E. The southern border of the basin is the eastward extension of the Oriente fault that follows

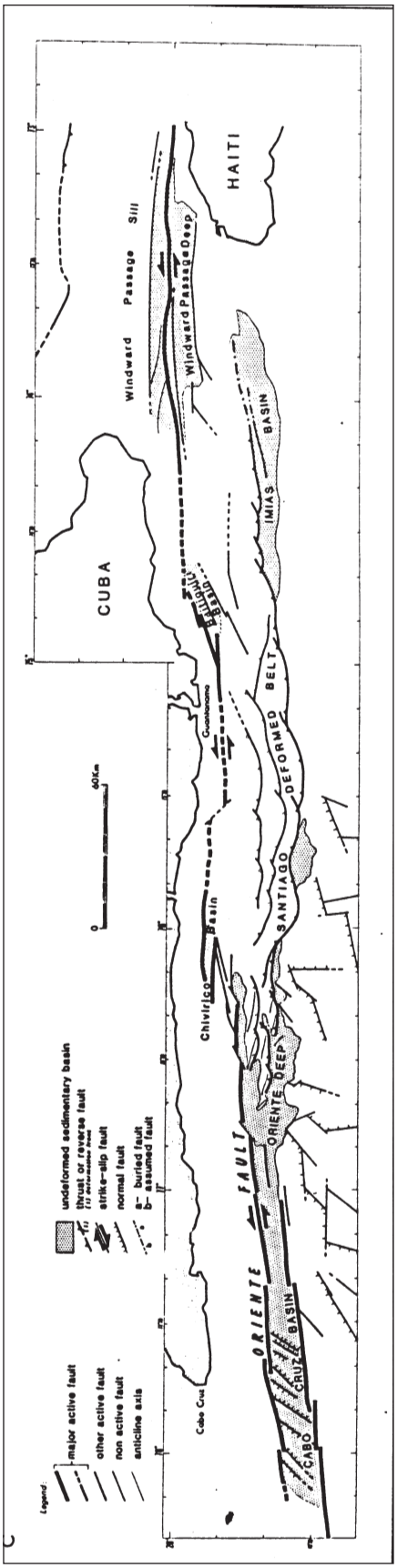

Figure 3. Tectonic map of the northern Caribbean plate boundary along the southern Cuban margin and through the Windward Passage.

the foot of the southern flank of the Cayman ridge (Fig. 1). This fault disappears to the east around 77°05W but is relayed by the fault that bounds the basin to the north. The northern fault does not extend westward of 78°20W but from this point on continues to the east along the Cuban margin. We interpret the Cabo Cruz depression as a pull-apart basin created by left-lateral shear along the two dextrally offset faults that bound it to the north and to the south. Left-lateral displacement along these faults imposes tensional strain in the relay area and causes extension and subsidence. In that context, the N45°–50°E–trending normal faults mapped within the basin can be interpreted as conjugate Riedel fractures.

Oriente Deep

East of the Cabo Cruz basin and morphologically connected to it, the Oriente Deep is an east-west–trending depression, located between 6,000 and 6,500 m deep (Fig. 3). To the north, the Oriente Deep is bounded by a prominent scarp, the Oriente Wall (Figs. 5, 6, and 7). The irregular slope and segmented trace of the Oriente Wall on map is due to two fault sets: (1) N90°E–trending faults showing significant vertical offsets, and (2) N60°E–trending faults relaying the previous ones in a sinistral offset pattern. These faults represent the trace of the plate boundary and have a significant left-lateral slip component in addition to the obvious vertical displacement along them (Calais and Mercier de Lépinay, 1991). Two small pull-apart basins (Chivirico and Baitiquiri basins, Fig. 3) have developed on tensional relays along the main left-lateral strike-slip fault. The Oriente Deep is filled with a sedimentary sequence thicker than 2,000 m in the northern part of the basin, along the active fault trace. The sediments thin to the south where they onlap the north-dipping basin substratum (Fig. 8). The sedimentary infilling of the Oriente Deep is most probably terrigenous, as suggested by the well-defined and continuous reflections on the seismic lines. The sediment supply mainly comes from the adjacent Cuban mountains (Sierra Maestra), but also from Jamaica by the way of submarine canyons (Mercier de Lépinay et al., 1989).

Santiago deformed belt

The flat bottom of the Oriente Deep is interrupted at 76°40′W by a narrow elliptic ridge, trending N130°E (Figs. 6 and 7). Seismic-reflection profiles show that this ridge is an anticline with its axial plane slightly inclined toward the south (Fig. 8). Further east, the compressional deformation progressively affects a greater width of the basin, defining a narrow east-west–trending band of hills (Fig. 8). The seismic-reflection profiles show that each of these hills corresponds to an anticline fold, 300–600 m high above the bottom of the basin, about 10 km long and 3 km wide. Continuing to the east, the deformation involves the whole width of the Oriente Deep and the basement of the Cuban margin, forming the Santiago Promontory (Fig. 7). These compressional tectonic structures extend as far east as the

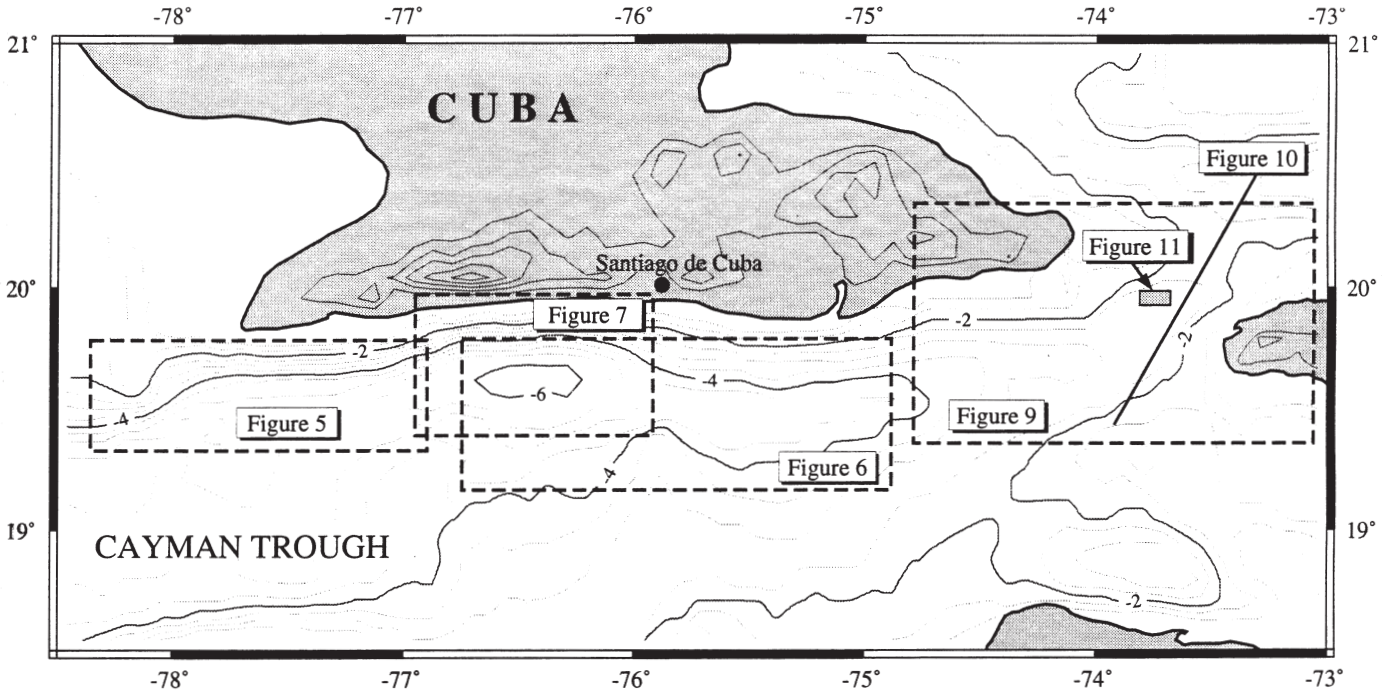

Figure 4. Location of Figures 5–7 and 9–11.

Windward Passage and form the Santiago deformed belt (Fig. 3). This 300-km-long and 10–30-km-wide belt extends parallel to the Oriente fault, that marks its northern boundary. Its southern boundary is a deformation front that usually corresponds to the surface trace of a north-dipping thrust or reverse fault. The deformation of the Santiago deformed belt is active and caused by transpression along the left-lateral Oriente strike-slip fault (Calais and Mercier de Lépinay, 1990, 1991).

Windward Passage

Between Cuba and Hispaniola, the Oriente fault runs straight through the Windward Passage into the Tortue channel (Figs. 3 and 9). Seismic reflection profiles and side-scan sonar imaging show that the two scarps that bound the Windward Passage Deep to the north and to the south are not associated with deformation of the recent basin sediments. We therefore believe that these scarps are not active faults (Fig. 10), which discards the interpretation of this basin as an active pull-apart (Mann and Burke, 1984). The Oriente fault actually crosses the Windward Passage Deep in its middle, affecting its youngest sediments. This structural arrangement of a single strike-slip fault cutting through a sedimentary basin has been classically reproduced in analogous clay and sand models (e.g., Odonne and Vialon, 1983) and is here naturally offered to direct observation. The main fault trace strikes N80°E in the western part of the basin, N90°E in its central part, and N95°E in its eastern part. Seismic profiles show that this fault is a south-verging reverse fault in the western part, which becomes vertical in the middle part and continues as a north-verging reverse fault in the eastern part as it enters the Tortue channel (Calais and Mercier de Lépinay, 1995). It is associated with minor folding and reverse faulting displaying a positive flower structure pattern (Fig. 10). The high-resolution side-scan sonar images show that the main fault is made of successive rectilinear segments. A slight offset and change of direction occur at each relay between two successive segments, giving the appearance of one continuous fault trace (Fig. 11). These relays are marked by a more intense deformation over a 500 m–1 km wide area, contrasting with the low deformation level along the rectilinear segments themselves. The deformation is mostly characterized by en echelon sigmoidal tensional fractures. Their S-shape and N60°E general trend indicate left-lateral displacement along the main east-west–trending strike-slip fault.

TRANSPRESSION IN THE ORIENTE DEEP

In the Oriente Deep, the lack of submarine erosion has clearly preserved the tectonic structures in the morphology. Our full Seabeam coverage of this area together with a dense seismic reflection coverage allowed a detailed analysis of the deformation and of its evolution in time and space.

Morphostructures

The western part of the Santiago deformed belt forms a narrow band of three N90°E–trending hills rising about 300 m above the bottom of the Oriente Deep. Each of them corresponds to a set of right-handed en echelon folds, which are clearly visible on the detailed bathymetric map (Fig. 7). This

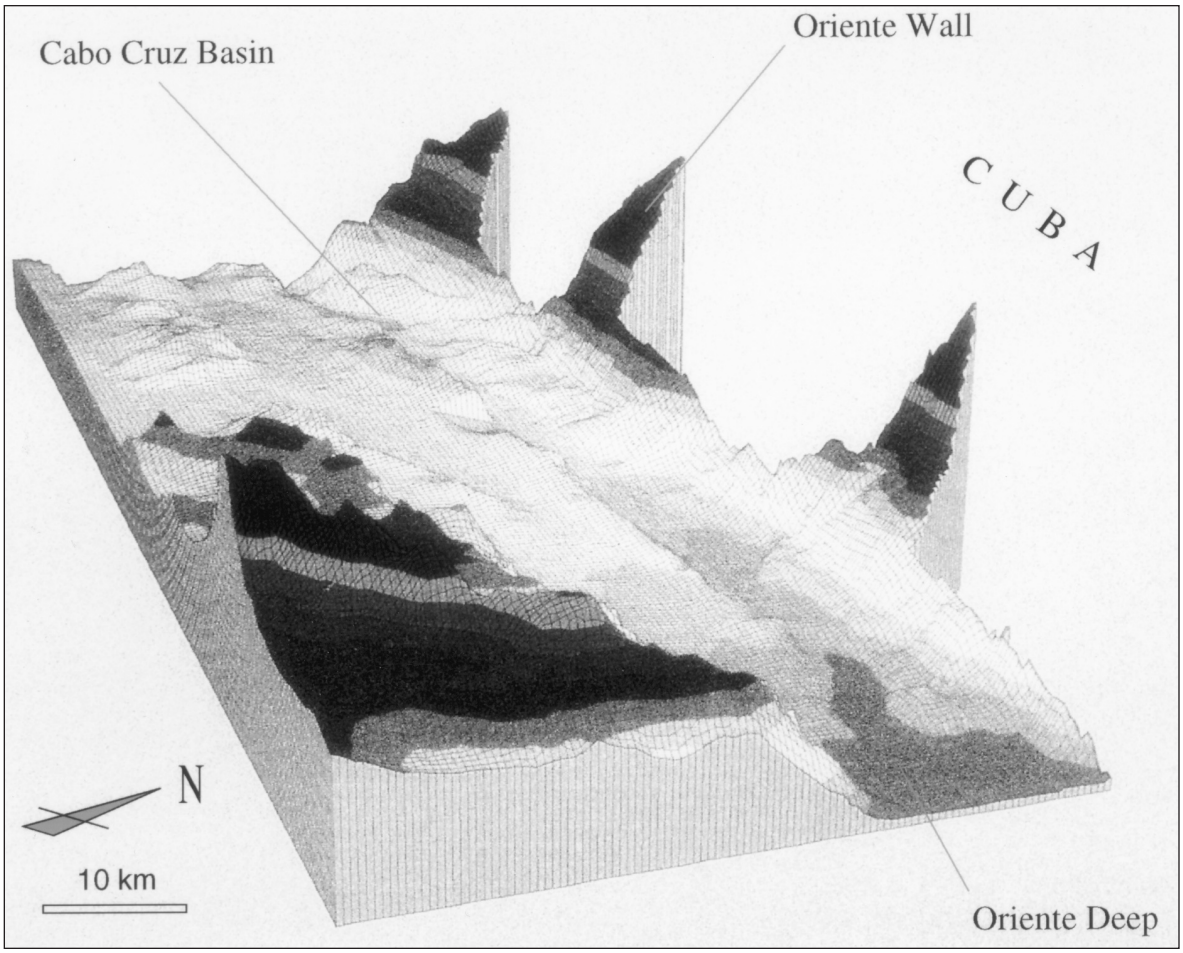

Figure 5. Three-dimensional bathymetry of the Cabo Cruz basin area.

arrangement is typical for folding in a left-lateral strike-slip tectonic regime. The axial trend of the folds, however, significantly varies within each set. On both the central and southern fold sets, the westernmost anticline trends N125°E–N130°E, making an angle of 35°–40° with the main strike-slip fault direction. Both are of small size and have a rectilinear axis. The other anticlines are bigger and have a curved axis striking 5°–20° from the main strike-slip fault direction. The stretched sigmoidal shape of these curved fold axes indicates left-lateral shear. The anticlines' wavelength is 9 km in the northern fold set, 7 km in the central fold set, and 5 km in the southern fold set, but remains constant within each fold set. The size of the anticlines shows that same gradient: they are 12 km long × 3 km wide in the northern fold set but only 5 km long × 2 km wide in the southern one. We interpret this geometry as the result of progressive northward deepening of the sedimentary infilling of the Oriente Deep, as suggested by analog models (Wilcox et al., 1973; Cobbold, 1975; Odonne and Vialon, 1983; Richard and Cobbold, 1989). The trend of the central set of folds occurs on an extension of the fault bounding the Cabo Cruz basin to the south. This suggests that this fault may extend farther east in the subsurface and act as a preexisting discontinuity that would passively initiate the folding.

SPACE AND TIME EVOLUTION OF FOLDING AND REVERSE FAULTING

An upper sequence of diverging reflections onlaps southward onto the northern flank of the anticlines (B′ on profile 59 shown in Fig. 8), with a thickness that progressively increases from the folds' crest down along their flank. This geometry characterizes a syntectonic sequence, deposited and progressively tilted during the folding of the underlying sequence. A sequence showing the same seismic characteristics is visible on profile 105 (A shown in Fig. 8), but is covered on that profile by a sequence of parallel reflections that uncomformably overlies the fold. A third sequence can be identified on profiles 59 and 105 (C or C′ shown in Fig. 8), with continuous and parallel reflections clearly affected by folding on both profiles. The most recent sediments on profile 59 are therefore syntectonic, whereas they are post-tectonic on profile 105. This result indicates that the fold on profile 59 is currently growing, whereas the fold on profile 105 is not. It suggests that

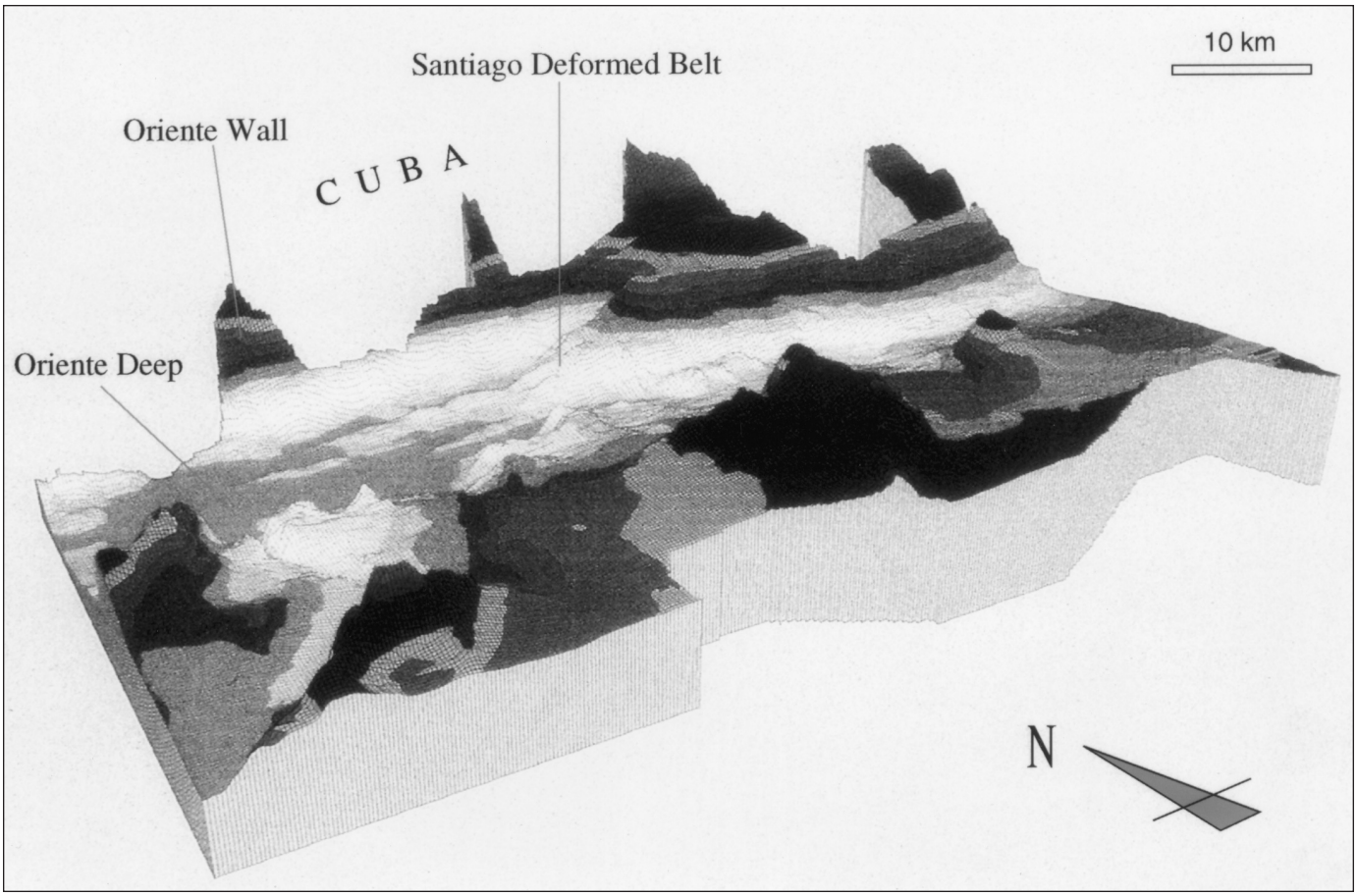

Figure 6. Three-dimensional bathymetry of the Oriente Deep area.

folding is diachronous and propagates westward. Profile 105 shows an active reverse fault at the base of its southern flank that affects the youngest sediments of the Oriente Deep (Fig. 8). Such a fault is not visible on profile 59, where folding is still active. These observations suggest that folding in the Oriente Deep is a short-lived process and that the compressive strain is taken up by reverse faulting as soon as the folds reach a sufficient size.

EARTHQUAKE DISTRIBUTION AND FOCAL MECHANISMS

Instrumental seismicity

We used the instrumental seismicity data published in the International Seismological Center (ISC) catalogs that provide location, time, and magnitude of global earthquakes for the past 35 yr (1960–1995). The focal mechanisms were taken from the Centroid Moment Tensor (CMT) solutions published by Dziewonsky et al. (e.g., 1981) and cover from 1977 to the present.

Earthquake distribution reveals rather little seismicity along the Swan and Oriente faults in the Cayman trough (Fig. 2). Shallow earthquakes associated with both faults show pure left-lateral strike-slip displacement along east-west–trending vertical fault planes. One focal mechanism in the vicinity of the mid-Cayman spreading center shows east-west extension related to oceanic accretion at the ridge axis. The seismicity pattern along the Oriente fault changes as it reaches the southern Cuban margin. The focal mechanisms of all but one of the events of the southern Cuban margin show a strike-slip component, as along the Cayman trough. It is, however, always associated with either a thrust component (in all but one case) or an extension component (in one case, the Cabo Cruz basin). One earthquake shows pure thrusting. All these events share a focal plane that trends between N30ºE and N130°E and dips between 21° and 69° to the north. Given the active north-dipping south-verging thrusts that we mapped in that area (cf. supra), we correlate this nodal plane with the fault plane and interpret these events as oblique thrusting on north-dipping rupture planes.

Two large earthquakes have recently been recorded in the Cabo Cruz basin area. The first one (mb = 5.7, August 26, 1990) has a focal mechanism that essentially shows east-west extension, with a little strike-slip component. It is probably caused by normal faulting related to extension in the Cabo Cruz basin. We propose to correlate the N30°E–trending nodal plane with faults of the same direction that we observed within the basin. In that hypothesis, these faults would mostly have a normal component,

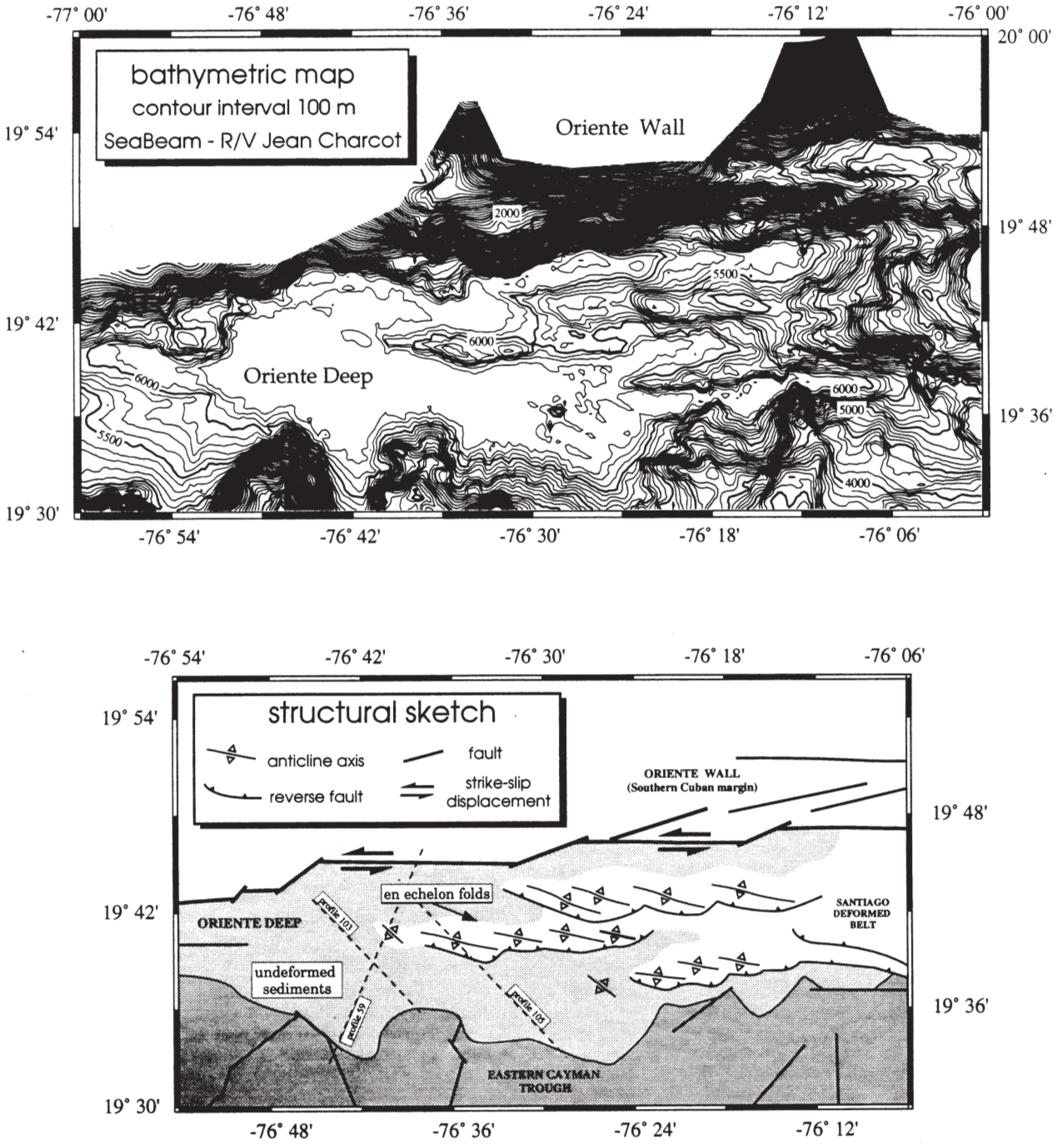

Figure 7. Detailed bathymetric map of the Oriente Deep and morphostructural interpretation. The dashed lines give the location of the seismic profiles of Figure 8.

combined with little left-lateral strike-slip. This result is in accordance with an interpretation of these faults as Riedel fractures associated with left-lateral shear along major east-west–trending faults. The most recent and biggest earthquake along the southern Cuban margin is a mb = 6.3 that struck the Cabo Cruz basin area on May 25, 1992 (Perrot et al., 1997). The main shock probably occurred along the northern edge of the basin, although the accuracy of teleseismic determinations does not give a precise enough location to undoubtedly point out the associated rupture. We modeled that earthquake using a hybrid ray-tracing method (Perrot et al., 1994) that enables us to use a two-dimensional crustal model around the seismic source. We used the crustal model obtained by Edgar et al. (1971) from seismic-refraction data. The best fit between the observed and synthetic seismo-

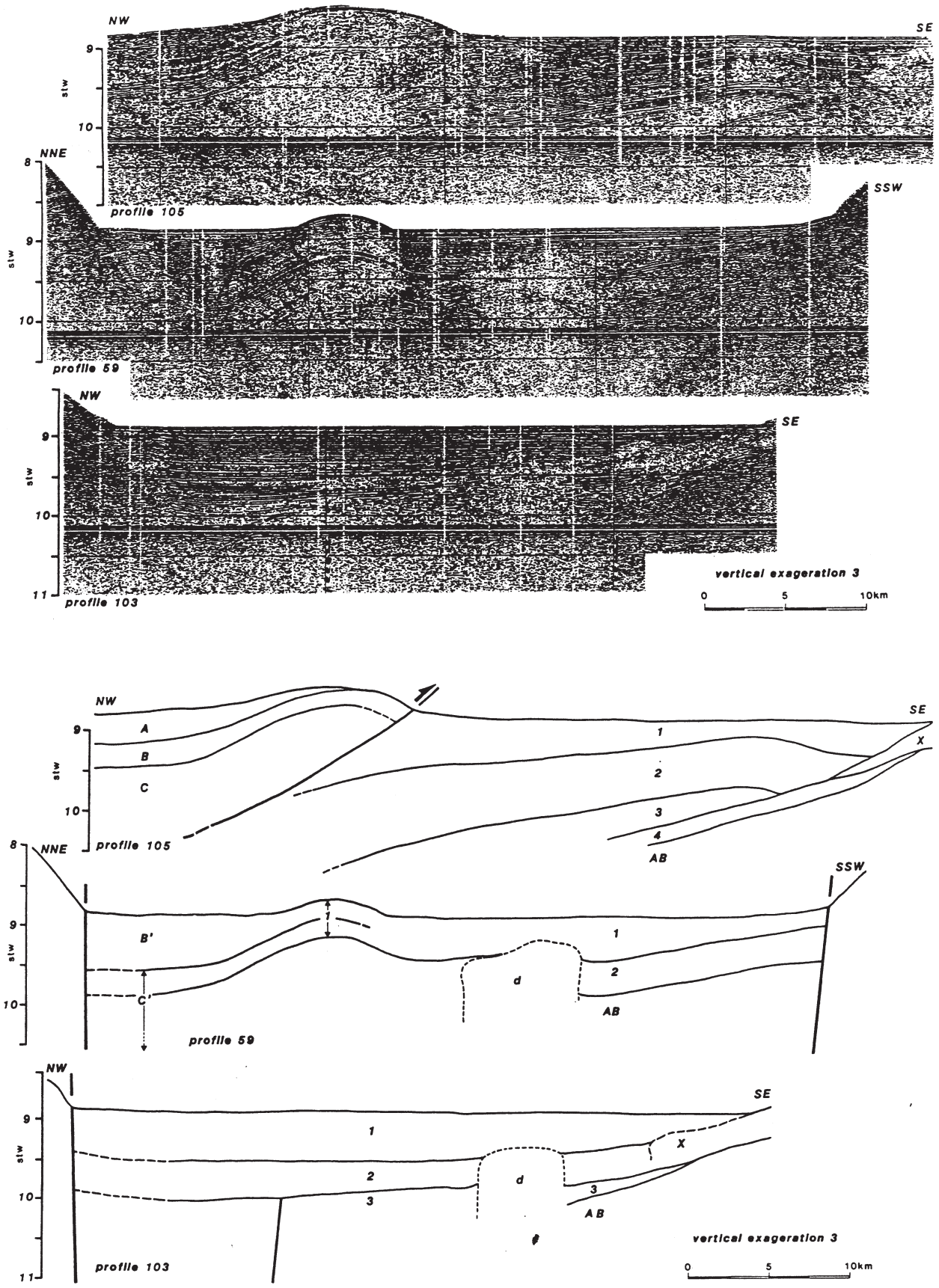

Figure 8. Single-channel seismic-reflection profiles 59, 103, and 105 across the Oriente Deep and corresponding interpretation.

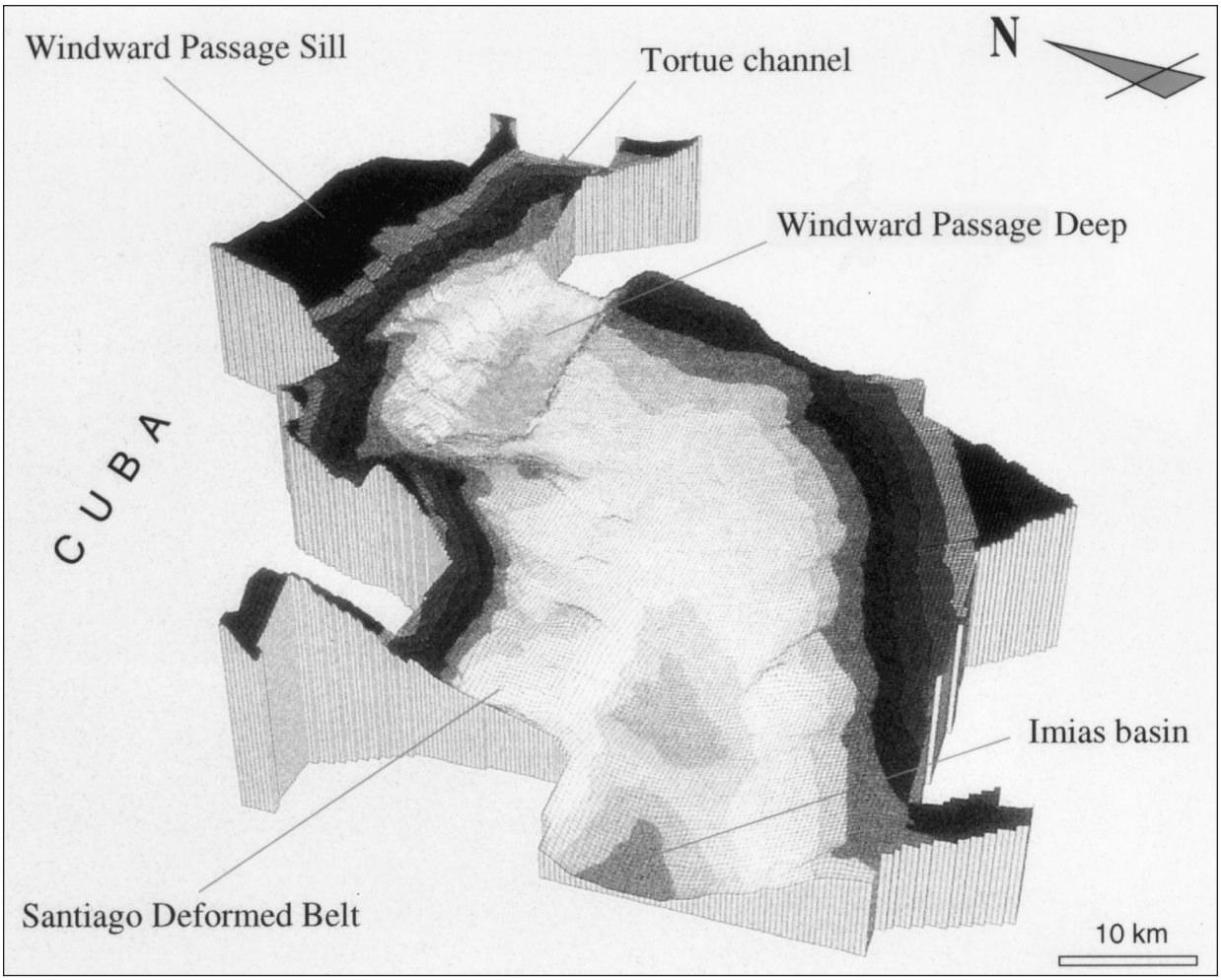

Figure 9. Three-dimensional bathymetry of the Windward Passage area.

grams is obtained for a 19-km-deep hypocenter with a focal plane trending N80°E and dipping 55° to the north (Fig. 12). Because of its coincidence with the Oriente fault direction and the consistency of this focal mechanism with others farther east, we interpret this focal plane as the rupture plane.

Historical seismicity

Reports of earthquakes in the Greater Antilles date as far back as the 16th century when the region was being colonized by the Spanish. On the basis of these reports, Salterain (1883) already noticed the significant seismic activity in southern Cuba. Before the 20th century, the only populated area in that region was the city of Santiago de Cuba (Fig. 4), which was founded in 1514. The history of Santiago therefore provides a precise calendar for major earthquakes in that region. Taber (1922, p. 211) noted that while strong shocks were usually felt over a large region, small events have been reported only from Santiago. The location of these old events is not accurate, but because the Oriente fault is the only major active fault in the area, it seems reasonable to assume that they occurred along it, as Taber already proposed in 1922: "Most of the earthquakes that have damaged property in eastern Cuba have probably their origins along the precipitous scarp that forms the north side of the Bartlett [Cayman] Trough." The first earthquake reported in Salterain's listing that caused serious damage to Santiago occurred in 1578. Two other strong and damaging shocks followed in 1675 and 1677, two years apart. One year later, on February 11, 1678, a strong shock caused extensive destruction in the city. In 1755, a severe earthquake was followed by a tsunami that flooded Santiago. The strongest earthquake ever felt in this region occurred on June 11, 1766, and almost completely destroyed the city of Santiago. Salterain lists 18 strong earthquakes between 1777 and 1852 and quotes a witness of the August 20, 1852, earthquake who reported that "the first shock consisted of a strong up and down motion, causing many of the inhabitants to flee from the city." This last information, and especially the 1755 tsunami, suggests that some of the historical

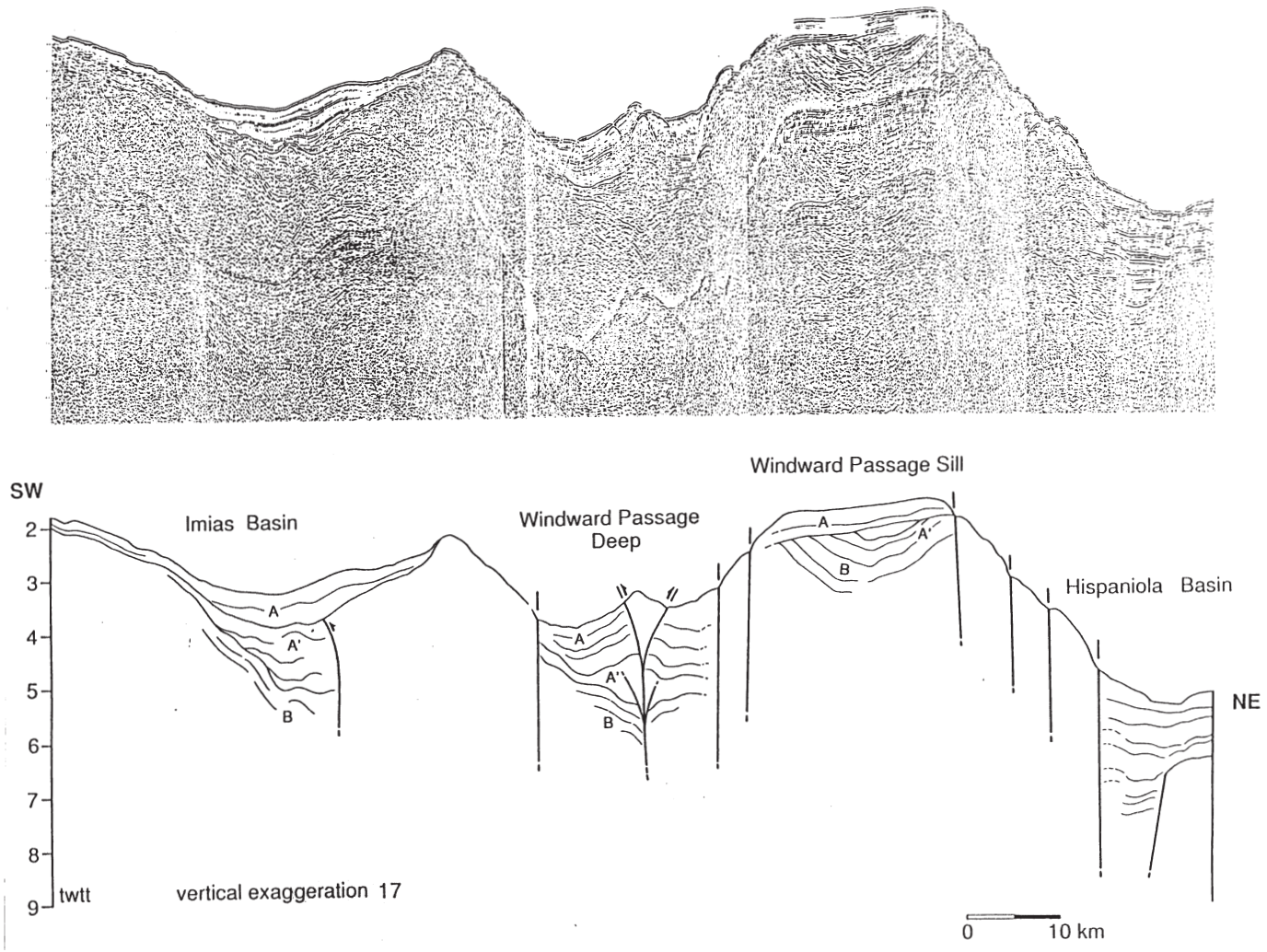

Figure 10. Multichannel seismic-reflection profile crossing the Windward Passage Deep and corresponding interpretation.

earthquakes of southern Cuba may have had a thrust component, as the instrumental seismicity has shown for most of the recent earthquakes in that region.

The earliest earthquake in the southern Cuban region for which an estimate of source parameters is available is dated 1887 (Mocquet, 1984). In about a century, five earthquakes with a magnitude Ms greater than 6.5 occurred along the southern Cuban margin (Table 1, from Mocquet, 1984). This provides us with a century of quantitative information on major earthquakes in this region.

SEISMIC SLIP, STRESS AND STRAIN

Seismic slip rates

The seismic energy released during earthquakes provides an estimate of the displacement due to earthquakes on a strike-slip fault (e.g., Brune, 1968; Thatcher et al., 1975; Anderson, 1979). In the following paragraphs, we estimate the slip rate along the southern Cuban margin from 78°W to 74°W (Fig. 2).

The average seismic slip is given by

$$\bar{u} = \frac{1}{\mu A \Delta T} \sum_{\Delta T} M_o \qquad (1)$$

where A is the total fault area, μ the shear modulus, ΔT the data time span, and M_o the seismic moment (Brune, 1968). We used $\mu = rV_s^2 = 3.3 \times 10^{11}$ dyn/cm^2, a 440-km-long × 15-km-deep fault plane (from 78°E to 74°E). We applied the above equation to the data listed in Table 1 and in the ISC catalog (1960–present). From 1887 to the present, we obtain an average seismic slip rate of 15 mm/yr, fairly close to the 12 ± 3 mm/yr NUVEL-1 slip estimate along the Oriente fault (Table 2, p. 211). However, using only the ISC data we obtain an average seismic slip rate of only 6.3 mm/yr. This probably indicates that the 35 yr span of the ISC catalog does not provide a record of the seis-

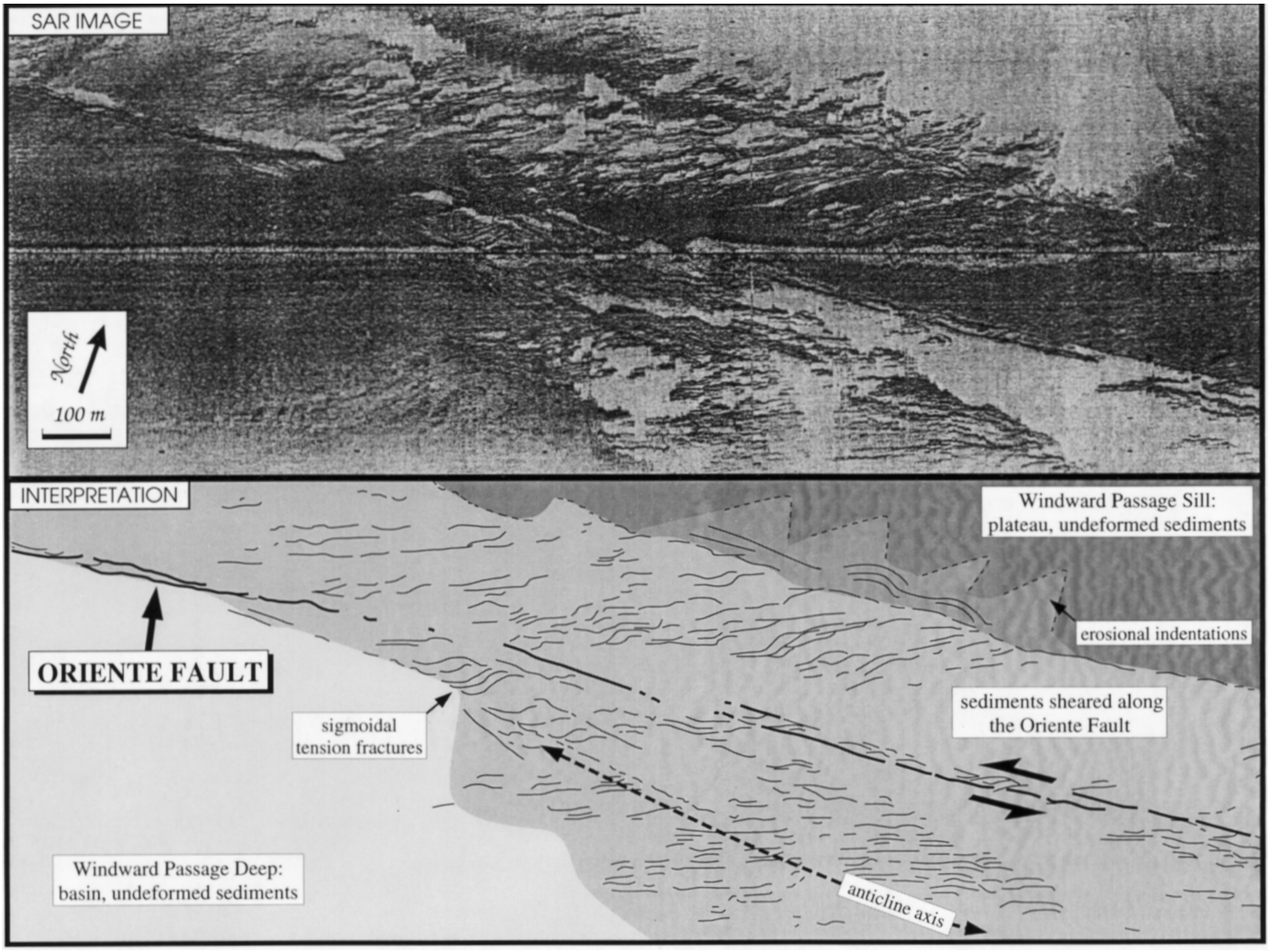

Figure 11. Side-scan sonar image of a segment of the Oriente fault in the Windward Passage Deep (SAR = side aperture radar).

micity typical of longer time spans. However, it could also mean that the magnitudes of the historical events have been overestimated.

To test these hypotheses, we used an alternative method based on the frequency-magnitude and moment-magnitude relations that characterize the seismic area (Anderson, 1979). In a given seismic area where $\log(N) = a - b\, m_b$ and $\log(M_o) = c\, m_b + d$, the average seismic slip is given by:

$$\bar{u} = \frac{1}{\mu A} \frac{10^{\alpha} 10^{(1-\beta)\gamma_{\max}}}{(1-\beta)\ln 10}, \qquad (2)$$

with $\beta = b/c$, $\alpha = a + db/c - \log(c)$, and $\gamma_{\max} = \log(M_o^{\max})$. We used the ISC catalog and obtained for the southern Cuban margin $\log(N) = 3.6 - 0.6m_b$, $\log(M_o) = 0.9m_b + 19.4$ (Fig. 13), and an average seismic slip rate of 13.3 mm/yr (Table 3).

This value is about twice as great as the 6.3 mm/yr obtained by summing the seismic moments provided by the ISC catalog only, but it agrees well with the 15 mm/yr obtained from using the historical seismicity and with the NUVEL-1 slip estimate of 12 ± 3 mm/yr. We therefore believe that the 6.3 mm/yr value was biased by a peculiar short-term seismicity pattern over the past 35 yr and that the magnitudes of the historical events were probably correct.

Seismic stress tensor

We computed a stress tensor by inverting the source parameters of 6 $m_b > 5$ thrust events of the southern Cuban margin (Angelier and Mechler, 1979). The source parameters are listed in Table 3 and the principal components of the resulting stress tensor are shown on Figure 14. We obtain a principal compressive stress s_1 trending N240°E and dipping 13° to the southwest and a principal tensional stress s_3 trending N134°E and dipping 50° to the southeast. This stress tensor characterizes a combination of thrust and strike-slip and is consistent with the tectonic observations. The principal compressive

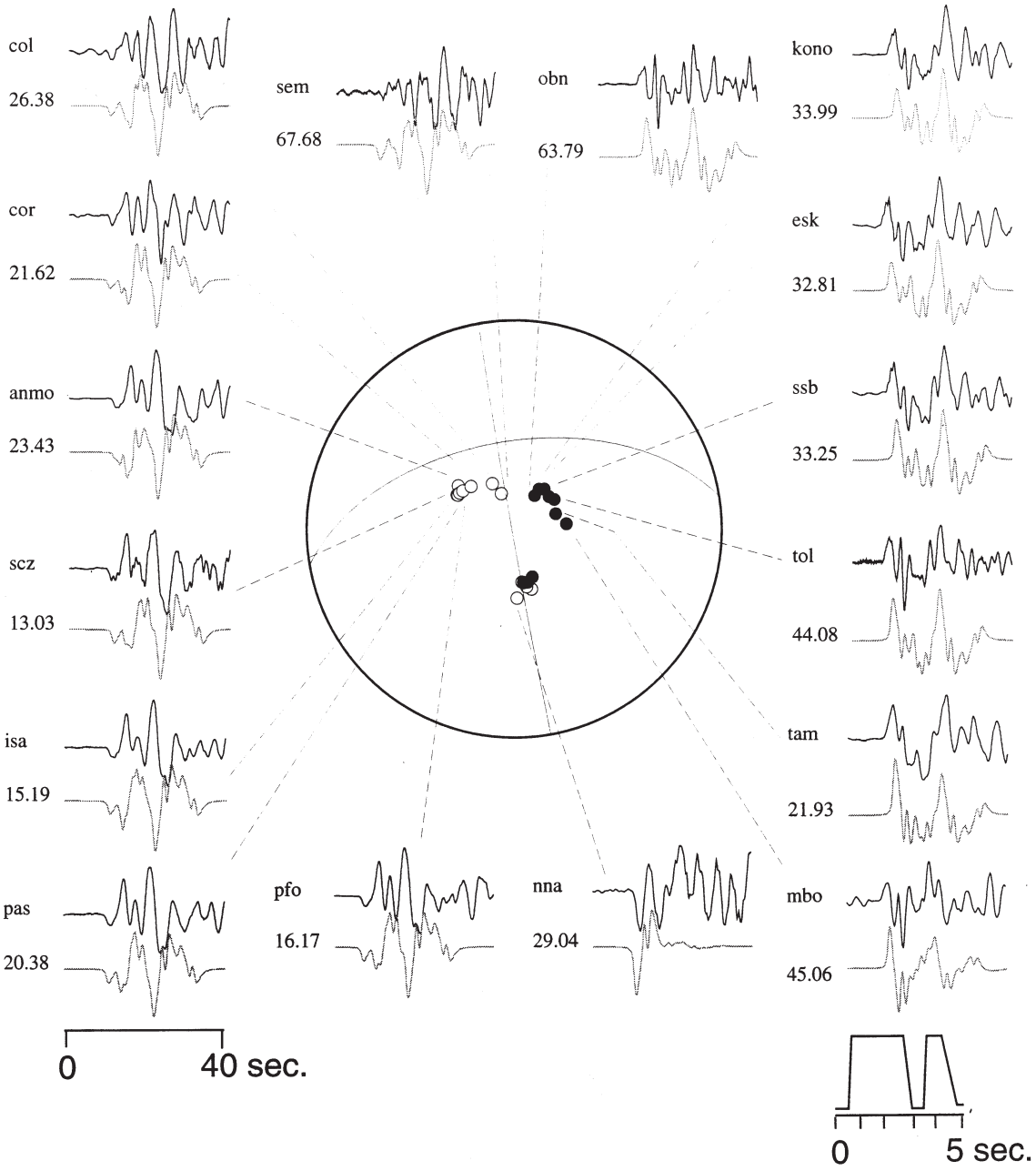

Figure 12. Focal mechanism of the Ms = 7.0 "Cabo Cruz" earthquake (May 25, 1992) from P-waves modeling. The observed (top) and synthetic (bottom) seismograms are displayed for each station with the station name on the left. Seismic moments are in 10^{-18} N.m. The source time function is at the bottom right of the figure.

stress is subperpendicular to the main strike-slip fault and perpendicular to the axis of the folds that we imaged in the Oriente Deep (Fig. 7).

This same stress pattern has been described along the San Andreas fault system in California (Mount and Suppe, 1987), where a small component of convergence is added to the general strike-slip displacement between the Pacific and North America plates. We tentatively apply the same interpretation to the northern Caribbean plate boundary along the southern Cuban margin and thus infer a small convergence component to be added to the general strike-slip displacement between the Caribbean and North America plates in that region. This convergence component could explain the transpressive tectonic regime revealed by the morphostructural analysis as well as the teleseismic data along the southern Cuban margin.

TABLE 1. HISTORICAL EARTHQUAKES REPORTED ALONG THE SOUTHERN CUBAN MARGIN*

Date	Location	Moment (10^{26} dyn.cm)	Magnitude M_s
Sept. 23, 1887	South of Cuba	25	7.5
Feb. 20, 1917	19.5°N/78.5°W	14	7.4
Feb. 3, 1932	19.8°N/75.8°W	1.5	6.7
July 7, 1947	19.9°N/75.3°W	1.5	6.7

*Source parameters have been estimated (from Mocquet, 1984). Numerical values are approximate.

Seismic strain rates

Kostrov (1974) showed that the average irrotational strain in a volume caused by slips on different rupture planes is given by

$$\bar{\varepsilon}_{ij} = \frac{1}{2\mu\Delta V}\sum_{x=1}^{n} M_{ij}^{(x)} \qquad (3)$$

where M_{ij} is the seismic moment components summed over n rupture planes and ΔV is the deformed volume. As before, we assumed a shear modulus μ of 3.3×10^{11} dyn/cm^2 and a 440-km-long × 40-km-wide × 15-km-deep deformed volume extending along the Oriente fault from 78°E to 74°E. Using the CMT source parameters (Table 3), we obtain the following strain tensor:

$$\bar{\varepsilon}_{ij} = \begin{pmatrix} 31.27 & 42.46 & -49.49 \\ 42.46 & -33.06 & 30.40 \\ -49.49 & 30.40 & 1.79 \end{pmatrix} \times 10^{-9}/\text{yr}, \qquad (4)$$

with the rows and columns corresponding to the east, south, and vertical components, respectively. The average slip corresponding to this strain tensor is 13.9 mm/yr in a N84.5°E direction. Given the uncertainties associated with the determination of earthquake source parameters, this direction is in fair agreement with the NUVEL-1 prediction of N78°E. The slip rate agrees well with the value of 13.3 mm/yr obtained using Anderson's method (Table 2) and with the NUVEL-1 prediction of 12 ± 3 mm/yr.

This strain tensor represents the strain released during earthquakes in the deformed area averaged over 18 yr (data time span). It shows east-west extension and north-south contraction of about the same amount and with little vertical extension. Figure 15 shows that the strain tensor is almost isotropic in a vertical east-west–trending plane, as one should expect within a shear plane. This agrees with the Oriente fault being the main shear zone. In the horizontal plane, the strain tensor shows left-lateral shear (Fig. 15) consistent with strike-slip displacement along the plate boundary. In a vertical north-south–trending plane, the strain tensor shows right-lateral shear and strong contraction along an axis dipping 45° to the north, both consistent with southward thrusting and north-south shortening in the Santiago deformed belt.

DISCUSSION: SEISMICITY, ACTIVE STRUCTURES, AND PLATE MOTION

Marine geophysical data and the seismicity characteristics show that the tectonic regime along the southern Cuban margin is a combination of left-lateral shear and north-south compression along the whole margin. This transpressive regime is not restricted to the Santiago deformed belt, where surficial evidence of transpression is pronounced, but also extends into the Cabo Cruz basin, where the major tectonic structures indicate transtension. However, transtension in the Cabo Cruz pull-apart area is related to the local geometry of the main fault zone, and does not preclude the existence of a regional compressional component along the fault zone.

The seismic slip rate along the Oriente fault deduced from different methods and from data spanning up to 108 yr agrees well with the 12 ± 3 mm/yr NUVEL-1 prediction (Table 2). This result suggests that all the stress accumulated by the Caribbean–North America plate motion is released seismically along the southern Cuban margin. On the other hand, 97% of the total seismic energy released along the southern Cuban mar-

TABLE 2. SLIP AND MOMENT RATES ALONG THE SOUTHERN CUBAN MARGIN*

	Geology (NUVEL-1)	Cumulative Seismic Moment, 1887 to Present	Cumulative Seismic Moment, 1960 to Present	Anderson (1979)	Kostrov (1974)
Moment rate (10^{24} dyn.cm/yr)	26	34	14	29	30
Slip rate (mm/yr)	12.0 ± 3	15	6.3	13.3	13.8
Time span (years)	3×10^6	108	35	35	18

*Rates estimated from five different methods (explanations in text).

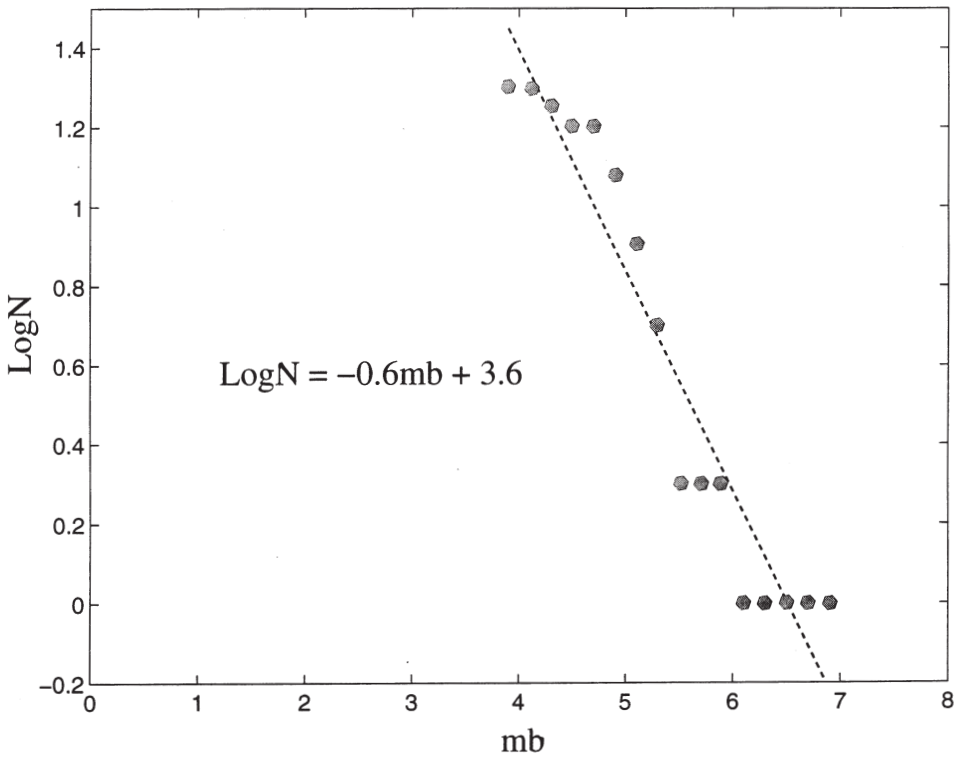

Figure 13. Cumulative frequency (N) versus magnitude (m_b) plot for the southern Cuban margin seismicity between 78°W and 74°W. The plotted regression line corresponds to the relation indicated in the figure.

TABLE 3. SOURCE PARAMETERS OF M_b >5 EARTHQUAKES ALONG SOUTHERN CUBAN MARGIN FROM 1970 TO PRESENT

Date	Time	Strike	Dip	Rake	m_b	M_s	M_o	M_{rr}*	M_{ss}*	M_{ee}*	M_{rs}*	M_{re}*	M_{se}*
11/13/78	07:43	330°	69°	73°	5.1	4.7	0.63	0.41	0.02	-0.43	-0.3	0.35	0.69
09/01/85	01:00	228°	53°	82°	5.1	4.5	0.44	0.44	-0.28	-0.17	-0.06	-0.11	-0.18
02/12/89	14:27	286°	29°	43°	5.2	4.6	0.75	0.44	-0.28	-0.16	0.11	-0.55	0.31
05/22/90	20:36	290°	43°	27°	5.0	4.9	0.13	0.57	-0.07	-0.50	-0.35	-0.82	0.74
08/26/90	07:53	039°	62°	57°	5.7	5.1	2.2	-1.4	-0.72	2.2	-0.69	-0.59	0.82
09/04/90	08:03	302°	21°	21°	5.2	4.5	0.73	0.24	-0.07	-0.17	-0.26	-0.63	0.23
05/25/92	16:55	248°	43°	01°	6.3	7.0	201	4	-85	81	81	-127	109

*M_{rr}, M_{ss}, M_{ee}, M_{rs}, M_{re}, and M_{se} are the moment tensor elements in 10^{24} dyn.cm expressed in an r-up, s-South, e-East coordinate system.

gin over the past 35 yr is due to the May 25, 1992, earthquake (Table 3). Also noticeable is the lack of moderate-size earthquakes ($5.0 < M_s < 6.0$) in this region, as shown by Figure 13. This tends to show that most of the seismic stress is released during a few strong earthquakes, such as the 1992 Cabo Cruz event, and is consistent with the historical seismicity that shows the occurrence of only one or two earthquakes with a magnitude greater than 7.0 per century.

These results single out this segment of the northern Caribbean strike-slip plate boundary from oceanic transform faults, where up to 95% of the total slip can occur aseismically (Trehu and Solomon, 1983; Steward and Okal, 1983; Dziak et al., 1991). In the case of oceanic transform faults, this process is usually related to an anomalously high heat flow that prevents seismic failure (Burr and Solomon, 1978; Kawasaki et al., 1985). Heat-flow measurements in the eastern part of the Cayman trough do not show any significant anomaly (Rosencrantz et al., 1988). Moreover, the Oriente fault along the southern Cuban margin crosses island-arc rocks, not oceanic material (Edgar et al., 1971; Mercier de Lépinay et al., 1989). We also show that the relative displacement of the Caribbean and North America plates is slightly oblique to the Oriente fault trend along the southern Cuban margin. This could participate in "locking" the fault zone by increasing the coupling between the Caribbean and North America lithospheres. These characteristics may explain the highly seismic nature of the northern Caribbean plate boundary along the southern Cuban margin.

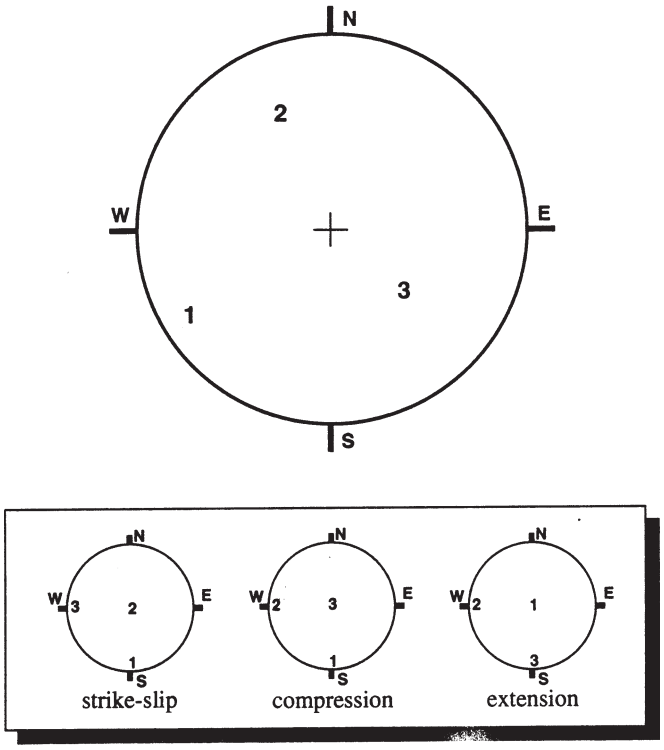

Figure 14. Principal axis of the stress tensor along the southern Cuban margin (Schmidt projection, lower hemisphere). Inset: theoretical stress tensor axis in the case of pure strike-slip, pure compression, and pure extension.

CONCLUSION

The analysis of the active tectonic structures along the northern Caribbean plate boundary from Cuba to Hispaniola reveals a narrow deformation zone dominated by left-lateral strike-slip faulting. The shear displacement is probably concentrated along the most prominent structural feature, the Oriente fault. This fault has a discontinuous trace with left-stepping offsets that generate tensional strain and cause the subsidence of pull-apart basins like the Cabo Cruz basin. However, the most striking tectonic structures display transpression (Santiago deformed belt) with active folding and reverse faulting. The earthquakes' distribution and their source parameters are well correlated with the active tectonic structures. Both types of data reveal the combination of north-south compression and left-lateral shear starting at about 78°W long. in the Cabo Cruz basin area and continuing all the way along the southern Cuban margin. We infer the existence of a component of convergence added to the shear displacement between the Caribbean and North America plates that would induce the transpressive strain regime and cause folding and reverse faulting along structures parallel to the main fault. We compute a seismic slip rate of 13–15mm/yr that agrees well with the 12 ± 3 mm/yr NUVEL-1 estimate along the northern Caribbean plate boundary. This result implies that all the slip along the southern Cuban margin occurs seismically and could suggest strong lithospheric coupling between the Caribbean and North America plates in that region.

ACKNOWLEDGMENTS

We are grateful to the ship crew and scientific members of the Seacarib II (R/V *Jean Charcot*) and Oriente (R/V *Le Suroit*) oceanographic campaigns during which most of the marine geophysical data presented here were collected. We thank Jim Dolan, William Dillon, and James Dewey for their helpful reviews. Géoscience Azur publication 167.

REFERENCES CITED

Anderson, J. G., 1979, Estimating the seismicity from geological structure for seismic-risk studies: Bulletin of the Seismological Society of America, v. 69, p. 135–158.

Angelier, J., and Mechler, P., 1979, A graphic method applied to the localization of principal stresses for fault tectonics and seismology; the right dihedral method: Bulletin de la Societé Géologique de France, v. 19, p. 1309–1318.

Brune J. N., 1968, Seismic moment, seismicity, and rate of slip along major fault zones: Journal of Geophysical Research, v. 73, p. 777–784.

Burr N. C., and Solomon, S. C., 1978, The relationship of source parameters of oceanic transform earthquakes to plate velocity and transform length: Journal of Geophysical Research, v. 83, p. 1193–1205.

Calais, E., and Mercier de Lépinay, B., 1990, A natural model of active transpressional tectonics: The en échelon structures of the Oriente Deep, along the northern Caribbean transcurrent plate boundary: Revue de l'Institute Francais du Pétrole et Annales des Combustible Liquides, v. 45, p. 147–160.

Calais, E., and Mercier de Lépinay, B., 1991, From transtension to transpression along the northern Caribbean plate boundary off Cuba: Implications for the recent motion of the Caribbean plate: Tectonophysics, v. 186, p. 329–350.

Calais, E., and Mercier de Lépinay, B., 1995, Strike-slip tectonic processes in the northern Caribbean between Cuba and Hispaniola (Windward Passage): Marine Geophysical Research, v. 17, p. 63–95.

Case, J. E., and Holcombe, T. L., 1980, Geologic-tectonic map of the Caribbean region: U.S. Geological Survey, Miscellaneous Investigations, Map I-1100, Scale 1:2,500,000.

Cobbold P. R., 1975, Fold propagation in single embedded layers: Tectonophysics, v. 27, p. 333–351.

DeMets, C., Gordon, R. G., Argus, D. F., and Stein, S., 1990, Current plate motions: Geophysical Journal of the Royal Astronomical Society, v. 101, p. 425–478.

Dziak R. P., Fox, C. G., and Embley, R. W., 1991, Relationship between the seismicity and geologic structure of the Blanco transform zone: Marine Geophysical Researches, v. 13, p. 203–208.

Dziewonski, A. M., Chou, T. A., and Woodhouse, J. H., 1981, Determination of earthquake source parameters from waveform data for studies of global and regional seismicity: Journal of Geophysical Research, v. 86, p. 2825–2852.

Edgar, N. T., Ewing, J. I., and Hennion, J., 1971, Seismic refraction and reflection in the Caribbean Sea: American Association of Petroleum Geology Bulletin, v. 55, p. 833–870.

Goreau, P. D. E., 1983, The tectonic evolution of the north-central Caribbean plate margin [Ph.D. thesis]: Cambridge, Massachusetts, Massachusetts Institute of Technology, 245 p.

Kawasaki, I., Yasutosi, K., Ikuko, T., and Kosugi, N., 1985, Mode of seismic

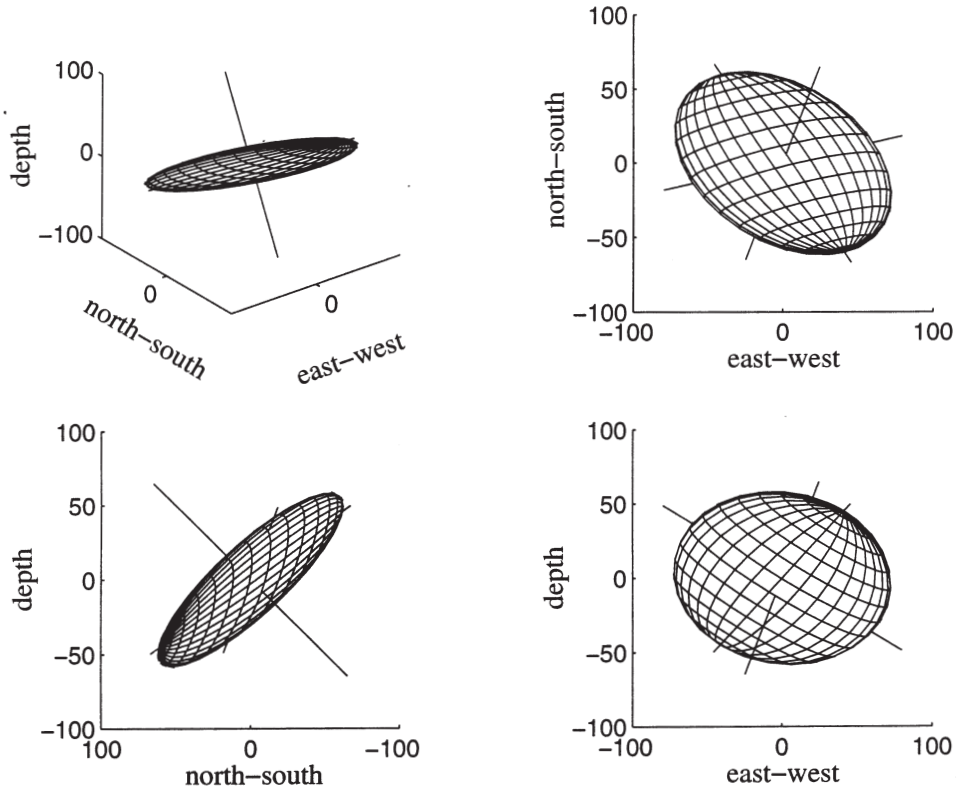

Figure 15. Ellipsoid representation of the strain tensor along the southern Cuban margin.

moment release at transform faults: Tectonophysics, v. 118, p. 313–327.

Kostrov, V. V., 1974, Seismic moment and energy of earthquakes, and seismic flow of rocks: Physics Solid Earth, v. 1, p. 13–21.

Mann, P., and Burke, K., 1984, Neotectonics of the Caribbean: Review of Geophysics and Space Physics, v. 22, p. 309–362.

Mascle, A., and Letouzey, A., 1990, Geological map of the Caribbean: Rueil-Malmaison, France, L'institute Français du Pétrole, Z sheets.

Mercier de Lépinay, B., Renard, V., Calais, E., Calmus T., Capet, X., Delteil, J., Gardner, O., Hernandez, G., Mauffret, A., Momplaisir, R., Quentric, I., Rodriguez, R., Ross, M., Tardy, M., and Vila, J. M., 1989, Morphology and structure along a major marine strike-slip fault zone: The northern Caribbean plate boundary between Cuba, Hispaniola and Jamaica, *in* Proceedings of the 28th International Geological Congress, July 9–19, 1989: Washington D.C.

Mocquet, A., 1984, Vitesses de déplacement discontinu le long d'une zone limite de plaques: Caraibes-Amérique du Nord (Discontinuous slip rates along the Caribbean–North America plate boundary) [unpublished M.A. thesis]: France, University of Rennes, 53 p.

Molnar, P., and Sykes, L. R., 1969, Tectonics of the Caribbean and Middle America regions from focal mechanisms and seismicity: Geological Society of America Bulletin, v. 80, p. 1639–1684.

Mount, V. S., and Suppe, J., 1987, State of stress near the San Andreas Fault; implications for wrench tectonics: Geology, v. 15, p. 1143–1146.

Odonne, F., and Vialon, P., 1983, Analogue models of folds above a wrench fault: Tectonophysics, v. 99, p. 31–46.

Perrot, J., Deschamps, A., Farra, V., and Virieux, J., 1994, Azimuthal distorsion of the seismic focal sphere: Application to earthquakes in subduction zone: Physics of the Earth and Planetary Interiors, v. 84, p. 240–270.

Perrot, J., Calais, E., and Mercier de Lépinay, B., 1997, Waveform simulation of the May 25th, 1992, Ms = 6.7 Cabo Cruz earthquake (Cuba): New constraints on the tectonic regime along the northern Caribbean plate boundary: PAGEOPH, v. 149, p. 475–487.

Richard, P., and Cobbold, P., 1989, Structures en fleur positives et décrochements crustaux: Modélisation analogique et interprétation dynamique (Positive flower structures and crustal strike-slip faults: analog models and dynamic interpretation): Comptes Rendus de l'Académie des Sciences des Paris, p. 553–560.

Rosencrantz, E., Ross, M. I., and Sclater, J. G., 1988, The age and spreading history of the Cayman Trough as determined from depth, heat flow and magnetic anomalies: Journal of Geophysical Research, v. 93, p. 2141–2157.

Salterain, P., 1883, Ligera resena de los tremblores de tierra ocurridos en la isla de Cuba (The earthquakes of the island of Cuba): Boletin de la Comision del Mapa Geologico de Espana, v. 10, p. 371–385.

Steward, L. M., and Okal, E. A., 1983, Seismicity and aseismic slip along the Eltanin fracture zone: Journal of Geophysical Research, v. 88, p. 10495–10507.

Taber, S., 1922, The seismic belt in the greater Antilles: Bulletin of the Seismological Society of America, v. 4, p. 199–219.

Thatcher W., Hileman, J. A., and Hanks, T. C., 1975, Seismic slip distribution along the San Jacinto fault zone, southern California, and its implications: Geological Society of America Bulletin, v. 86, p. 1140–1146.

Tréhu, A. M., and Solomon, S. C., 1983, Earthquakes in the Orozco transform zone: Seismicity, source mechanisms, and tectonics: Journal of Geophysical Research, v. 88, p. 8203–8225.

Wilcox, R. E., Harding, T. P., and Seely, D. R., 1973, Basic Wrench Tectonics: American Association of Petroleum Geologists Bulletin, v. 57, p. 74–96.

MANUSCRIPT ACCEPTED BY THE SOCIETY JANUARY 9, 1998

Geological Society of America
Special Paper 326
1998

The 1943–1953 north-central Caribbean earthquakes: Active tectonic setting, seismic hazards, and implications for Caribbean–North America plate motions

James F. Dolan
Department of Earth Sciences, University of Southern California, Los Angeles, California 90089
David J. Wald
U.S. Geological Survey, Pasadena, California 91125

ABSTRACT

The 1943 northern Mona Passage earthquake and the 1946 northeastern Hispaniola earthquake were two of the largest events to strike the north-central Caribbean region in more than 400 yr. Both were oblique, left-lateral thrust events generated by the rupture of large parts of the gently south-dipping, plate-interface fault that separated the obliquely subducting North America (Atlantic) slab from the overriding Hispaniola and Puerto Rico blocks of the northern Caribbean plate boundary zone (NCPBZ). These ruptures occurred at strongly coupled collisional asperities associated with active, collisional underthrusting of high-standing carbonate banks of the southeastern Bahamas. This is particularly well illustrated by the 1946 mainshock, where the 200-km-long aftershock zone exactly matches the limits of the active collision zone between northern Hispaniola and Silver and Navidad carbonate banks. A large aftershock of the 1946 earthquake in 1948 deepened the mainshock rupture plane, and another major aftershock in 1953 extended the rupture 15 km westward to the leading edge of the oblique, westward-propagating Bahamas collision.

Bathymetric data reveal a 7-km-deep pull-apart basin along a major left-lateral strike-slip fault in the Hispaniola slope between the 1943 and 1946 rupture planes, suggesting that this section of the plate-interface oblique thrust fault may not be undergoing active collision. We speculate that such noncollisional parts of the plate-interface fault may not be as strongly coupled as the collisional asperities. The occurrence of both the 1943 and 1946 events—the two largest thrust events known to have occurred on the plate-interface fault since at least 1787—suggests that in the northern Caribbean such large thrust earthquakes may typically nucleate only at strongly coupled collisional asperities.

Rakes derived from focal mechanisms that we calculated for the 1943 and 1946 mainshocks (030° and 034°, in map view, respectively) indicate that slip along the plate-interface fault is oblique to the 080–110° trend plate margin in the northeastern Hispaniola–northwestern Puerto Rico area. Much of the plate-boundary slip in this region, however, is partitioned onto the left-lateral, Septentrional fault onshore Hispaniola. This fault probably merges into the south-dipping plate interface along the top of the underthrust Atlantic slab at ~15 km depth beneath northern Hispaniola. The exact location of the downward termination of the Septentrional fault is

Dolan, J. F., and Wald, D. J, 1998, The 1943–1953 north-central Caribbean earthquakes: Active tectonic setting, seismic hazards, and implications for Caribbean–North America plate motions, *in* Dolan, J. F., and Mann, P., eds., Active Strike-Slip and Collisional Tectonics of the Northern Caribbean Plate Boundary Zone: Boulder, Colorado, Geological Society of America Special Paper 326.

unknown, but it probably occurs downdip from the 1943 and 1946 rupture planes. Thus, the rakes derived from the 1943 and 1946 mainshocks show that relative plate motion in the region must be oriented more easterly than ~030°. Furthermore, the oblique-thrust mechanism of the 1943 mainshock indicates that plate motion along the 080°-trending plate boundary off northwestern Puerto Rico must be oriented more northerly than 080°. This is supported by geological data that reveal evidence for a slight component of convergence across this part of the plate margin. Thus, the direction of relative motion between the obliquely subducting North America (Atlantic) plate and the Hispaniola and Puerto Rico blocks of the NCPBZ is between 030° and 080°. These data support several published models that predict east-northeast relative plate motion in the region. Conversely, the earthquake data rule out several models that predict that relative motion between the North America plate and the Puerto Rico block of the NCPBZ plate motion is oriented east-west. The transpressional regime revealed by the earthquake data also preclude models in which Puerto Rico has been proposed to be (1) actively rotating counterclockwise or (2) underlain by an active, south-dipping extensional decollement.

Evidence for a component of oblique left-lateral slip on the plate-interface thrust, coupled with published, preliminary Global Positioning System geodetic data, suggests that a significant portion of the relative motion between the North America plate and the Hispaniola and Puerto Rico blocks of the NCPBZ may be accommodated along the south-dipping plate-interface thrust fault. This fault thus represents a major seismic hazard to the densely populated northern parts of Hispaniola and Puerto Rico. Other major seismic sources in the region include the Septentrional fault, large normal faults in the Mona Passage between Hispaniola and Puerto Rico, and the left-lateral Enriquillo-Plantain Garden strike-slip fault and north-dipping Los Muertos plate-interface thrust fault along the southern edge of the NCPBZ.

The 1943–1953 earthquakes were the most recent major events in a cluster of large events that have occurred on faults along the northern margin of the NCPBZ since 1842. Available historical data suggest that this cluster of activity in the northern deformation belt is anti-correlated—both temporally and geographically—with a similar cluster of earthquakes that occurred between the early 1600s and 1860 on a parallel system of left-lateral strike-slip and thrust faults that stretches along the southern boundary of the NCPBZ. The cause of the intriguing pattern of "deformation switching" remains unknown but represents an important target of future research.

INTRODUCTION

Although the densely populated northern Caribbean islands of Hispaniola and Puerto Rico (Fig. 1) have the longest historical earthquake record in the Americas, dating back to the mid-16th century (Scherer, 1912; Kelleher et al., 1973; Chalas-Jimenez, 1989; W. R. McCann and L. Feldman, written communication, 1995), seismic hazards in the north-central Caribbean region remain relatively poorly understood. One of the main reasons for this is that, although the general tectonic setting of the northern Caribbean plate margin has been known for some time (e.g., Molnar and Sykes, 1969; Bracey and Vogt, 1970; Schell and Tarr, 1978), the major active faults in the plate boundary have not been studied in detail until recently. In many cases, basic faulting parameters, such as location, extent, geometry, kinematics, and earthquake history have not been known. For example, although the Septentrional fault is a major left-lateral strike-slip fault that stretches for several hundred kilometers across the length of northern Hispaniola, it was not fully identified as such until the early 1980s (Mann et al., 1984; Mann and Burke, 1984). The study of Mann et al. (this volume) is the first detailed study to be published on this major fault. The offshore part of the plate boundary in the Hispaniola region was, until recently, even less well studied than the onshore faults. Austin (1983) and Dillon et al. (1992) recognized active thrust faulting off northwestern Hispaniola, but a companion chapter by Dolan et al. (this volume) is the first detailed description of the active structures and tectonics of a 400-km length of the offshore plate boundary between north-central Hispaniola and northwestern Puerto Rico.

Major earthquakes in the region have also received relatively little study until recently. Prior to the 1943–1953 sequence discussed in this chapter, which was studied by Kelleher et al. (1973), only a few historic events have been documented in any detail (e.g., the 1842 northwest Hispaniola earthquake *in* Scherer, 1912; and the 1918 Mona Passage earthquake *in* Reid and Taber, 1919) despite the long historic record in the region.

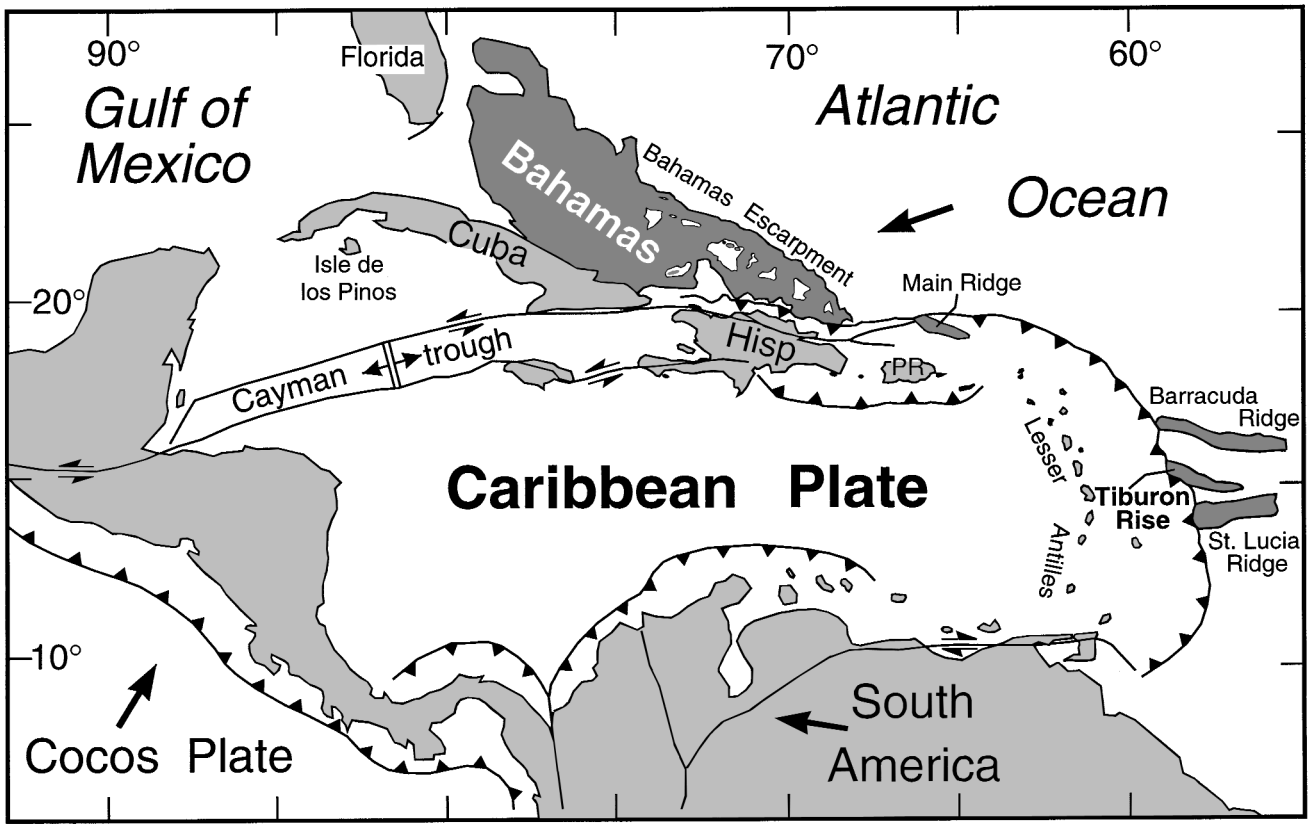

Figure 1. Location map of the Caribbean region (after Mann et al., 1984). Arrow in northeast denotes best estimate of northern Caribbean plate boundary zone (NCPBZ)–North America (Atlantic) plate relative motion vector determined in this study. Other arrows show plate motion directions from Mann et al. (1984). Westward motion of both the North America and South America plates relative to the Caribbean plate south of the NCPBZ results in predominantly left-lateral strike-slip motion along the northern boundary, and right-lateral strike-slip motion along the southern margins of the Caribbean plate, respectively; the Caribbean plate is stationary relative to a hot-spot reference frame. Dark shading denotes Bahamas carbonate province. PR is Puerto Rico; Hisp is Hispaniola.

Furthermore, paleoseismological studies have only just begun in the region. Prentice et al. (1993) published the first paleoseismologic data from the northern Caribbean based on their trench studies of the Septentrional fault in north-central Hispaniola (see also Mann et al., this volume).

Another major factor in our lack of knowledge about the seismotectonics and seismic hazards of the northern Caribbean is the fact that relatively few large earthquakes have occurred along the plate boundary during the instrumental era. This chapter focuses on the two largest instrumentally recorded earthquakes—the 1943 northern Mona Passage earthquake and the 1946 northeastern Hispaniola earthquake—that have occurred in the northern Caribbean region. In this study we (1) examine the relationship between these earthquakes and zones of active, collisional underthrusting along the northern Caribbean plate boundary zone (NCPBZ); (2) discuss the significance of these collisions for seismic hazard assessment in the region; (3) use the earthquake focal mechanisms that we have determined to address the long-standing disagreement about relative plate motions in the north-central Caribbean region; and (4) discuss the 1943 and 1946 earthquakes in the context of the temporal and spatial patterns of strain release along the NCPBZ.

GEOLOGIC SETTING

As a result of long-lived and ongoing interactions with the surrounding North America and South America plates, the margins of the Caribbean plate are extremely complex, both structurally and kinematically (Fig. 1). The north-central Caribbean islands of Hispaniola, Puerto Rico, and Cuba represent the dismembered remnants of one or more Cretaceous to Eocene island arcs that developed above a southwest-dipping subduction zone (Pindell and Barrett, 1991). Since middle Eocene time both the North and South America plates have moved westward relative to the Caribbean plate (in a hot-spot reference frame), with active arc volcanism occurring in the Lesser Antilles in response to west-dipping subduction of Atlantic oceanic lithosphere beneath the Caribbean plate (Pindell and Barrett, 1990). This relative motion

results in predominantly left-lateral motion along the northern boundary of the Caribbean plate (Molnar and Sykes, 1969; Bracey and Vogt, 1970; Schell and Tarr, 1978; Mann et al., 1984, 1990; Pindell and Barrett, 1990). Despite a general consensus on this point, both the direction and velocity of Caribbean–North America relative plate motion have been the subject of long-standing debate, with a range of proposed directions from 090° to 065°, and a range of proposed rates from 11 to 37 mm/yr (Molnar and Sykes, 1969; Jordan, 1975; Minster and Jordan, 1978; Sykes et al., 1982; Stein et al., 1988; DeMets et al., 1990; DeMets, 1993; Deng and Sykes, 1995; Farina et al., 1995).

Global plate motion model NUVEL-1, which is relatively poorly constrained for the northern Caribbean region, yielded near east-west relative plate motion at an overall rate of ~11 ± 3 mm/yr in the Hispaniola region (De Mets et al., 1990; DeMets, 1993). Analysis of magnetic lineations in the Cayman trough suggests that the long-term average plate motion rate is ~15 mm/yr along the Caribbean–North America plate boundary (Rosencrantz et al., 1988). However, more recent analysis of only post-early Miocene to Holocene magnetic lineations yielded a slightly faster estimate of ~19–22 mm/yr (Rosencrantz, 1995). MacDonald and Holcombe (1978) obtained a similar estimate (20 ± 4 mm/yr) using magnetic anomaly data for the past 2.3 Ma. Sykes et al. (1982) and Rosencrantz and Mann (1991), however, argued that these values underestimate total Caribbean–North America motion because some plate-boundary slip bypasses the northern part of the Cayman trough and is accommodated along the left-lateral Enriquillo-Plantain Garden fault zone in Jamaica and southern Hispaniola (Fig. 1) (Mann et al., 1984). Sykes et al. (1982), using the configuration and thermal character of the subducted Atlantic slab and slip vectors from plate-boundary earthquakes in the eastern and northeastern Caribbean, estimated a rate of 37 ± 5 mm/year along an azimuth of 065°. Deng and Sykes (1995) argued that this rate is probably an overestimate, and they use their calculated Euler pole together with GPS geodetic data from Dixon (1993) to estimate a rate of 20–30 mm/yr, with a best estimate of 23 mm/yr, along an azimuth of 070° in the north-central Caribbean. Dewey and Suarez (1991) obtained a rate of 27 mm/yr by assuming that the Caribbean is fixed with respect to a hotspot reference frame. Preliminary GPS geodetic data from a network of northern Caribbean stations yielded an overall Caribbean–North America plate relative plate motion rate of ~24 mm/yr in the Hispaniola region (Farina et al., 1995; Dixon et al., 1998). Collectively, these estimates indicate that the relative motion rate between the Caribbean and North America plates is ~20–25 mm/yr.

In the north-central Caribbean the plate boundary forms a complex, 250-km-wide zone of deformation known as the northern Caribbean plate boundary zone (NCPBZ) (Fig. 2; Mann et al., 1984). The NCPBZ in this region is highlighted by two major zones of deformation that occur along the northern and southern boundaries of the islands of Puerto Rico and Hispaniola (Mann et al., 1984, 1990; Burke, 1988). The northern zone, which is the focus of this study, is associated with south-dipping underthrusting of Atlantic oceanic lithosphere of the North America plate (McCann and Sykes, 1984; McCann and Pennington, 1990; Deng and Sykes, 1995; Dolan et al., this volume), whereas the southern deformation zone involves north-dipping underthrusting of Caribbean lithosphere at the Los Muertos trench (Ladd and Watkins, 1978; Byrne et al., 1985; Ladd et al., 1990; Dillon et al., 1994; Dolan et al., this volume). The northern deformation zone exhibits well-developed strain partitioning in Hispaniola (Dolan et al., this volume), with much of the plate-boundary, left-lateral strike-slip motion accommodated on the Septentrional fault system (Mann et al., 1984, 1990, this volume; Calais et al., 1992; Prentice et al., 1993). The Septentrional fault system extends westward into the Oriente fault zone, which forms the northern boundary of the Cayman trough pull-apart basin (Fig. 1) (Calais et al., 1989, 1992, this volume; Edgar, 1991; Rosencrantz and Mann, 1991). East of Hispaniola, left-lateral strike-slip motion occurs on the eastern Septentrional and northern Puerto Rico slope fault zones north of Puerto Rico (Masson and Scanlon, 1991; Dolan et al., this volume). Development of a small accretionary prism offshore northern Hispaniola attests to an active component of convergence across the plate boundary in the Hispaniola region (Austin, 1983; Dillon et al., 1992; Dolan et al., this volume).

Hispaniola–Bahamas collision zone

One of the most notable features of the plate boundary in the Hispaniola area is a zone of active collision between Hispaniola and high-standing carbonate banks of the southeastern Bahamas. SeaMARC II side-scan sonar data collected offshore northern Hispaniola reveal that two Bahamas carbonate banks are actively colliding with Hispaniola over a front more than 200 km long (Dolan et al., this volume). The collision, which extends along the plate boundary between ~70° 00′W and 68° 30′W, involves the southern margins of Silver and Navidad banks, which rise 5.5 km above the surrounding Atlantic abyssal plain (Fig. 2). The collision is best illustrated offshore of north-central Hispaniola, between 70° 05′W and 69° 42′W, where Silver Spur, a bathymetrically high-standing ridge of Silver bank carbonate, impinges on the Hispaniola slope and projects beneath the Rio San Juan Peninsula of the Dominican Republic (Dolan et al., this volume). Throughout the rest of the collision zone, high-reflectivity carbonate bank material directly abuts lower reflectivity material of the Hispaniola slope.

To the west of the collision zone, the high-standing Mouchoir bank is separated from the deformation front at the base of the northern Hispaniola slope by the 20–30-km-wide Hispaniola basin (Fig. 3). Thus, this part of the Hispaniola margin is not experiencing active collision with the buoyant Bahamas block. In contrast, to the east of the Silver-Navidad bank collision zone, the Bahamas ridge has already been obliquely subducted beneath the Puerto Rico block of the NCPBZ (Dolan et al., this volume). These major differences in the structural style of the plate margin are due to the diachronous nature of the Bahamas collision—the

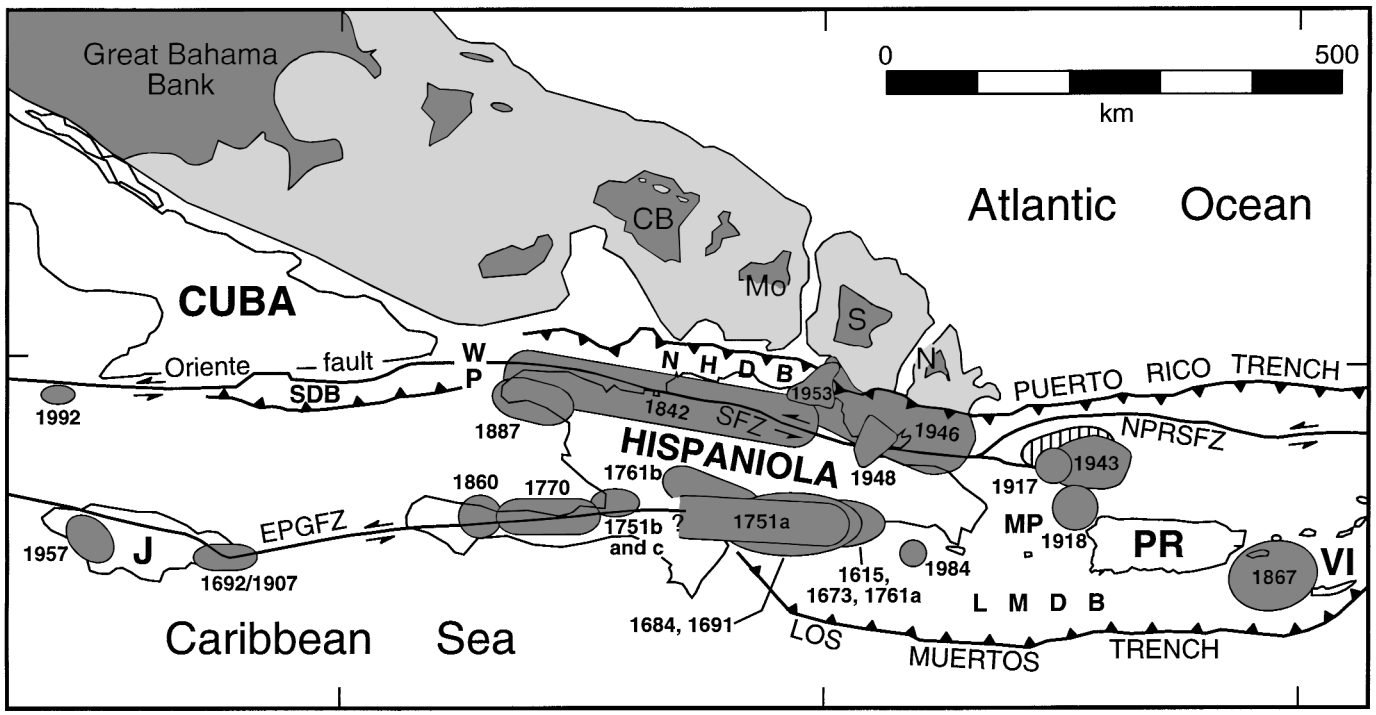

Figure 2. Neotectonic map of north-central Caribbean showing great width (250 km) and complexity of the northern Caribbean plate boundary zone (NCPBZ) as well as the location of major historical earthquakes (year of occurrence shown for each event; 1751a event occurred in October and 1751b earthquake occurred in November). Geologic data compiled from Dolan et al. (this volume), Mann et al. (1984, this volume), Masson and Scanlon (1991), Edgar (1991), Dillon et al. (1992), and Case and Holcombe (1980). Earthquake data compiled from Kelleher et al. (1973), Chalas-Jimenez (1989), McCann and Pennington (1990), and Mann et al. (this volume). CB is Caicos bank; EPGFZ is Enriquillo-Plantain Garden fault zone; J is Jamaica; LMDB is Los Muertos deformed belt; Mo is Mouchoir bank; MP is Mona Passage; N is Navidad bank; NHDB is northern Hispaniola deformed belt; NPRSFZ is northern Puerto Rico slope fault zone; PR is Puerto Rico; S is Silver bank; SDB is Santiago deformed belt; SFZ is Septentrional fault zone; VI is Virgin Islands; WP is Windward Passage.

generally westward motion and more northwesterly strike of the Bahamas ridge relative to the NCPBZ results in a westward-younging zone of active collision. Based on this reasoning, Dolan et al. (this volume) proposed that the Bahamas ridge collision has progressed much farther beneath northern Mona Passage than it has within the Silver-Navidad collision zone. They suggest that a zone of relatively shallow bathymetry in the northern part of Mona Passage (their Mona block) is the sea-floor manifestation of ongoing collisional underthrusting of an already subducted southeastern Bahamas bank, which they named Mona bank.

Dolan et al. (this volume) also used recent seismicity data to construct a structure-contour map on the top of the south- to south-southwest–dipping, underthrust Atlantic (North America) slab (Figs. 3 and 4). The strike and dip of the slab changes markedly at the proposed Mona bank collision. North of the Virgin Islands, at ~65° W, local network data reveal that the slab dips 45° south (Frankel, 1982; McCann and Sykes, 1984; Fischer and McCann, 1984). The dip of the slab shallows markedly westward toward the postulated Mona bank collision zone. At the locus of the collision at 67° 30′ the slab dips ~25° south (Fig. 3; Dolan et al., this volume). West of the collision the strike of the shallow part of the slab changes to west-northwest. Along the Silver-Navidad collision zone in northeastern Hispaniola the shallow part of the underthrust slab dips ~30° south-southwest.

THE 1943–1953 NORTH-CENTRAL CARIBBEAN EARTHQUAKE SEQUENCE

On July 29, 1943, a major earthquake occurred offshore of northwestern Puerto Rico (Fig. 5) (Kelleher et al., 1973). This event, which we refer to as the northern Mona Passage earthquake, was the first in a sequence of large earthquakes that struck the north-central Caribbean region during the decade 1943–1953. Three years after the northern Mona Passage earthquake, the region experienced an even larger event when, on August 4, 1946, a great earthquake occurred beneath the coast of northeastern Hispaniola, ~200 km west of the 1943 epicenter (Fig. 5) (Lynch and Bodle, 1948; Small, 1948; Kelleher et al., 1973).

In the following discussion of these earthquakes and their aftershocks we use the surface-wave magnitude (M_s) estimates of

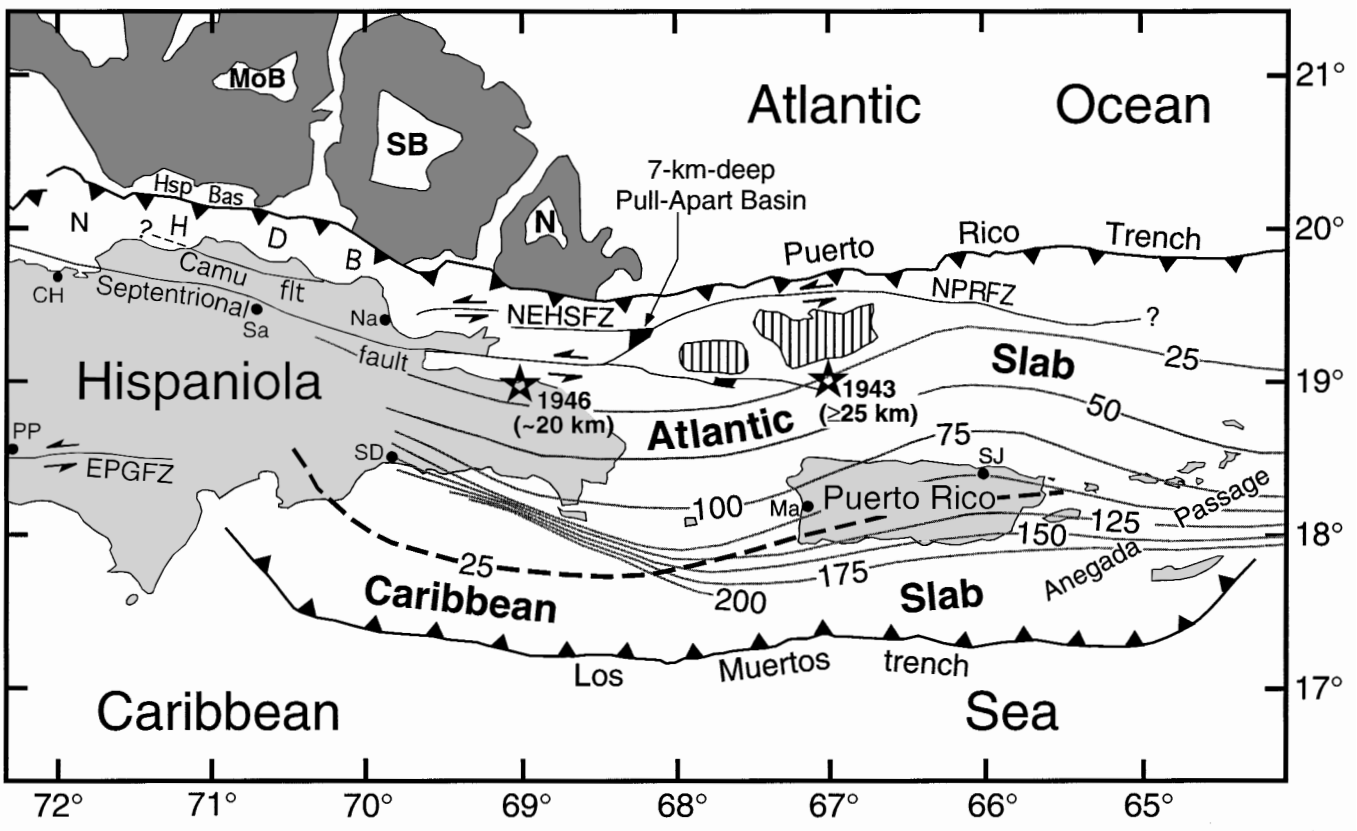

Figure 3. Structure contour map of underthrust Atlantic and Caribbean slabs in north-central Caribbean region. Depth contour interval is 25 km. Contours are from Dolan et al. (this volume) and are based on cross sections of recent seismicity that occurred between 1962 and 1994 and that were taken from the International Seismological Centre (ISC) Catalog of Earthquakes (1994). Slab contours shown as solid gray lines are constructed along the top of a south-dipping zone of seismicity interpreted to represent the top of the underthrust slab of Atlantic oceanic lithosphere of the North America plate. Slab contour shown by black dashed line is constructed along top of north-dipping upper limit of a north-dipping zone of seismicity thought to represent the top of underthrust Caribbean lithosphere. Note the epicenters and approximate focal depths of the 1943 northern Mona Passage and 1946 northeastern Hispaniola earthquakes, which are discussed in this chapter. The minimum focal depth shown for the 1943 event was determined in this study. The approximate focal depth for the 1946 event is from Russo and Villaseñor (1995). Dark shading denotes limits of Bahamas carbonate province (from Dolan et al., this volume). Black circles show locations of major cities. CH is Cap Haitien, Haiti; EPGFZ is Enriquillo-Plantain Garden fault zone from Mann et al. (1984); Hsp Bas is Hispaniola basin; Ma is Mayaguez, Puerto Rico; MoB is Mouchoir bank; N is Navidad bank; Na is Nagua, Dominican Republic; NEHSFZ is northeast Hispaniola slope fault zone; NHDB is northern Hispaniola deformed belt, which includes the northern Hispaniola accretionary prism; NPRFZ is northern Puerto Rico fault zone compiled from Masson and Scanlon (1991) and Dolan et al. (this volume); PP is Port-au-Prince, Haiti; Sa is Santiago, Dominican Republic; SB is Silver bank; SD is Santo Domingo, Dominican Republic; SJ is San Juan, Puerto Rico. Irregular black areas northeast of Hispaniola denote pull-apart basins at left-steps along the Septentrional fault system (from Dolan et al., this volume).

Kelleher et al. (1973), despite the fact that subsequent studies suggest that these estimates are systematically too large. For example, Kelleher et al. (1973) estimated an M_s of 8.1 for the 1946 mainshock, whereas Abe (1981) estimated M_s 8.0, and both Pacheco and Sykes (1992) and Russo and Villaseñor (1995) estimated M_s 7.8. Nevertheless, for the sake of consistency we use the Kelleher et al. (1973) estimates because only their study estimated magnitudes for all of the events we discuss below. Where available, we include more recent magnitude estimates in parentheses after the Kelleher et al. (1973) estimate. For example, the 1946 northeast Hispaniola earthquake is referred to as M_s 8.1 (Kelleher et al., 1973; M_s 8.0 in Abe, 1981; M_s 7.8 in both Pacheco and Sykes, 1992, and Russo and Villaseñor, 1995); the 1943 northern Mona Passage earthquake is referred to as M_s 7.8 (Kelleher et al., 1973; M_s 7.7 in Abe, 1981; M_s 7.5 in Pacheco and Sykes, 1992).

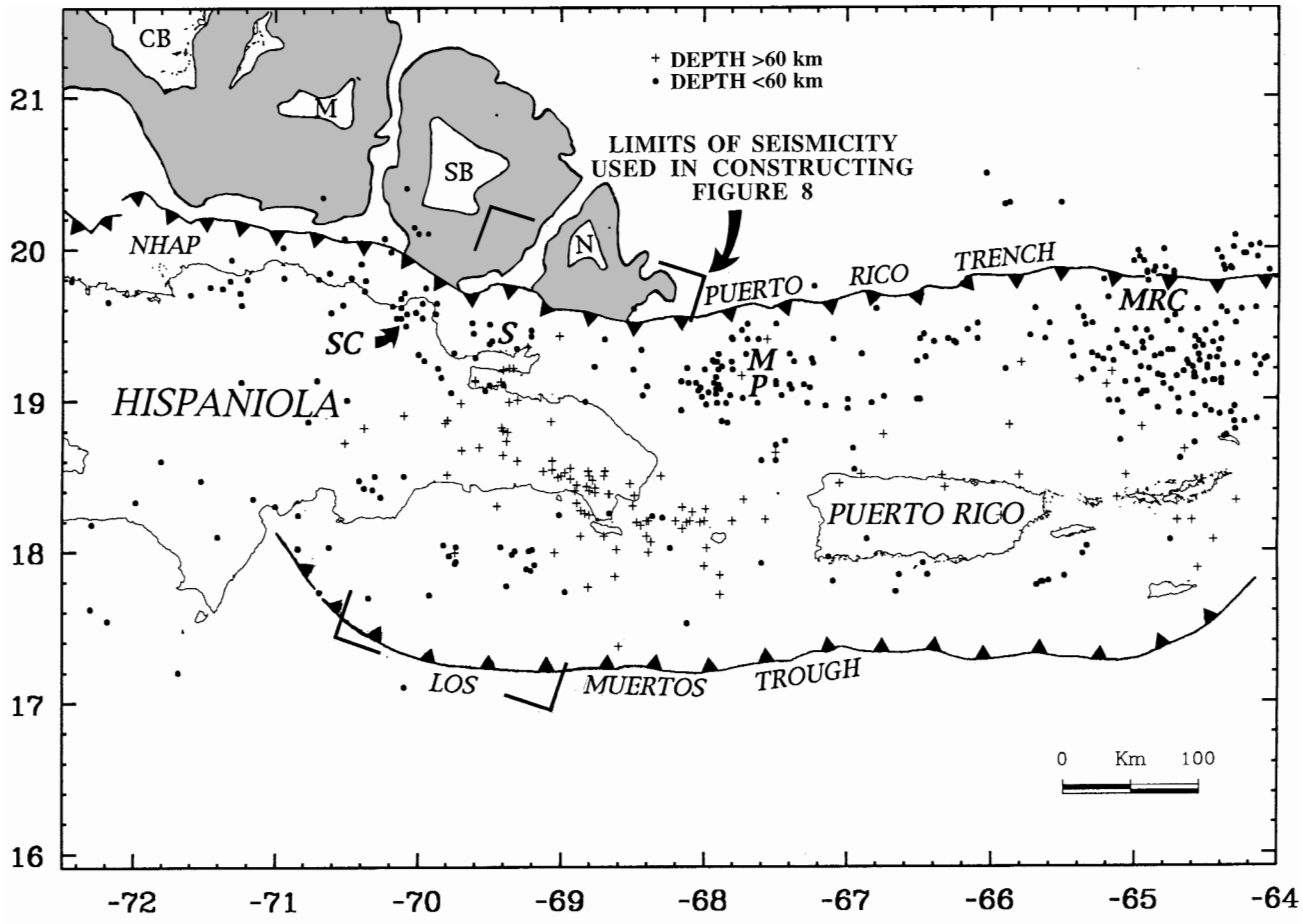

Figure 4. Map of recent seismicity (1962–1992) from ISC catalog (slightly modified from Dolan et al., this volume). Gray shading denotes limits of southeastern Bahamas carbonate province. Box denotes limits of seismicity used to construct cross section shown in Figure 8. CB is Caicos bank; M is Mouchoir bank; MP is Mona Passage seismicity cluster; MRC is Main Ridge seismicity cluster; N is Navidad bank; NHAP is northern Hispaniola accretionary prism; S is Samana seismicity cluster; SB is Silver bank; SC is Sosua seismicity cluster. See Dolan et al. (this volume) for detailed discussion of seismicity distribution.

The north-central Caribbean region was first settled permanently during Columbus's second voyage in 1494, and consequently the area has the longest historical earthquake record in the New World, dating back to the mid-16th century (Scherer, 1912; Kelleher et al., 1973; Chalas-Jimenez, 1989; W. R. McCann and L. Feldman, written communication, 1995). Based on this historical record, the 1943 and 1946 mainshocks appear to be the largest earthquakes that have struck the northeastern Hispaniola–Mona Passage–northwestern Puerto Rico area since at least November 2, 1564, when a large earthquake destroyed the northern Hispaniola cities of Santiago and La Vega (Scherer, 1912; McCann and Pennington, 1990; W. R. McCann and L. Feldman, written communication, 1995).

Despite the large magnitudes of the 1943 and 1946 earthquakes, they have been studied little; prior to this study and the recent study by Russo and Villaseñor (1995), neither their focal mechanisms or focal depths had been determined. To better understand the seismotectonics and seismic hazards of the area, we have determined focal mechanisms for the six largest earthquakes from the 1943–1953 sequence, including both the 1943 and 1946 mainshocks, and the four largest aftershocks of the 1946 event (August 8, 1946; October 4, 1946; April 21, 1948; and May 31, 1953) (Figs. 6 and 7). We initially determined the range of possible first motion mechanisms for each event (Fig. 6). For all but one of the six events (the M_s 7.6 event on August 8, 1946, discussed in a following section), one nodal plane is well constrained to strike west-northwest and dip ~70–75° north-northeast. The best-fitting conjugate planes are consistent with shallowly dipping thrust faulting with fault dips ranging from south-southeast to due west. To resolve the strike of the shallowly dipping planes, we used the well-constrained, steeply dipping nodal planes as a constraint in body-waveform inversions to determine the conjugate plane most consistent with available P and S bodywaves for each earthquake. The detailed results of our waveform inversions will be reported in detail in a later paper by Wald and Dolan. Because the number of high-qual-

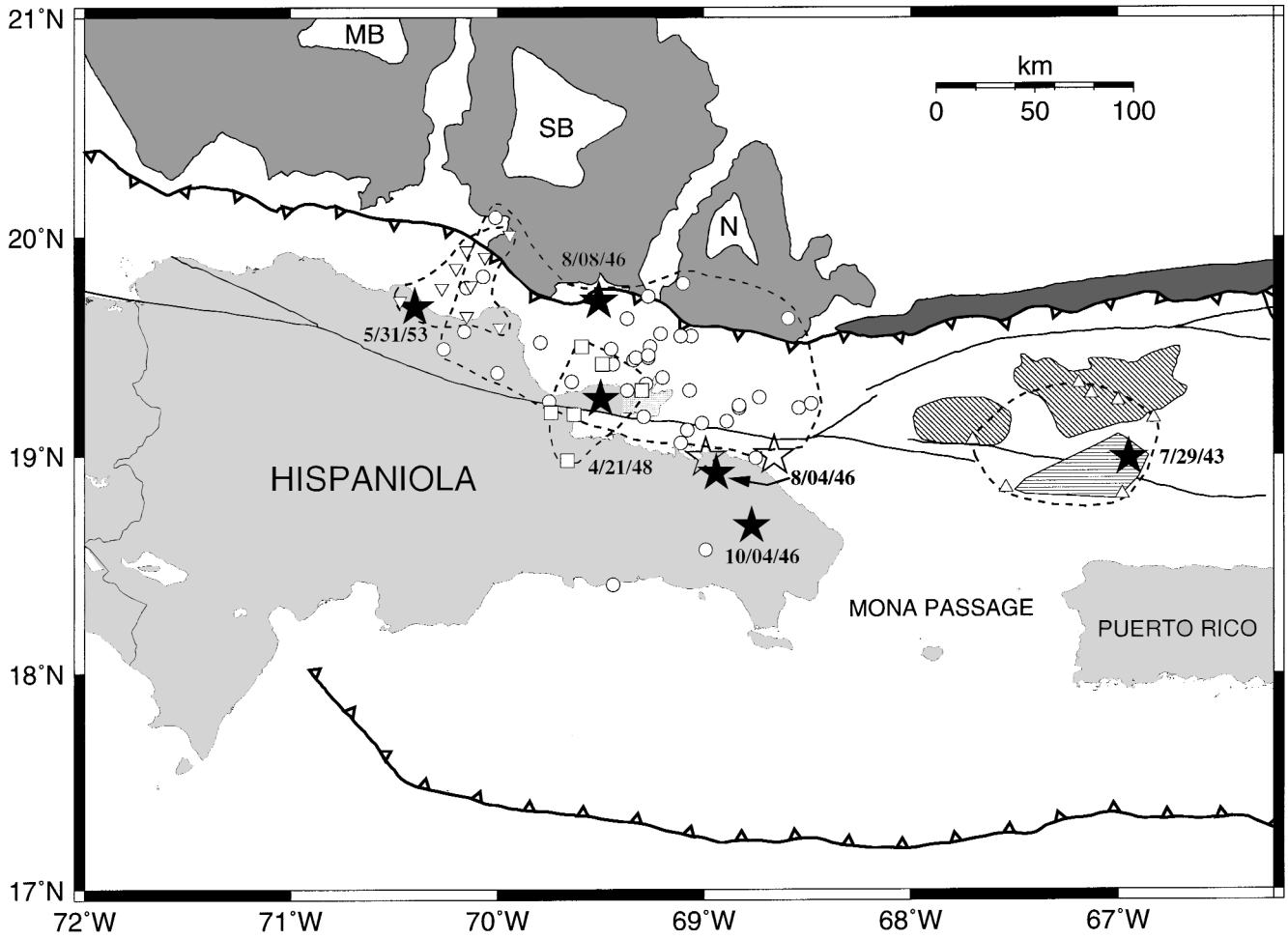

Figure 5. Relocated mainshocks and aftershocks of the 1943 northern Mona Passage earthquake and the 1946 northeastern Hispaniola earthquake from Kelleher et al. (1973). Mainshocks and large aftershocks, including the four largest aftershocks of the 1946 event (August 8, 1946; October 4, 1946; April 21, 1948; and May 31, 1953), are denoted by black stars. Smaller aftershocks denoted by various open symbols. Open stars show relocations of the 1946 mainshock and October 4, 1946, aftershock by Russo and Villaseñor (1995). Russo and Villaseñor's (1995) relocation of the 1946 mainshock epicenter does not change significantly from that of Kelleher et al. (1973). Russo and Villaseñor's (1995) relocation of the October 4, 1946, aftershock does change significantly, however, shifting 20 km to the north-northeast of the Kelleher et al. (1973) location. Note coincidence of 1946 aftershock zone with the 200-km-long Silver-Navidad bank collision zone. Solid lines with teeth are deformation fronts of the Puerto Rico trench–northern Hispaniola accretionary prism system (north of Hispaniola and Puerto Rico) and the Los Muertos trench accretionary prism (south of the islands). Dark shading denotes limits of southeast Bahamas carbonate banks (Dolan et al., this volume). The two irregular zones of diagonal hatching north-northwest of Puerto Rico represent areas of anomalously shallow bathymetry ("anomalous block" of McCann and Sykes, 1984). Dolan et al. (this volume) interpret these shallow regions as the surficial manifestation of collisional underthrusting of a southeastern Bahama bank, which they named Mona bank. The triangular zone of horizontal hatching north of Puerto Rico denotes the rupture plane of the 1943 northern Mona Passage earthquake, as determined in this study. Note the proximity of the 1943 rupture zone to the proposed Mona bank collision. Solid lines without teeth are major, left-lateral strike-slip faults of the Septentrional fault system (SFS). Note the bifurcation of the SFS in the northern Mona Passage and the divergence of two eastern strands around the Mona bank zone of anomalously shallow bathymetry. Dark shading represents basinal sediments in the Puerto Rico trench. Geologic data compiled from Dolan et al. (this volume), Mann et al. (1984), Dillon et al. (1991), Edgar (1991), Masson and Scanlon (1990), and Case and Holcombe (1980). MB is Mouchoir bank; N is Navidad bank; SB is Silver bank.

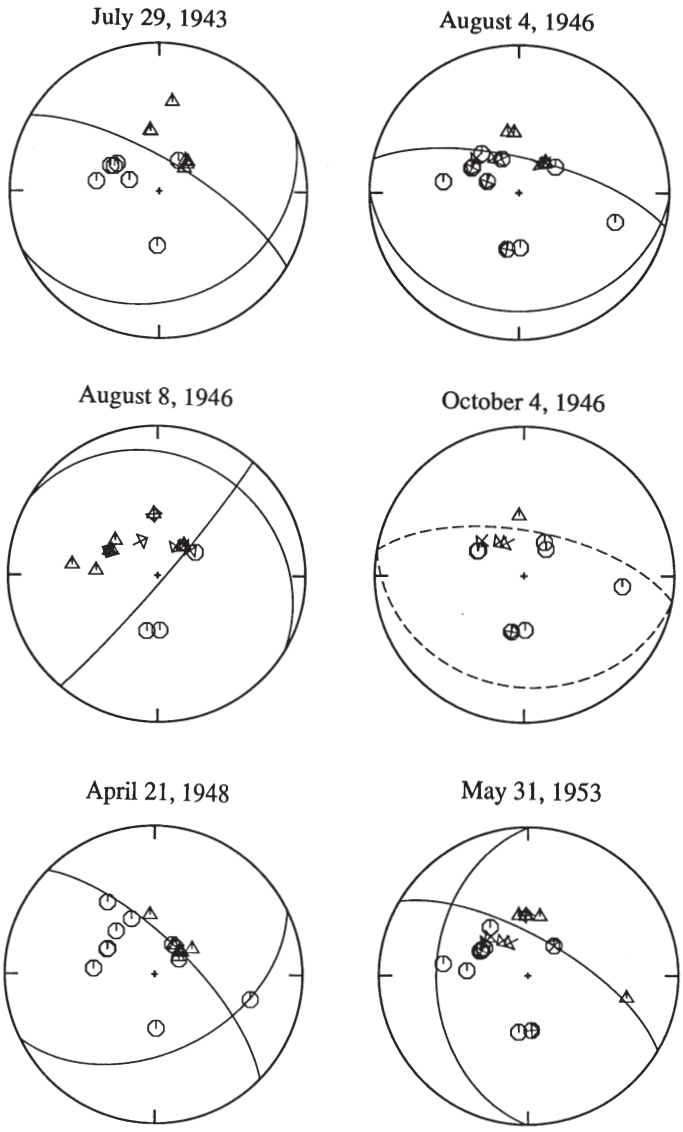

Figure 6. Focal mechanisms determined in this study for the six largest earthquakes in the 1943–1953 north-central Caribbean sequence (lower hemisphere projections). Mechanisms for July 29, 1943, northern Mona Passage mainshock; the August 4, 1946, northeastern Hispaniola mainshock; and the May 31, 1953, Sosua earthquake (an aftershock of the 1946 mainshock) show the results of our body-waveform inversions. The mechanisms for the other three events are P-wave first-motion focal mechanisms. Circles, triangles, and plus symbols denote dilational, nodal, and compressional arrivals, respectively.

ity waveforms is limited for this time period, constraining one nodal plane based on the more numerous polarity observations (for the steeply dipping plane) is beneficial in adding stability to the waveform inversion. We used the methodology of Kikuchi and Kanamori (1991), which we modified to accommodate both the nodal plane constraint and the varied mechanical and electromagnetic instrument types available during this time period.

Our body-waveform inversions were most successful for three events—the 1943 and 1946 mainshocks and the 1953 Silver Spur aftershock (discussed in following sections)—and these are shown in Figures 6 and 7. The focal mechanisms shown for the other three events—the two large 1946 aftershocks and the April 21, 1948, Samana earthquake—are first-motion mechanisms only. In general it proved difficult to accurately constrain the exact strike of the shallowly dipping thrust plane for these events; rotating the strike of this plane by as much as 60°, from near east-west to north-northwest, does not result in significantly different waveform results. For these events we assumed that the strike of the shallowly dipping plane, which we interpret as the faulting plane, was parallel to the west-northwest–trending long axis of the 1946 aftershock zone (Fig. 5). Given the parallelism of the aftershock zone with the ~275–290° orientation of all major active faults in this part of the plate boundary, including the Septentrional strike-slip fault and the offshore deformation front, we feel that this is an appropriate assumption. In the following section we discuss each of the six earthquakes we studied in detail.

1946 northeastern Hispaniola earthquake

The tectonic setting of the 1946–1953 northeastern Hispaniola earthquake sequence is somewhat better defined than that for the 1943 northern Mona Passage earthquake, and we therefore discuss the northeastern Hispaniola earthquake and its aftershocks first. The M_s 8.1 mainshock (Kelleher et al., 1973; M_s 8.0 in Abe, 1981; M_s 7.8 in both Pacheco and Sykes, 1992, and Russo and Villaseñor, 1995) occurred on August 4, 1946, and was followed by numerous small to moderate aftershocks. Kelleher et al. (1973) relocated 53 of the largest aftershocks. Their relocated aftershocks define a 195-km × 95-km zone that extends west-northwest along the northern slope of Hispaniola, basically between the offshore deformation front and the coast of Hispaniola; several early aftershocks (i.e., before the first large aftershock on August 8, 1946) extend northward almost to the deformation front (Fig. 5). Russo and Villaseñor (1995) also relocated 61 aftershocks of the 1946 mainshock. Their distribution is generally similar to that shown by Kelleher et al. (1973), although the spatial clustering of their relocated events is somewhat tighter than that shown by Kelleher et al. (1973). The aftershock zone (as defined both by Kelleher et al., 1973, and Russo and Villaseñor, 1995) exactly matches the limits of the Hispaniola–Bahamas collision zone as defined by SeaMARC II sidescan sonar and seismic reflection data, from the southeast edge of Navidad bank to the western margin of Silver Spur (Fig. 5; Dolan et al., this volume). Our body-waveform inversions yielded a focal mechanism for the 1946 mainshock that shows that it was a thrust fault event that occurred on either a shallowly south-dipping plane that strikes 085°, or a steeply northeast-dipping plane that strikes 110° (Fig. 6).

As noted above, the strike of the shallowly dipping plane is rather poorly constrained. Several lines of evidence, however, show that the event occurred on the shallowly south-dipping plane. The great width of the 1946 aftershock zone relative to its length is incompatible with a steeply dipping fault plane and

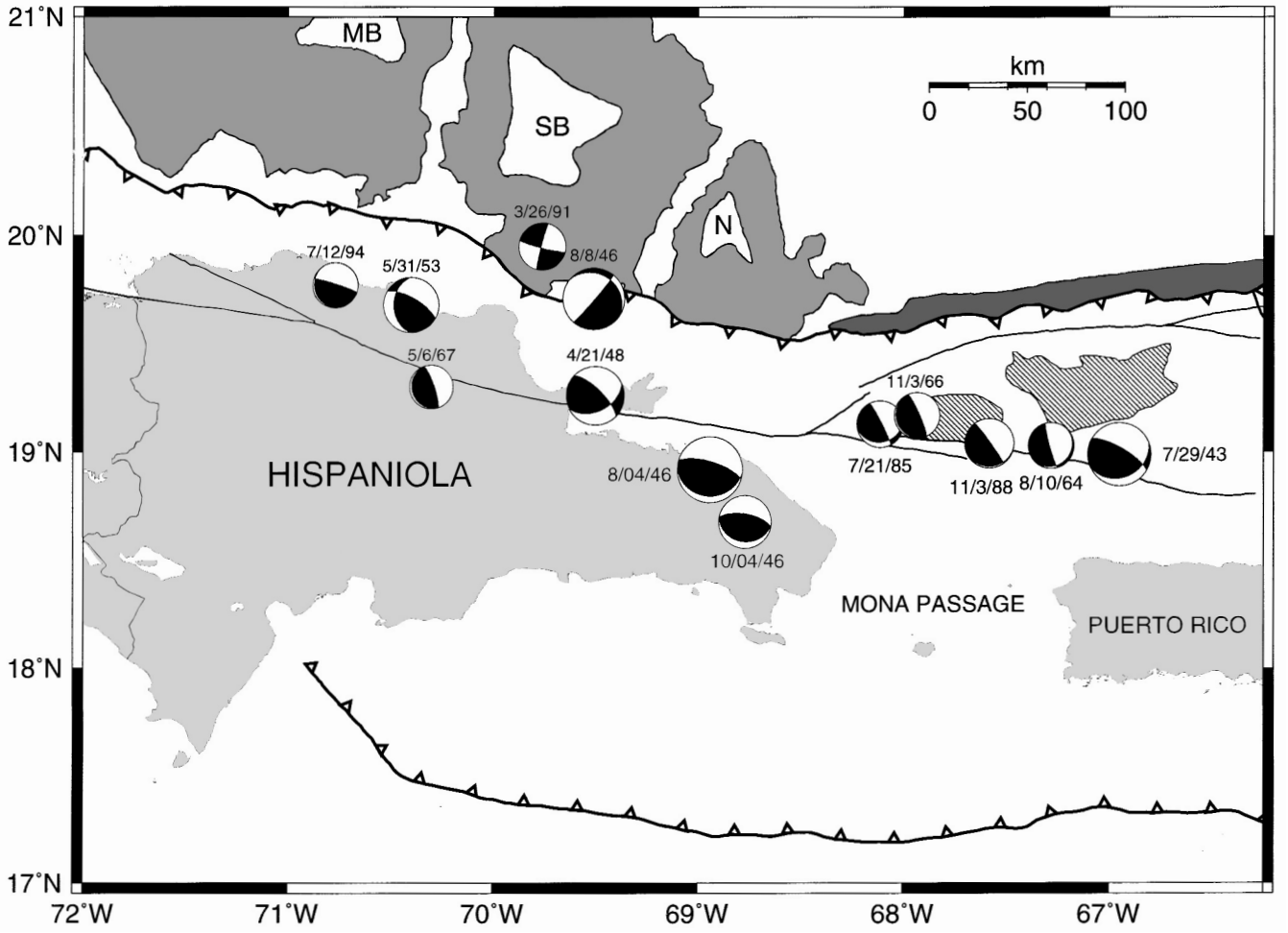

Figure 7. Map of the six focal mechanisms determined in this study (large mechanisms) as well as seven other instrumentally recorded events (small mechanisms) compiled from Molnar and Sykes (1969); Kafka and Weidner (1979); and Harvard Centroid Moment Tensor Catalog (1994). Focal mechanisms are lower hemisphere projections; black areas denote compression, white areas show dilation. MB is Mouchoir bank; N is Navidad bank; SB is Silver bank.

shows that the earthquake occurred along the shallowly dipping nodal plane (Fig. 5). Furthermore, the coincidence of the northern edge of the aftershock zone with the collisional deformation front indicates that the rupture plane dipped south beneath Hispaniola. Finally, Russo and Villaseñor's (1995) relocated aftershocks define a gently south- to southwest-dipping plane that extends from the deformation front toward the mainshock focus (Fig. 8). In our body-waveform inversion, the depth of the mainshock focus is relatively poorly constrained but was between 15 and 40 km. Russo and Villaseñor (1995) estimate a depth of ~20 km. The dip of the shallowly south-dipping nodal plane on our focal mechanism is 23° (Fig. 6). If we fit a plane extending from the deformation front at the sea floor, through the south-dipping cluster of aftershocks, to the mainshock focus at 20-km depth, we calculate a dip of the fault plane of ~20°, nearly identical to that derived from our focal mechanism (Fig. 8). The mainshock focus occurred near the downdip (southern) edge of the rupture plane, near the southeastern edge of the aftershock zone. These data suggest that the 1946 mainshock rupture propagated updip and to the west-northwest.

In addition to the shallow, gently south-dipping cluster of aftershocks extending downdip to the mainshock focus, Russo and Villaseñor (1995) also relocated 22 deeper 1946 events that they interpret as aftershocks (all events relocated by Russo and Villaseñor, 1995, shown by triangles in Fig. 8). These deep 1946 events occurred in a diffuse zone that encompassed most of the thickness of the underthrust Atlantic slab. As can be seen from Figure 8, the deep 1946 events are part of a long-lived sequence of intraplate seismicity associated with the underthrust Atlantic slab, probably related to bending stresses within the slab (and possibly also deep extension as the slab sinks, as suggested by McCann and Sykes, 1984). In contrast, the shallow, south-dipping zone of aftershocks was temporally anomalous, and relatively few events have occurred in this region during the past

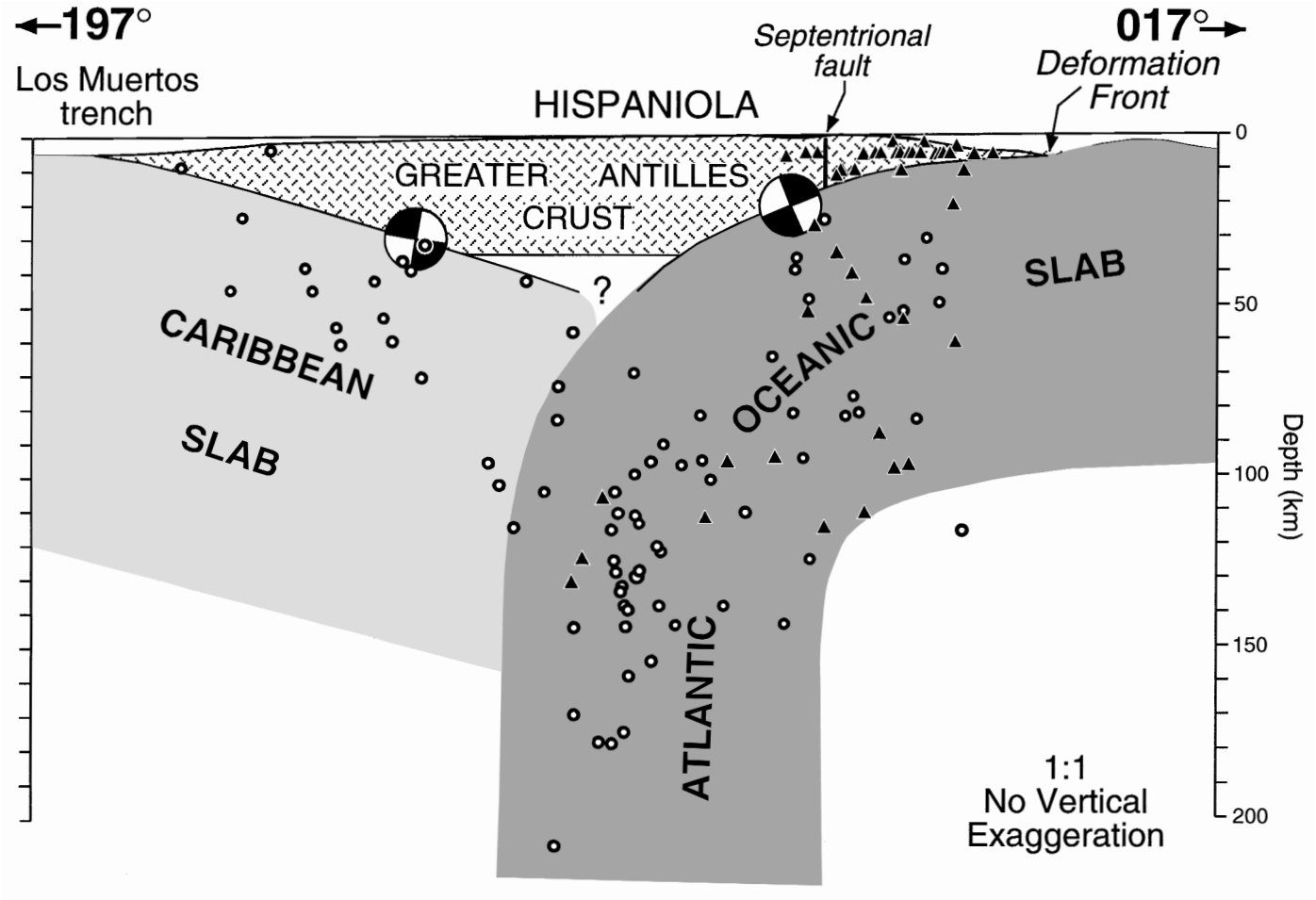

Figure 8. Cross section oriented 017° showing recent seismicity in the region of the 1946 northern Hispaniola earthquake (modified from Dolan et al., this volume). Heavy line at top of figure represents bathymetry-topography along center line of cross section. No vertical exaggeration. Note that although profile is oriented approximately perpendicular to regional strike, the profile is oblique to some tectonic and topographic features. Shading denotes approximate thickness of different lithospheric plates, based on assumptions that the Atlantic plate consists of normal oceanic lithosphere ~90–100 km thick and that the thicker crust of the Caribbean plate (Edgar et al., 1971; Case et al., 1990) results in a thicker lithosphere. All seismicity data from National Earthquake Information Center Catalog of Earthquakes (1994) 1962–1992 except as noted. Only earthquakes with well-defined depths have been used; earthquakes assigned default depths of 10 km and 33 km were not used in constructing these sections. Triangles denote 1946 aftershocks relocated by Russo and Villaseñor (1995). Note the well-defined, shallowly southwest-dipping zone of 1946 aftershocks. Also note the diffuse, southward-dipping zone of aftershocks associated with underthrusting of Atlantic oceanic crust and Bahamas platform carbonates. These shallow aftershocks extend almost to the deformation front defined by the SeaMARC II data, suggesting that the 1946 mainshock may have locally ruptured all the way to the sea floor in this collisional region of enhanced mechanical coupling. Note the near-total absence in the recent ISC data of well-located earthquakes associated with the south-dipping plate interface between underthrust Atlantic oceanic crust and Hispaniola that ruptured during the 1946 northeastern Hispaniola earthquake. In contrast, the relocated 1946 aftershocks define a shallowly southwest-dipping plane approximately along our proposed 1946 mainshock rupture surface. Note that the deeper relocated 1946 aftershocks occur within a long-lived zone of deep background seismicity defined by the past 30 yr of ISC catalog data. The gentle southwestward dip of the shallow 1946 aftershock zone, coupled with its location north of the Septentrional fault, confirms that the 1946 mainshock occurred along the shallowly southwest-dipping plate interface, rather than along a strand of the Septentrional fault system as has been suggested by Russo and Villaseñor (1995). Focal mechanisms are shown for the 1946 northeast Hispaniola mainshock (from this study) and for the M_s 6.7 earthquake of June 24, 1984, which occurred along the north-dipping Los Muertos trench zone of underthrusting (from Byrne et al., 1985).

30 yr. These observations indicate that the shallow aftershocks were directly related to afterslip on or near the rupture plane of the 1946 mainshock.

Russo and Villaseñor (1997) note that the deep aftershock activity increased 15-fold in the year after the 1946 mainshock and suggest that this indicates that the earthquake occurred on a steeply northeast-dipping plane. There are two major problems with this interpretation. First, it does not explain the shallow, south-dipping aftershock zone. Second, it merely suggests mechanical continuity of the slab, not necessarily that the deep slab ruptured in the earthquake. Such mechanical continuity of the slab is entirely consistent with our model, and in fact would be predicted by it. We would expect that as the Atlantic slab underwent 5–10 m of coseismic underthrusting during the 1946 mainshock, the slab would respond to the consequent change in internal stresses by producing the intraslab earthquakes observed as Russo and Villaseñor's deep "aftershocks." We would expect these to be most frequent right after the mainshock, as has been shown to be the case by Russo and Villaseñor (1995). In summary, while the deep 1946 events relocated by Russo and Villaseñor (1995) were technically aftershocks of the 1946 event (having occurred within one rupture length of the mainshock), they do not define the rupture plane, as suggested by Russo and Villaseñor. Rather, the 1946 rupture plane is defined by the temporally anomalous, gently south-dipping zone of shallow aftershocks.

1946 tsunamis. Immediately after the August 4, 1946, mainshock, a tsunami struck ~30 km off the eastern coastline of the Rio San Juan Peninsula, drowning nearly 100 people in the village of Mantanzas (then known as Julia Molina), just south of the present city of Nagua (Fig. 3) (Lynch and Bodle, 1948; Small, 1948). Although the tsunami height was only 2.5 m at Mantanzas, the low beach relief in the area allowed the tsunami to propagate inland for several kilometers, accounting for the high loss of life (Lynch and Bodle, 1948). Farther north, at the mouth of Rio Boba, higher beach relief overtopped by the tsunami required tsunami heights of 4–5 m (Lynch and Bodle, 1948; Small, 1948). Anecdotal accounts noted that the tsunami propagated from north to south down the coast, indicating a source to the north. The location of the tsunami implies that it was probably caused by either: (1) sea-floor uplift associated with propagation of the mainshock rupture to the sea floor at the collisional deformation front; or (2) widespread, earthquake-induced slumping of the Hispaniola slope or the southern slopes of Silver or Navidad banks. The southern slopes of the carbonate banks exhibit numerous slump scars and avalanche chutes, some of which are very large (Mullins et al., 1991, 1992; Dolan et al., this volume). Similarly, the Hispaniola slope within the collision zone is highlighted by widespread, recent slumping (Dolan et al., this volume). The location of the most widespread zone of major slumps on the Hispaniola slope 100 km east of the tsunami landfall, however, suggests that the 1946 tsunami was probably not directly related to the widespread slumping of the northeastern Hispaniola slope. In addition to the large tsunami immediately after the August 4 mainshock, smaller tsunamis continued for several days after the mainshock (Seismological Notes, 1946). The post-mainshock occurrence of these tsunamis suggests that they may have been caused by submarine slumps and slides triggered by aftershocks.

Large 1946 aftershocks

The M_s 7.6 earthquake of August 8, 1946 (Kelleher et al., 1973; M_s 7.3 in Russo and Villaseñor, 1995), represents the largest aftershock of the 1946 northeast Hispaniola earthquake. Our preliminary analysis of the waveforms for the August 8 event indicates that it was a complex rupture, probably involving several subevents. Because of this complexity, the first-motion-only focal mechanism we show for the August 8 earthquake is poorly constrained and should be considered uncertain; we plan to continue our attempts to model the waveforms of this complex event. Despite our lack of confidence in the focal mechanism shown in Figure 6, one aspect of the August 8 earthquake is quite clear: The preliminary focal mechanism is markedly different from all the other events in the 1943–1953 sequence. Unlike the other events, all of which show thrust faulting on shallowly south- or southwest-dipping planes, the August 8, 1946, earthquake exhibits either right-lateral motion on a near-vertical plane striking 040°, or left-lateral motion on a moderately north-dipping plane that strikes 126° (Fig. 6).

Kelleher et al. (1973) calculate an M_s of 7.0 for a second major aftershock on October 4, 1946. Their results show this event as having occurred at the extreme southeastern edge of the 1946–1953 earthquake sequence, more than 25 km southeast of the 1946 mainshock (Fig. 5). In contrast, Russo and Villaseñor (1995) calculated an M_s of 6.1 for this event. Furthermore, their relocation shows that the earthquake actually occurred much closer to the mainshock, 20 km north-northeast of the position calculated by Kelleher et al. (1973) (Fig. 5). Although we have calculated only a first-motion mechanism for this earthquake, it appears to be remarkably similar to the mechanism that we determined for the 1946 mainshock, with thrust faulting on a plane that dips 17° south (Fig. 6).

1948 Samana earthquake

The 1946 earthquakes were followed by two other large events within the collision zone. On April 21, 1948, an M_s 7.3 event occurred beneath the Samana Peninsula, within the central part of the 1946 aftershock zone (Fig. 5). Relocated aftershocks for this event (Kelleher et al., 1973) indicate a rather narrow aftershock zone that extended only ~50 km along strike, but ~65 km perpendicular to strike (Fig. 5). Our first-motion focal mechanism shows that this earthquake was similar to the 1946 mainshock, with oblique left-lateral–thrust motion occurring on a shallowly south-dipping plane (Fig. 5). The relatively large strike–perpendicular width of the aftershock sequence of this event strengthens our interpretation of a low-angle, south-dipping 1946 rupture plane (Fig. 6). Aftershocks of the 1948 earthquake extend ~15 km south of the aftershock zone of the 1946 earthquakes, suggesting

that the 1948 event may have extended the 1946 rupture plane downdip in the central part of the collision zone.

1953 Silver Spur earthquake

On May 31, 1953, an M_s 7.0 earthquake occurred beneath northern Hispaniola, just south of the coast, along the southwestern projection of the western edge of the Silver Spur collision (Fig. 2) (International Seismological Summary of 1953, 1961); Sykes and Ewing, 1965). Our body-waveform inversion yielded a focal mechanism for this earthquake that is similar to the 1946 and 1948 ruptures, revealing thrust faulting on a shallowly south-southwest–dipping plane (Figs. 6 and 7). Aftershocks for this earthquake define an elongated triangle that extends northeastward from the mainshock along the western edge of the Silver Spur collision (Fig. 5). Although the 1953 mainshock occurred ~15 km west of the western edge of the 1946 aftershock zone, the eastern half of the 1953 aftershock zone overlaps with the westernmost part of the 1946 aftershock zone (Fig. 5). The focal depth of the Silver Spur earthquake was ~15–25 km.

1943 northern Mona Passage earthquake

The July 29, 1943, M_s 7.8 northern Mona Passage earthquake (Kelleher et al., 1973; M_s 7.7 in Abe, 1981; M_s 7.5 in Pacheco and Sykes, 1992) ruptured a large segment of the plate boundary north of the Mona Passage between Hispaniola and Puerto Rico (Fig. 5). Our body-waveform inversion yielded a focal mechanism that is generally similar to the 1946, 1948, and 1953 northeastern Hispaniola earthquakes in that it shows thrust faulting on either a shallowly south-dipping plane, or a steeply west-northwest–dipping plane (Fig. 6). However, the focal mechanism indicates that the 1943 event exhibited slightly more oblique, left-lateral motion than the 1946 mainshock (Fig. 6).

We have used the waveform inversion to constrain the dimensions of the main rupture area for the 1943 mainshock. These data reveal a roughly triangular asperity that extends westward from the mainshock focus for ~50 km; almost no strain release occurred east of the mainshock (Fig. 5). The rupture plane is ~40 km wide (viewed perpendicular to the shallowly dipping faulting plane) along its eastern edge and narrows to a point at its western end. Seven aftershocks of the 1943 earthquake (relocated by Kelleher et al., 1973) define a 90-km × 65-km "halo" that extends well beyond the rupture plane (Fig. 5). The aftershock zone closely corresponds to the zone of anomalously shallow bathymetry at the north end of Mona Passage, which Dolan et al. (this volume) interpret as the sea-floor manifestation of the Mona bank collision. The rupture zone of the earthquake is parallel to, and just south of the zone of shallow bathymetry (Fig. 5). Unlike the 1946 mainshock, the 1943 northern Mona Passage event does not appear to have ruptured to the sea floor at the deformation front. Rather, the waveform analysis indicates that slip occurred no shallower than ~25 km depth. The absence of shallow rupture probably explains the lack of any reported tsunamis for this earthquake. A 25–30-km-deep focus for the 1943 mainshock places the event near the top of a long-lived, south-dipping cloud of small to moderate earthquakes identified by Dolan et al. (this volume) as the top of the underthrust Atlantic (North America) slab (Fig. 3; see also Dolan et al., this volume).

Furthermore, although the 1943 mainshock epicenter was located close to the sea-floor trace of the southeastern strand of the left-lateral Septentrional strike-slip fault defined by SeaMARC II side-scan sonar data (Dolan et al., this volume), the large strike–perpendicular width of the 1943 aftershock zone relative to its along-strike length, with the occurrence of aftershocks almost 40 km north of the surface trace of the fault as well as 25 km to the south, suggests that the earthquake occurred on a shallowly south-dipping plane. This observation, coupled with the occurrence of the earthquake along the inferred top of the underthrust slab and the similarity of the 1943 focal mechanism to the shallowly south- to southwest-dipping thrust earthquakes of the 1946–1953 sequence to the west, indicates that the 1943 earthquake did not occur on the Septentrional fault. Rather, as with the 1946–1953 earthquakes beneath Hispaniola, the focal mechanism and aftershock data indicate that the 1943 earthquake ruptured the shallowly south-dipping, interplate thrust interface along the top of the underthrust Atlantic slab (Fig. 6).

Focal mechanisms for recent (1962–1994) moderate earthquakes

In addition to our focal mechanisms for the 1943–1953 earthquakes, focal mechanisms of seven moderate earthquakes that have occurred in the region since 1962 have been published (Molnar and Sykes, 1969; Kafka and Weidner, 1979; Harvard Centroid Moment Tensor Catalog, 1994). Six of the seven published focal mechanisms are similar to the 1943–1953 earthquakes, showing predominantly thrust motion along shallowly south- and southwest-dipping planes (Fig. 7). As with the larger 1943–1953 events, rake angles of the six recent moderate thrust-fault events indicate that motion was oblique to the strike of the plate margin. Obliquity of slip during these earthquakes to the plate margin ranges from ~30° to near 90°, indicating a range of motion from mixed thrust–left-lateral displacement to left-lateral strike-slip offset nearly parallel to the strike of the underthrust Atlantic slab (Fig. 7). In general, the focal mechanisms for the smaller events show more highly oblique motion than the larger 1943–1953 earthquakes. The seventh moderate earthquake, which occurred just north of the deformation front near 69° 45′W, exhibited near-pure strike-slip motion on vertical planes, either left-lateral slip on a 100°-striking plane, or right-lateral slip on a 015°-striking plane.

DISCUSSION

The most striking characteristic of the 1943 and 1946 earthquakes is their spatial coincidence with active collision zones involving buoyant, high-standing carbonate banks of the south-

eastern Bahamas. This relationship is particularly clear in the case of the 1946–1953 north Hispaniola sequence. When compared with the structure contour map of the underthrust Atlantic slab beneath Hispaniola, the focal depth, the shallow southward dip, and the west- to west-northwest strike of the 1946–1953 faulting planes are all consistent with the earthquakes having occurred on the plate interface along the top of the underthrust North America (Atlantic) slab (Fig. 7). This observation, coupled with the spatial coincidence of the aftershock zones of the 1946–1953 earthquakes with the Silver-Navidad bank collision zone defined by Dolan et al. (this volume), suggests that the earthquake ruptured the strongly coupled interface between Hispaniola and the underthrust portions of the colliding Bahama banks. The fact that the shallow, gently south-dipping zone of 1946 aftershocks extends to the deformation front further implies that the earthquake may have ruptured updip from the focus at ~20 km all the way to the sea-floor deformation front.

The tectonic significance of the August 8, 1946, M_s 7.6 (Kelleher et al., 1973; M_s 7.3 in Russo and Villaseñor, 1995) aftershock that struck offshore Hispaniola just south of the collisional deformation front is still somewhat unclear because of the uncertain nature of the focal mechanism and the absence of a well-constrained focal depth. One possibility is that the earthquake represents right-lateral tear faulting within the underthrust Bahama bank as part of collisional readjustment of the colliding block to slip during the northeastern Hispaniola earthquake.

The focal mechanism and location of the October 4, 1946, M_s 7.0 (Kelleher et al., 1973; M_s 6.1 in Russo and Villaseñor, 1995) aftershock suggest that this earthquake may have re-ruptured the extreme downdip (southern) limit of the 1946 mainshock rupture plane. We speculate that the October 4 earthquake may have ruptured down to the extreme downdip edge of underthrust, buoyant Bahamas material.

The location of the 1948 Samana earthquake suggests that this event re-ruptured, and deepened, the central part of the shallowly south-dipping 1946 mainshock rupture plane (Fig. 5). Aftershocks of the 1946 mainshock and recent moderate earthquakes are both anomalously sparse in the eastern part of the 1946 rupture zone to the east of the 1948 rupture (Figs. 4 and 5). These data suggest that the 1948 earthquake may have ruptured a zone of incomplete strain release during the 1946 mainshock. The Samana earthquake also occurred directly downdip (southward) of the projection of Navidad Channel—the deep, linear, north-northeast–trending channel that separates Silver and Navidad banks (Dolan et al., this volume)—suggesting the possibility that the 1948 rupture occurred along a zone of weakness associated with the underthrust portion of Navidad Channel. The 1948 earthquake occurred beneath the Samana Peninsula, which exhibits much more rugged topography than areas to the east or west (de Zoeten et al., 1991; Dolan et al., this volume; their fig. 11A). This observation suggests a third possibility, that the Samana earthquake may have been localized at a collisional asperity beneath the Samana Peninsula. We speculate that the anomalously high topography of the peninsula may be related to underthrusting of a particularly shallow portion of the underthrust Bahama banks, in much the same way that we propose that the zone of anomalously shallow bathymetry in the northern part of Mona Passage is caused by underthrusting of Mona bank.

The coincidence of the western limit of 1953 aftershock zone with the leading (western) edge of the Silver Spur collision suggests that this earthquake ruptured the area of strong coupling between Hispaniola and the underthrust portion of Silver Spur. The 1953 aftershock zone extended ~10–15 km west of the western limit of the 1946 aftershocks (Fig. 5), indicating that the 1953 earthquake may have extended the 1946 rupture to the extreme western edge of colliding carbonate basement. Molnar and Sykes (1969) have determined a focal mechanism for a 1967 M 5.3 event that occurred at a depth of 39 km, ~15 km southeast of the 1953 event (Fig. 7). Their mechanism is consistent with west-southwestward underthrusting along a shallowly west-southwest–dipping fault plane. Comparison of the depths of the 1953 and 1967 earthquakes with the structure contour map of the underthrust Atlantic slab shows that both earthquakes were generated by rupture of the plate-boundary thrust interface along the top of the underthrust slab (Fig. 7).

On the basis of recent seismicity, the 25- and 50-km depth contours of the top of the underthrust Atlantic slab can only be confidently traced northwestward to ~69° 45′W (Fig. 3; Dolan et al., this volume). However, based on the similarity of the 1953 and 1967 focal mechanisms with those of the 1943, 1946a, 1946c, and 1948 earthquakes, we suggest that the shallowly south-dipping North America (Atlantic) slab extends at least as far west as 70° 15′W, the western edge of the 1953 rupture. Furthermore, the consistent southerly dip of structures in the accretionary prism of the northern Hispaniola deformed belt west of the Silver Spur collision, and the shallow southward dip of underthrust carbonate basement beneath the deformation front along the southern edge of the Hispaniola basin (Dolan et al., this volume), imply that the underthrust Atlantic slab may exist west of the collision. The slab is not seismically resolvable in north-central and northwestern Hispaniola, however, and the deep crustal–upper mantle structure west of 70° 15′W remains poorly understood.

As with the 1946 northeastern Hispaniola earthquake, the 1943 northern Mona Passage earthquake appears to have been localized along an active collision. As discussed above, Dolan et al. (this volume) have proposed that the anomalously shallow bathymetry of the northern Mona Passage area has developed in response to underthrusting of a buoyant Bahama bank, which they named Mona bank. Since the Bahamas ridge strikes more northwesterly than the plate boundary deformation front, collisional underthrusting is diachronous, younging from east to west (Dolan et al., this volume). Thus, the collision has progressed farther in the Mona Passage area than to the west in the region of the 1946 earthquake. Based on this reasoning, Dolan et al. (this volume) suggest that the Mona bank has already been thrust beneath the insular slope, which has been uplifted in response to the collision.

Comparison of the 1943 mainshock focal mechanism data with the structure contour map of the underthrust Atlantic slab

indicates that the 1943 rupture occurred along the shallowly south-dipping interface between the underthrust Atlantic slab and the overriding Caribbean margin (Figs. 3 and 7). The focal mechanisms and focal depths of several moderate, recent earthquakes from beneath the northwest part of Mona Passage also support this interpretation (Dolan et al., this volume). All three recent events were shallowly dipping thrust-faulting earthquakes that occurred at depths that plot along the top of the slab interface (Fig. 7).

One of the most puzzling aspects of the 1943 mainshock rupture was the absence of widespread damage from the event in northwestern Puerto Rico, which is only ~50 km south of the epicenter. We suggest that the answer lies in the rupture characteristics of the earthquake. The mainshock focus is located at the extreme eastern edge of the rupture plane, and our body-waveform inversion suggests that several subevents propagated westward along the rupture plane. These data indicate a strong westward directivity during this event. If so, then most of the energy from the earthquake probably propagated west, away from Puerto Rico, and dissipated along the northern, offshore slope of Hispaniola. Furthermore, the relatively great depth of the earthquake (>25 km) precluded generation of any significant tsunami, thus sparing low-lying coastal areas in northwestern Puerto Rico and northeastern Hispaniola from inundation.

Implications of the 1943–1953 earthquake sequence for seismic versus aseismic strain release along the plate-interface thrust fault

What do the 1943 and 1946 earthquakes tell us about the degree of seismic coupling along the plate boundary? We have proposed that the 1943 and 1946 earthquakes were generated by rupture of strongly coupled, collisional asperities along the plate-interface thrust fault. We suspect that elastic strain energy along these collisional parts of the plate-interface is released predominantly during coseismic slip. What can we say about the degree of coupling along the noncollisional parts of the plate boundary?

The absence of rupture in the 200-km-wide section of the plate boundary between the 1943 and 1946 earthquakes is an interesting anomaly. As noted above, our waveform inversions suggest that the 1943 earthquake ruptured unilaterally westward, which probably resulted in a large dynamic strain pulse that may have loaded the section of the plate interface to the west of the 1943 earthquake toward failure. The fact that the western segment did not rupture could be because of either: (1) the recent occurrence of a moderately large earthquake that relieved the strain along the fault between the 1943 and 1946 ruptures or (2) a long-term, slower strain accumulation rate along the unruptured part of the plate-interface thrust fault.

If the absence of rupture on the fault between the 1943 and 1946 earthquakes was due to the recent release of strain in a large, pre-1943 earthquake, then that earthquake was either not felt in Puerto Rico or Hispaniola, or it was not recorded historically. The only large historical event that might have occurred on the plate-interface thrust fault in this area is the M_s 7.0 event of 1917 (Kelleher et al., 1973; McCann and Sykes, 1984). Rupture of the entire unruptured part of the fault could have produced an M ~7.5 earthquake comparable to that in 1943, but even farther from Puerto Rico than the 1943 event. Thus, it was possible that such an event would have not been felt strongly in Puerto Rico. This would place the event closer to Hispaniola, however, making it more likely that the postulated event would have been felt and recorded there. The directivity of the event could also play an important role. As noted above, the 1943 mainshock, despite its proximity to coastal Puerto Rico, produced only a maximum Modified Mercali Intensity of V in northwestern Puerto Rico (W. R. McCann, personal communication, 1995). It would be especially easy for an event not to be recorded the farther back in time it occurred. This, however, would allow a longer period of strain accumulation on the plate-interface thrust fault.

Alternatively, the portion of the plate-interface thrust fault plane between the 1943 and 1946 ruptures may not store elastic strain energy as efficiently as the collisional asperities along the fault that ruptured in those two earthquakes. The bathymetry of the Hispaniola slope provides important constraints on the location of active collisional underthrusting (Dolan et al., this volume). Although the eastern part of the unruptured zone overlaps with the western part of the zone of shallow bathymetry in the northern Mona Passage, most of the unruptured zone lies in an area of complicated bathymetry associated with a major bifurcation of the Septentrional strike-slip fault system at ~68° 25′W (Fig. 3). Centered in the middle of the unruptured zone is a 7-km-deep, 35-km-long pull-apart basin at a major left-step in the left-lateral strike-slip fault system (Dolan et al., this volume). The presence of this deep basin contrasts markedly with the slopes to the east and west, and seems incompatible with collisional underthrusting of a bathymetrically high-standing block beneath the unruptured part of the plate boundary. Based on this reasoning, we suggest that the Mona bank and Silver-Navidad bank collision zones are separated by a section of the plate boundary that is not undergoing collisional underthrusting of buoyant Bahamas material. If so, then the degree of seismic coupling between the plates in the unruptured segment of the plate interface may be less than that along the collisional asperities. Thus, the elastic strain necessary to generate slip in earthquakes may be stored more slowly than in the surrounding, more strongly coupled parts of the plate-interface thrust fault, and a significant portion of the interplate slip may be accommodated aseismically along the noncollisional parts of the plate-interface thrust fault. This leads us to speculate that the noncollisional parts of the fault may participate in large thrust earthquakes less frequently than more strongly coupled portions of the fault. This inference is supported by the fact that the two largest instrumentally recorded events to strike the region—the 1943 and 1946 earthquakes—both occurred at sites of presumed collisional underthrusting and consequent strong interplate coupling. The exact degree to which aseismic slip contributes to interplate slip along the thrust interface, however, remains unknown.

Based on the observations discussed above, we speculate that large interplate thrust earthquakes most commonly nucleate

at collisional asperities. This does not mean that large thrust ruptures cannot nucleate outside the zones of active collisional underthrusting, only that the inferred higher degree of interplate coupling in the collision zones results in faster, more effective strain accumulation necessary to generate large earthquakes. Furthermore, although large earthquakes may commonly nucleate at collisional asperities, the earthquake ruptures may propagate beyond those asperities into less strongly coupled, noncollisional parts of the plate-interface thrust fault.

Extent of underthrust, buoyant Bahamas province in the north-central Caribbean

If large thrust earthquakes along the northern margin of the NCPBZ nucleate more effectively at collisional asperities, then it is of obvious importance to understand the three-dimensional distribution of underthrust, buoyant Bahamas material. Furthermore, the extent of buoyant Bahamas material along the plate boundary represents one of the key elements that must be understood before attempting any reconstruction of the tectonic and mechanical evolution of the NCPBZ. The southern margin of the Bahamas province, however, has already been subducted beneath the NCPBZ. We must therefore use indirect means to infer the subducted extent of the Bahamas province.

First, and most basically, the Bahamas province is thought to have developed above a northwest-striking oceanic fracture zone associated with opening of the Atlantic Ocean (Mullins and Lynts, 1977). The linear, fracture-zone–parallel nature of the Bahamas is reflected most prominently in the Bahamas escarpment, the steep, northeastern wall of the Bahamas (Fig. 1). As discussed above, the northwest strike of the Bahamas, coupled with the overall near–east-west relative North America (Atlantic) plate–NCPBZ motion, indicates that the Bahamas collision is diachronous, younging from the west. Thus, the collision has progressed farther in the east than in the west. Dolan et al. (this volume) propose that Mona bank, which they hypothesize has been subducted beneath the northern Mona Passage, represents the easternmost extent of underthrust, buoyant Bahamas.

As noted above, the bathymetry of the Hispaniola slope also places important constraints on the distribution of underthrust Bahamas material. Specifically, the presence of the 7-km-deep pull-apart basin above the middle of the unruptured section of the thrust fault suggests that this part of the plate boundary is not undergoing active collisional underthrusting. We suggest that this zone of noncollision probably extends from the eastern edge of the 1946 rupture plane at ~68° 30′W to the western edge of the northern Mona Passage zone of anomalously shallow bathymetry at ~68° 00′W (Fig. 5).

If, as we propose, 1943 and 1946 mainshocks nucleated at collisional asperities, then we can use the rupture planes of the 1946 and (with slightly less confidence) the 1943 earthquakes as proxies for the presence of underthrust buoyant Bahamas material. The clear spatial correlation between the rupture plane of the 1946 northeastern Hispaniola earthquake and the active Silver-Navidad bank zone of collisional underthrusting provides strong support for this inference.

Finally, side-scan sonar data show that collisional underthrusting terminates at the western edge of the Silver Bank collision zone (Dolan et al., this volume). West of the collision, the southern edges of high-standing Mouchoir and Caicos banks lie to the north of the deformation front (Fig. 2). For example, seismic-reflection data from the Hispaniola basin west of Silver Spur show a sharply defined southern limit to high-standing Mouchoir bank 8–25 km north of the deformation front; carbonate material underthrust beneath the Hispaniola slope consists of gently south-dipping slope deposits that lie more than 4.5 km below the crest of Mouchoir bank (Dolan et al., this volume). In other words, because of the highly irregular shape of the southern margin of the Bahamas province, and the diachronous, westward-younging nature of the oblique collision, collisional underthrusting of high-standing carbonate bank material has not yet occurred west of the Silver Spur collision, with a few minor exceptions (e.g., Mouchoir Spur; Dolan et al., this volume).

Based on these observations, we have constructed a map of the probable approximate downdip, southern limit of underthrust Bahama carbonates (Fig. 9). Note that although we have drawn the southern edge of postulated Mona bank along the southern edge of the 1943 rupture plane, the actual downdip limit of underthrust Mona bank basement in this area is unknown.

Relative plate motions in the north-central Caribbean based on earthquake focal mechanisms

To understand the mechanics and evolution of the NCPBZ, we must know the direction of relative plate motion between the North America plate (Bahamas province) and the Hispaniola and Puerto Rico blocks, which lie within the NCPBZ; the true Caribbean plate lies to the south of the NCPBZ. The direction of motion along the NCPBZ has been the subject of much debate during recent years. Regional plate models, based primarily on analysis of magnetic lineations formed during opening of the Cayman trough, the presence of left-lateral strike-slip faults along the northern plate boundary and right-lateral faults along the southern boundary, and active volcanism in the Lesser Antilles island arc indicate that both the North and South America plates have moved generally westward with respect to the Caribbean (relative to the hot-spot reference frame) since Eocene time (Pindell and Barrett, 1990; Mann et al., 1990). However, current absolute and relative plate motions in the north-central Caribbean region remain relatively poorly constrained. One of the major reasons for this is that, in marked contrast to most other plate boundaries worldwide, attempts to model Caribbean–North America plate motion vectors have largely proved unsuccessful (e.g., DeMets et al., 1990; DeMets, 1993). These results indicate that the Caribbean plate cannot be modeled as a rigid plane with discrete boundaries (DeMets, 1993). Rather, the Caribbean plate must be undergoing significant internal deformation. The validity of this concept is demonstrated by numerous geological and geophysical studies

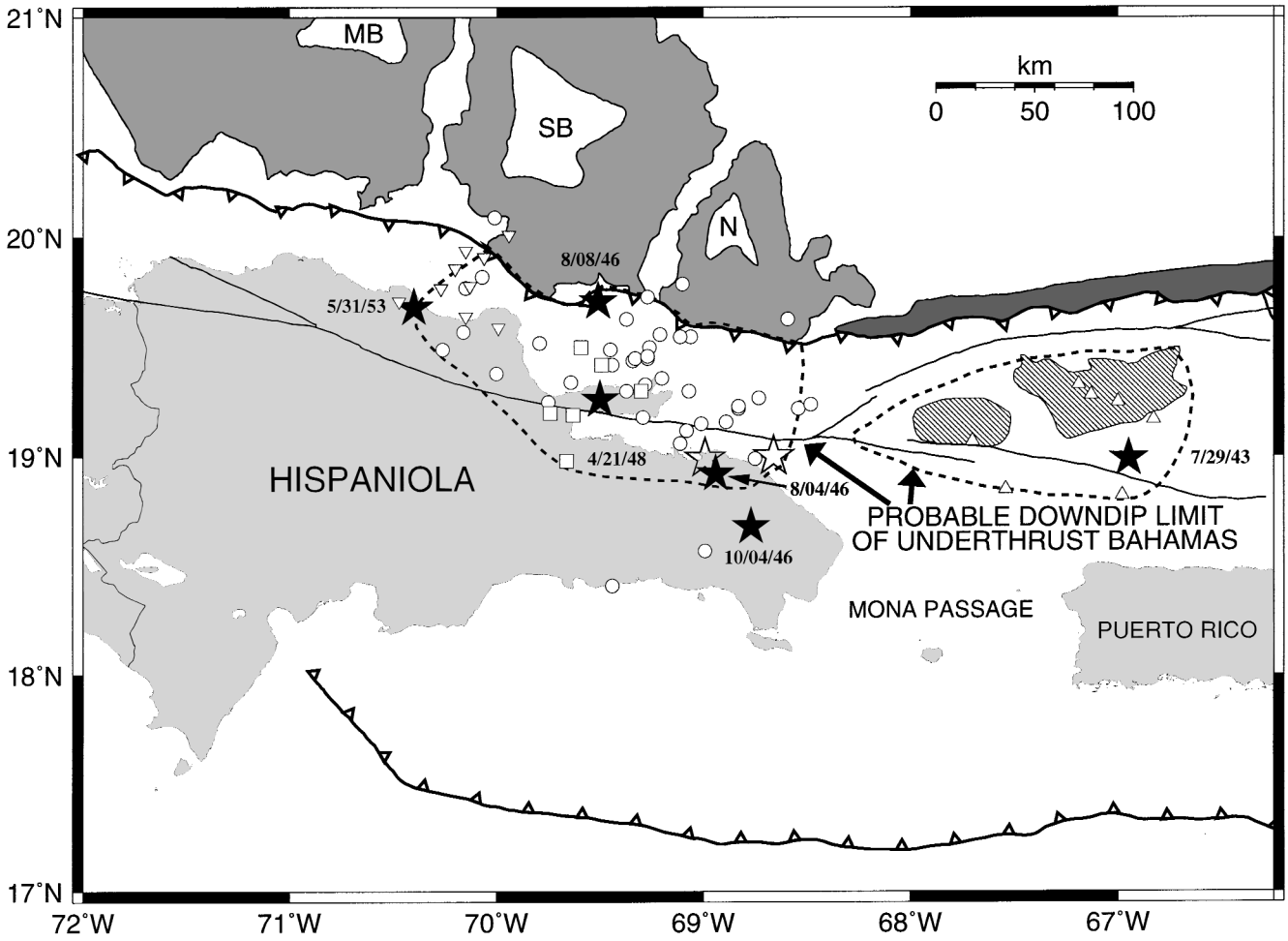

Figure 9. Map of proposed extent of underthrust Bahama bank material based on earthquake locations, limits of Silver-Navidad bank collision zone, and extent of Mona bank zone of anomalously shallow bathymetry. MB is Mouchoir bank; N is Navidad bank; SB is Silver bank.

that show that the margins of the Caribbean plate are characterized by wide, extremely complex zones of deformation (see overview in Mann et al., 1990). In the north-central Caribbean, for example, the 250-km-wide plate boundary zone is characterized by relative motions between several microplates and numerous smaller structural blocks (Mann et al., 1984, 1995; Byrne et al., 1985; Masson and Scanlon, 1991; Dolan et al., this volume).

As noted above, global plate motion models do not adequately constrain Caribbean–North America plate motions, and consequently there is disagreement about the exact relative plate motion along the NCPBZ (e.g., Sykes et al., 1982; McCann and Sykes, 1984; Stein et al., 1988; DeMets et al., 1990; DeMets, 1993). There is general agreement that both the North and South America plates are moving predominantly westward with respect to the Caribbean plate, resulting in a significant component of left-lateral strike-slip motion across the NCPBZ. Differences arise, however, in terms of the amount of oblique motion occurring along the margin, and even in the direction of any oblique motion.

Most models indicate either east-west relative motion (e.g., DeMets, 1993; Farina et al., 1995) or east-northeast motion (Bracey and Vogt, 1970; Schell and Tarr, 1978; Sykes et al., 1982; Deng and Sykes, 1995). All of these models predict predominantly left-lateral motion along the NCPBZ, with varying degrees of convergence. Masson and Scanlon (1991), on the basis of their analysis of the neotectonics of the Puerto Rico area, proposed an alternative scenario in which Puerto Rico behaves as a distinct platelet that is actively rotating counterclockwise between the Puerto Rico trench and Los Muertos trench within the overall left-lateral NCPBZ. Still other models suggest active transtensional and extensional deformation of the Hispaniola–Puerto Rico region (Larue and Ryan, 1990; Larue et al., 1990; Speed and Larue, 1991).

In the absence of high-resolution geodetic data for the northern Caribbean region, which are just becoming available (Farina et al., 1995; Dixon et al., 1998), the focal mechanisms that we have calculated, when coupled with geologic data, provide one of the most accurate means for placing constraints on the directions of relative plate motions in the region. The 1943 and 1946 earth-

quakes are among the largest (and the 1946 mainshock may, in fact, be the largest) events to have struck the northeast Hispaniola–northwest Puerto Rico area in at least 430 yr, and they record most of the strain released seismically along the plate interface during that time. It is therefore likely that they represent a significant portion of the long-term pattern of strain release along the margin. This inference is supported by the internal similarity of the focal mechanisms calculated for the individual earthquakes in the 1943–1953 sequence, as well as by the overall similarity of those focal mechanisms to mechanisms calculated for recent, moderate earthquakes that have occurred along the plate interface.

The rake that we calculated for the 1943 earthquake (030° in map view) indicates that during the earthquake motion along the east-northeast–trending plate interface (080° trend at the sea floor; ~065° trend at 25 km depth; Fig. 3) was highly oblique, with approximately equal amounts of convergence perpendicular to the margin and left-lateral motion parallel to it. The rake for the 1946 event (034° in map view) shows that motion along the plate interface during that earthquake was also oblique, but with only about one-half as much left-lateral motion parallel to the 100°-trending margin as thrust motion perpendicular to the margin (margin-parallel:margin-perpendicular ratio ~1:2). The rakes calculated for the other earthquakes from the 1946–1953 sequence give similar results (Fig. 6).

The earthquake data are supported by Dolan et al.'s (this volume) analysis of the active tectonics of the north-central Caribbean, which shows evidence of a convergent component of deformation along the entire northern boundary of the NCPBZ, from north of the Virgin Islands to north-central Hispaniola. Similarly, marine geophysical data from northwestern Hispaniola (Dillon et al., 1992) and southeastern Cuba (Calais et al., 1989, 1992, this volume) indicate that the contractional component of deformation continues as far west as the eastern end of the Cayman trough (Fig. 2). Even in a regime in which pure left-lateral motion would occur on east-west planes (e.g., NUVEL-1; DeMets et al., 1990), such contractional structures would be expected along the west-northwest–trending plate margin in the Hispaniola restraining bend (Mann et al., 1984). The occurrence of active contractional structures along the 080–085°-trending plate margin off northern Puerto Rico, however, requires that the relative motion vector between the North America plate and the Hispaniola and Puerto Rico blocks of the NCPBZ must be oriented more northerly than 080° to the north of Puerto Rico, given that the eastern strand of the Septentrional fault and the northern Puerto Rico slope fault zone—the only major strike-slip faults in the region—strike approximately east-west and northeast, respectively.

The relative motion data discussed above are based on the mechanisms of earthquakes that occurred at depths of 19–49 km along the south-dipping plate interface. Dolan et al. (this volume) have shown that the Hispaniola–Puerto Rico margin exhibits well-developed strain partitioning, with contractional deformation largely decoupled from left-lateral strike-slip motion. In northern Hispaniola, most transcurrent motion is accommodated along the Septentrional fault system (Mann et al., 1984, this volume; Prentice et al., 1993). East of 68° 15′W strike-slip motion appears to be accommodated along both the Septentrional system and the northeastern Hispaniola slope–northern Puerto Rico slope fault systems (Fig. 2) (Masson and Scanlon, 1991; Dolan et al., this volume). In such a strain-partitioned regime, motions along the decoupled contractional and transcurrent structures sum to the overall relative plate motion. These partitioned structures must merge at depth, with the deep portions of the transpressional plate boundary moving in the overall (oblique) relative plate motion direction (i.e., east-northeast). In the north-central Caribbean region, the partitioned strike-slip and contractional faults probably merge along a shallowly south-dipping decollement at the top of the underthrust North America (Atlantic) slab (Dolan et al., this volume).

For the rake of an earthquake to represent the true relative plate motion, partitioning of the overall oblique slip onto parallel strike-slip and contractional faults must occur *updip* of the rupture plane of the plate-interface earthquake. In other words, if a strike-slip fault merges with the decollement deeper than the rupture zone of a plate-interface earthquake, then the earthquake will exhibit a focal mechanism that is more contractional than the overall relative plate motion. Overall relative plate motion in such cases will depend on the relative slip directions and slip rates along the plate-interface thrust fault and the parallel strike-slip fault. Thus, the exact nature and location of the mechanical interaction between the strike-slip faults and the plate-interface decollement are critical for correctly interpreting the earthquake rake data.

Although we do not have definitive data on the location at which the partitioned strike-slip faults of the north-central Caribbean merge with the decollement, the marine geophysical data discussed in Dolan et al. (this volume) provide a general idea of where such interactions must take place. The mainshock focus of the 1943 northern Mona Passage earthquake was located almost directly beneath the eastern strand of the left-lateral Septentrional fault system, well to the south of the northern Puerto Rico slope fault zone (NPRSFZ) (Fig. 3). Thus, strike-slip on the NPRSFZ is partitioned off the south-dipping plate-interface oblique-thrust fault *updip* from the 1943 rupture plane. The rake from the 1943 earthquake can therefore be used to define the relative motion direction between the Puerto Rico block and the North America (Atlantic) slab for the area to the north (i.e., updip) of the 1943 rupture plane. In contrast, the rupture plane lies beneath, and locally slightly to the south of, the seafloor trace of the Septentrional fault (Fig. 5). Although we do not known the exact nature and location of the interaction of the eastern strand of the Septentrional fault with the decollement, it would appear from the location of the surface trace of the fault that at least some left-lateral strike-slip motion may be partitioned off the decollement *downdip* from the 1943 earthquake plane. If so, then the rake derived from the 1943 earthquake focal mechanism would indicate more of a compressional component of deformation than the overall relative plate motion that is occurring downdip of the zone of strain partitioning. In other words, overall relative plate motion between the North America

plate and the Puerto Rico block is probably more easterly than the 030° direction implied by the 1943 focal mechanism.

The data from the 1946 northeastern Hispaniola earthquake are similar. The sea-floor trace of the northeastern Hispaniola slope fault zone (NEHSFZ), a left-lateral strike-slip splay of the Septentrional fault system, is located only ~10–20 south of the deformation front, more than 40 km north of the epicenter of the 1946 mainshock (Fig. 3). Thus, assuming that the NEHSFZ dips steeply or vertically, most strike-slip motion on this fault is partitioned off the south-dipping plate interface updip from the major part of the 1946 rupture plane. In contrast, the 1946 epicenter was located just south of the surface trace of the Septentrional fault. Most of the aftershocks of the 1946 earthquake that were associated with the rupture plane, as well as the 1953 earthquake, occurred to the north of the Septentrional fault, indicating that the rupture plane extends well to the north of the Septentrional fault. The location of the Septentrional fault therefore suggests that a large percentage of the left-lateral motion is partitioned off the plate-interface fault to the south (i.e., downdip) of the 1946 rupture plane. As with the 1943 event, the rake determined for the 1946 earthquake therefore exhibits motion that is more contractional than the overall relative plate motion.

The data for the 1943 and 1946 earthquakes show that overall relative motion between the underthrust North America (Atlantic) plate and the Hispaniola and Puerto Rico blocks of the NCPBZ cannot be oriented more northerly than ~030°. Furthermore, the oblique-thrust focal mechanism for the 1943 event, together with geologic evidence showing some convergence along the margin north of Puerto Rico, requires that overall relative motion cannot be oriented more easterly than ~080° north of Puerto Rico. Thus, the relative plate motion direction along the northern deformation belt of the NCPBZ in the Puerto Rico–Hispaniola region lies between ~030° and 080°. These data cast doubt on models in which the direction of relative plate motion along the northern edge of the NCPBZ is oriented east-west (e.g., DeMets, 1993; Farina et al., 1995).

The exact relative plate motion vector depends on the ratio of slip rates on the left-lateral Septentrional fault system and the plate-interface oblique-thrust fault. The higher the slip rate on the Septentrional fault system, the closer the overall relative plate motion vector will be to 080°. Conversely, the higher the slip rate along the plate-interface thrust fault, the closer the overall relative motion vector will be to 030°. No well-constrained slip-rate data are currently available for motion along either the plate interface or the left-lateral strike-slip faults of the Septentrional fault system, although Mann et al. (this volume) show two independent estimates of the maximum possible slip rate for the Septentrional fault of 17 ± 6 and 19 ± 5 mm/yr.

Recent GPS geodetic data suggest that the Septentrional fault may accommodate only about 40% to 50% of the total motion along the NCPBZ (Dixon et al., 1998). Furthermore, these data imply that significant left-lateral motion occurs to the north of the Septentrional fault, offshore of Hispaniola. Because the oblique-left-lateral–thrust fault along the south-dipping plate interface is the dominant structure offshore northern Hispaniola, we suggest that it is likely that much of this off-Septentrional fault motion probably occurs during oblique slip on the south-dipping plate-interface fault. If so, then the offshore oblique thrust fault may have a relatively fast slip rate. Alternatively, some of the offshore left-lateral motion suggested by the GPS data may be accommodated on the northeastern Hispaniola slope fault and/or the Camu fault. Determination of the true slip rates of the major faults within the northern deformation belt of the NCPBZ will require more occupations of the recently established northern Caribbean geodetic network (Dixon et al., 1998), as well as the use of more sophisticated models that incorporate realistic fault geometries and the rakes derived from our focal mechanisms derived from events on the offshore plate-interface thrust fault.

The lack of detailed slip-rate data, coupled with our inability to determine exactly where strike-slip motion is partitioned off the plate interface, precludes an exact assessment of relative plate motion in north-central Caribbean, beyond placing maximum limits on the orientation of the relative motion vector between 030° and 080°. Even with detailed GPS geodetic data, care must be taken to model the effects of interseismic strain accumulation on the offshore oblique-thrust fault, as well as the Septentrional strike-slip fault. Other possible complications include the strain fields generated by the northeastern Hispaniola slope and Camu left-lateral strike-slip faults.

The similarity of the focal mechanisms of the 1943 and 1946–1953 earthquakes argues against active rotation of Puerto Rico as a separate microplate, as proposed by Masson and Scanlon (1991). The Masson and Scanlon (1991) model predicts transtensional deformation northwest of Puerto Rico, in the region of the 1943 earthquake. Our focal mechanism for that event, however, reveals oblique convergence along this part of the plate boundary. As noted above, marine geophysical data offshore northern Puerto Rico also show transpressional deformation across the entire margin (Larue and Ryan, 1998; Dolan et al., this volume). We believe that the post–10.9 Ma clockwise rotation of Puerto Rico observed in paleomagnetic data (Reid et al., 1991) record an earlier, since-terminated tectonic event.

The data discussed above also rule out models in which the NCPBZ is currently undergoing transtensional deformation (e.g., Larue and Ryan, 1990; Larue et al., 1990; Speed and Larue, 1991). We do not mean to imply by this that normal faults do not exist along the plate margin. Masson and Scanlon (1991) and Dolan et al. (this volume) describe large, oblique-normal faults along the northern margin of the Puerto Rico trench. Minor normal faults also occur along the southern edges of Navidad and Silver banks. Furthermore, it is possible that some predominantly strike-slip faults that Dolan et al. (this volume) describe from the northeastern Hispaniola slope also exhibit local transtensional motion (e.g., bounding faults of the two large pull-apart basins northeast of Hispaniola). However, the earthquake data discussed above indicate that motion along the NCPBZ is fundamentally transpressional, not transtensional, in the Hispaniola–Puerto Rico region.

In summary, the earthquake data presented in this chapter, coupled with geological evidence for a minor component of contractional deformation along the 080–085°-trending plate boundary north of Puerto Rico (Dolan et al., this volume), indicate that overall relative plate motion between the North America (Atlantic) plate and the Hispaniola and Puerto Rico blocks of the NCPBZ is oriented between ~030° and 080°. These data support earlier models in which relative plate motion is east-northeast in the region (e.g., Bracey and Vogt, 1970; Schell and Tarr, 1978; Sykes et al., 1982; Deng and Sykes, 1995).

Dolan et al. (this volume) point out that some north-south shortening also occurs along north-dipping thrust faults within the Los Muertos deformed belt (Fig. 2). This observation indicates that the relative motion vector between the true Caribbean plate, which lies south of the NCPBZ, and the North America plate, which lies north of the NCPBZ, must be oriented more northeasterly than the relative motion vector between the North America plate and the Hispaniola and Puerto Rico blocks. The true orientation of the plate motion vector between the Caribbean and North America plates depends on the slip rates of the plate-boundary–parallel, left-lateral Septentrional–northern Puerto Rico slope and Enriquillo-Plantain Garden fault systems, relative to the slip rates of the oblique-contractional and contractional fault systems of the northern Hispaniola and Los Muertos deformed belts—the higher the contractional slip rates relative to the strike-slip rates, the more northerly the true plate motion vector will be oriented; the higher the left-lateral strike-slip rates, the more easterly the relative motion vector will be oriented. Recent GPS geodetic data, however, suggest that rates of north-south shortening across the northern Caribbean plate boundary are probably only a few mm/yr (Dixon and Mao, 1997). Their data show that north-south convergence between the North America and South America plates is ~3.5 mm/yr at 65° W, increasing steadily to ~6 mm/yr at 75° W. Because some of this north-south motion must be accommodated along contractional structures along the southern Caribbean plate boundary zone (see Mann et al., 1990, for an overview of southern Caribbean tectonics), north-south shortening across the Los Muertos deformed belt is probably slow.

SEISMIC HAZARDS OF THE NORTHERN CARIBBEAN REGION

In this section we discuss the seismic hazards associated with major faults within the northern Caribbean plate boundary zone in the Hispaniola–Puerto Rico region. Historic earthquakes define two major belts of active faulting along the northern and southern boundaries of the NCPBZ (Fig. 2). The northern deformation belt comprises the offshore, plate-interface, oblique-thrust fault as well as the Septentrional, northern Puerto Rico slope, and northeastern Hispaniola slope left-lateral strike-slip faults. The southern deformation belt comprises the north-dipping Los Muertos plate-interface thrust fault and the Enriquillo-Plantain Garden left-lateral strike-slip fault.

Northern deformation zone of the NCPBZ

Earthquakes generated by slip on the plate-interface oblique thrust fault. In this chapter, we have documented the faulting parameters and tectonic setting of the 1943 and 1946 earthquakes, which we interpret to have occurred on the south-dipping, oblique-thrust fault separating the downgoing North America (Atlantic) slab from the overriding Hispaniola and Puerto Rico–Virgin Island blocks of the NCPBZ. The interplate thrust fault can certainly generate M ~8 earthquakes, such as the 1946 event, that are capable of producing extensive damage (Lynch and Bodle, 1948; Small, 1948). The gentle southward dip of this fault results in much greater potential fault-plane area relative to fault length than for the more steeply dipping strike-slip faults of the Septentrional system. Balancing this, however, is the fact that the subduction thrust fault lies well offshore of both Hispaniola and Puerto Rico. Even with the gentle dip of this fault, it lies ~25–30 km deep beneath the population centers of northern Hispaniola, and 75–100 km deep beneath the north coastal region of Puerto Rico (Fig. 3). Furthermore, as with most subduction-zone thrust-fault earthquakes worldwide, rupture in both the 1943 and 1946 mainshocks initiated near the base of the fault plane and propagated updip toward the deformation front—away from populated areas. In the case of the 1943 mainshock, rupture also appears to have propagated unilaterally to the west, directly away from the population centers of coastal Puerto Rico. Source directivity is not always so beneficial, however, as in the case of the 1946 mainshock, where probable unidirectional westward propagation—inferred from the location of the earthquake focus at the far eastern end of the rupture plane—probably directed much of the energy toward the major cities of the Cibao Valley and northern coast of Hispaniola.

In addition to the 1943 and 1946 thrust earthquakes, a poorly reported earthquake in 1787 caused strong ground shaking (Modified Mercalli Intensity [MMI] VIII) over a 150-km length of the northern coastal region of Puerto Rico (McCann and Sykes, 1984). This is the only potential great earthquake to have affected northern Puerto Rico during the >400-yr-long historic period (McCann and Sykes, 1984). The widespread nature of these reports of strong ground shaking led McCann and Sykes (1984) to propose that the 1787 earthquake was generated by rupture of a large part of plate-interface thrust fault (Fig. 2). The poorly defined location of the 1787 event suggests that it, like the 1943 and 1946 events, may have nucleated at a collisional asperity. We speculate that the 1787 earthquake may have nucleated at a collision involving Main Ridge, a west-northwest–trending ridge located 125 km north-northeast of Puerto Rico (Fig. 1). McCann and Sykes (1984) suggest that the Main Ridge is an aseismic ridge that, like the Bahamas, developed along a fracture zone associated with Mesozoic opening of the Atlantic Ocean. The proposed Main Ridge collision is the site of a persistent cluster of seismicity (McCann and Sykes, 1984; Dolan et al., this volume). Historical accounts of the 1787 event must be better documented to determine whether this event was, or was not, a great thrust earthquake.

The damage patterns reported for the 1787 event could also have been generated by a large, offshore strike-slip earthquake on the eastern continuation of the Septentrional fault system.

Accurate estimates of the seismic hazard posed by the south-dipping plate-interface thrust to the population centers of northern Hispaniola and Puerto Rico are complicated by the absence of a well-constrained slip rate for the fault (see discussion above), as well as by our lack of knowledge about the ratio of seismic to aseismic slip that occurs along the plate-interface thrust outside the collisional asperities. Determination of this parameter is of obvious importance for seismic hazard assessments for the region. If the plate-interface thrust fault is strongly coupled, even in non-collisional areas, then the seismic hazard to the Virgin Islands, Puerto Rico, and Hispaniola is much higher than if the noncollisional parts of the plate boundary are slipping largely aseismically.

Septentrional fault system. Slip on the Septentrional fault probably generated the large northwestern Hispaniola earthquakes of 1842 and 1887 (Fig. 2) (McCann and Pennington, 1990; Mann et al., this volume). The great length of the zone of high shaking intensities during the 1842 event suggests that it may have been a great earthquake (Scherer, 1912; Mann et al., 1984, this volume). Other evidence for the potential of the Septentrional fault system to produce large earthquakes comes from paleoseismological trenching along the central reach of the fault in Hispaniola. There, Prentice et al. (1993) and Mann et al. (this volume) have shown that the most recent surface rupture on the fault produced several meters of slip. These data indicate that this earthquake was almost certainly in excess of M 7. The recurrence of such a large event today in the rapidly developing northern part of Hispaniola would have devastating consequences given the high population density and frequently poor quality of construction in the region. The city of Santiago, Dominican Republic, in particular, with a population of ~750,000, lies within a few kilometers of the fault (Fig. 3) (Prentice et al., 1993; Mann et al., this volume). Old Santiago was destroyed in the earthquake of November 2, 1564, although it remains unclear what fault generated that event (Prentice et al., 1993; Mann et al., this volume).

Strike-slip faults offshore northern Puerto Rico Dolan et al. (this volume) show that the Septentrional fault system (SFS) extends eastward offshore Hispaniola. The fault bifurcates at ~68° 30′W, with one strand extending eastward toward the northern slope of Puerto Rico, and another strand extending northeastward to connect with the northern Puerto Rico slope fault zone (NPRSFZ) (Fig. 3) (Masson and Scanlon, 1991; Dolan et al., this volume). The presence of at least one active strike-slip fault of the eastern SFS beneath the northern Puerto Rico slope, within ~60 km of the northwestern tip of the island, represents a major potential hazard to the densely populated northern coastal region of Puerto Rico. In contrast, the NPRSFZ probably does not represent a major, independent seismic hazard of concern for northern Puerto Rico. The fault is located more than 110 km north of the Puerto Rico coast (Fig. 2). Furthermore, the location of the fault within a few kilometers of the deformation front of the south-dipping subduction thrust indicates that the NPRSFZ must merge downward into the subduction thrust at a depth of only a few kilometers (Dolan et al., this volume). Thus, the NPRSFZ is probably not capable of generating damaging earthquakes by itself, independently of major earthquakes generated by slip on the plate-interface, oblique-subduction thrust fault.

Normal fault earthquakes in Mona Passage. Mona Canyon, offshore of northwestern Puerto Rico, is controlled by large normal faults (Dolan et al., this volume). The steep eastern wall of the canyon, in particular, appears to be controlled by a single normal fault. These faults must be considered a potential seismic source, particularly in light of the fact that they lie within ~25 km of the northwestern tip of Puerto Rico. The location of the 1918 M_s ~7.5 Mona Passage earthquake suggests that it may have been generated by slip on a normal fault within Mona Passage (McCann and Sykes, 1984). The 1918 event resulted in extensive damage and loss of life in cities along the western coast of Puerto Rico (Reid and Taber, 1919, 1920).

Normal fault earthquakes in the underthrust Atlantic slab. Dolan et al. (this volume) ascribe the normal faults observed along the northern edge of the Puerto Rico trench to bending of the Atlantic slab during highly oblique underthrusting. On December 25, 1969, an M_s 7.5 normal fault earthquake occurred in the Atlantic oceanic slab being subducted beneath the Lesser Antilles island arc (Stein et al., 1982, 1983). Similar normal fault earthquakes along the northern margin of the Caribbean plate may pose a significant seismic hazard to the region. The direction of underthrusting in the northern Caribbean is highly oblique, however, and consequently the rate of slab bending is much slower than along the Lesser Antilles subduction zone. Thus, normal fault earthquakes associated with slab bending along the northern plate boundary will be less frequent and/or smaller than those along the Lesser Antilles margin where subduction is nearly perpendicular to the plate boundary. Nevertheless, the increase in deep, intraslab seismicity following the 1946 northeast Hispaniola mainshock shows that the oblique thrust component of motion associated with oblique underthrusting does cause readjustment of the underthrust slab after major slab-interface thrust earthquakes.

Tsunami hazards. Earthquakes on the offshore subduction thrust fault can cause destructive tsunamis (e.g., numerous small- to moderate-sized tsunamis generated by the 1946 northeastern Hispaniola earthquake) that are a cause for concern for the many low-lying coastal communities in Hispaniola and Puerto Rico. Such tsunamis can be generated either by displacement of the sea floor associated with updip rupture of the thrust fault to the sea floor, as well as by underwater landsliding. Because strong ground motions can trigger these underwater landslides, earthquakes on offshore strike-slip faults (e.g., eastern Septentrional fault system; northeastern Hispaniola slope fault; northern Puerto Rico slope fault), although they may not directly cause major elevation changes in the sea floor through fault slip, must also be considered potential triggers for destructive tsunamis. The numerous tsunamis that occurred for several days after the 1946 northeastern Hispaniola mainshock were probably generated by landsliding triggered by aftershocks.

Southern deformation zone of the NCPBZ

Los Muertos deformed belt. The Los Muertos deformed belt (LMDB) forms the southern edge of the NCPBZ for more than 650 km, from the Anegada Passage in the east to the San Pedro basin south of central Hispaniola in the west (Fig. 3). Active accretionary prism development within the LMDB is characterized by offscraping of Caribbean sediments and the development of north-dipping thrust faults and folds above a gently north-dipping thrust fault. This thrust fault defines the boundary between the overriding Puerto Rico–Virgin Islands and Hispaniola blocks of the NCPBZ and the true Caribbean plate, which lies to the south of the NCPBZ (Ladd and Watkins, 1978; Masson and Scanlon, 1991). The 1984 M_s 6.7 San Pedro basin thrust earthquake, the largest instrumentally recorded event to occur within the LMDB, demonstrates that the subduction thrust along the top of the underthrust Caribbean slab is seismogenic (Byrne et al., 1985). Little is known about this major seismic source, save its basic geometry as defined by side-scan sonar and seismic-reflection surveys and the dip of the Wadati-Benioff zone (Ladd and Watkins, 1978; Byrne et al., 1985; Ladd et al., 1990; Masson and Scanlon, 1991; Dolan et al., this volume). No known large historical earthquakes can be reliably associated with the Los Muertos subduction thrust, despite the >400-yr-long historic record in Puerto Rico.

Anegada Passage. The Anegada Passage, which extends northeastward across the Virgin Islands, connects the Los Muertos deformed belt with the Puerto Rico trench at ~63° W (Fig. 3). The Anegada Passage appears to encompass a zone of northeast-trending strike-slip faults and several pull-apart basins (Murphy and McCann, 1979; Jany et al., 1990). Isoseismals and maps of seismic seawaves generated by the large earthquake of 1867 indicate that the event occurred within the Anegada Passage (Reid and Taber, 1920). McCann and Sykes estimated a magnitude of ~7.75 for this event.

Enriquillo-Plantain Garden fault. First identified by Mann et al. (1984), the Enriquillo-Plantain Garden fault zone is a major left-lateral strike-slip fault that extends from near the western termination of the Los Muertos deformed belt in south-central Hispaniola westward for >800 km through the southern peninsula of Haiti and offshore through Jamaica to the southern edge of the Cayman trough (Fig. 2). No paleoseismological information is available for this fault, but it may have generated many of the major earthquakes that have struck southern Hispaniola (Fig. 2) (Mann et al., 1984, this volume; Chalas-Jimenez, 1989; McCann and Pennington, 1990). By analogy to the strain-partitioned system of faults beneath the northern zone of deformation of the NCPBZ, earthquakes generated by slip on thrust faults oriented parallel to the Enriquillo-Plantain Garden fault zone must also be considered a potential hazard to the southern Hispaniola and Jamaica regions (Mann et al., this volume).

Temporal occurrence of major earthquakes in the NCPBZ

Earthquakes in the NCPBZ in the Hispaniola area have clustered in two major temporal and geographic sequences—a period of numerous large events along the southern deformation belt during the 17th and 18th centuries, and a period of elevated activity along the northern belt of the NCPBZ during the 19th and 20th centuries (Figs. 2 and 10) (Scherer, 1912; Reid and Taber, 1919, 1920; Lynch and Bodle, 1948; Kelleher et al., 1973; Chalas-Jimenez, 1989). We refer to this alternation of major earthquake activity between the two deformation belts as "deformation switching."

Since 1842, the northern deformation zone of the NCPBZ has been in an active period of relatively frequent earthquakes (Fig. 10). These earthquakes include large events in 1842 and 1884 that probably occurred on the Septentrional fault system in northwestern Hispaniola (Mann et al., 1984, this volume), the 1917 and 1918 Mona Passage earthquakes (which may have occurred on either normal faults within Mona Passage [McCann and Sykes, 1984], the eastern Septentrional fault system, or the plate-interface thrust), and the 1943 northern Mona Passage and 1946 northeastern Hispaniola earthquakes, which occurred on the plate-interface oblique-thrust fault (this study) (Fig. 2). The 1953 Silver Spur earthquake was the most recent major event in this active period.

The active period along the southern deformation belt of the NCPBZ began in the early 1600s and included large earthquakes in October and November 1751, 1770, and 1860 (Fig. 2) (Scherer, 1912). These four events define a westward-propagating sequence that may have occurred along the Enriquillo-Plantain Garden fault system in southern Hispaniola (Fig. 2) (Mann et al., this volume). The occurrence of a tsunami during the October 1751 event, however, led McCann and Sykes (1984) to suggest the alternative possibility that this event may have occurred along the westernmost part of the north-dipping, plate-interface thrust fault beneath the Los Muertos deformed belt. The occurrence of a tsunami during an earthquake, however, does not provide definitive proof of an offshore source, as strong ground shaking generated by an earthquake on a nearby onshore fault could also trigger submarine landslides. The most likely possibility is that the 1751–1860 southern Hispaniola earthquake sequence was a domino-like, east-to-west "cascade" of events similar to the 1939–1967 sequence of earthquakes along the North Anatolian fault in Turkey, in which ~1,000 km of that large strike-slip fault broke in a westward-propagating series of large to great earthquakes (Ambraseys, 1970; Barka, 1992).

Although the first major event in the northern active sequence (1842) occurred before the final major event in the southern active period (1860), during most of the 250-yr-long southern active period, no large earthquakes appear to have occurred within the northern zone of deformation. Conversely, no large events—aside from the moderate-sized (M_s 6.7) 1984 San Pedro basin earthquake beneath the Los Muertos deformed belt—have occurred along the southern deformation belt since 1860 (Fig. 10). The southern active period was preceded by the 1564 earthquake, which devastated the city of Santiago in the Cibao Valley of northern Hispaniola (Scherer, 1912; Prentice et al., 1993; Mann et al., this volume; L. Feldman and W. R. McCann, written communication, 1995). This is apparently the earliest well-recorded event in

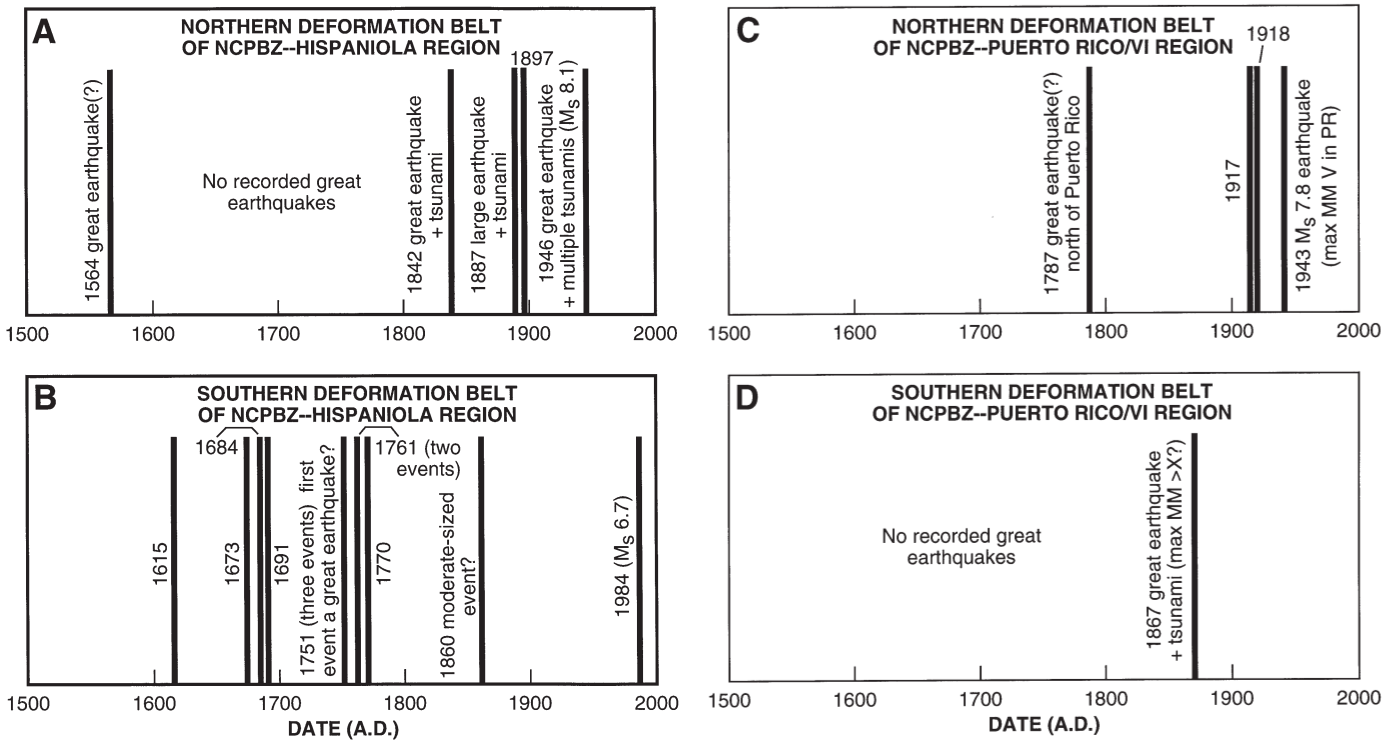

Figure 10. Plots of temporal and geographic distribution of major historical earthquakes in the Hispaniola–Puerto Rico region of the northern Caribbean plate boundary zone (NCPBZ) (modified from Chalas-Jimenez, 1989). Catalog is probably complete for large to great earthquakes since ca. 1800. Although some large offshore events may be missing during this period, it is unlikely that any great earthquakes were not recorded during the past 200 yr (Kelleher et al., 1973). Catalog prior to 1800 is of variable quality and may be incomplete, especially for offshore earthquakes. Events listed here had maximum Modified Mercali Intensities of >VIII, and many exhibited MM Intensities of X and XI. (A) Occurrence of large recorded earthquakes in the northern belt of deformation of the NCPBZ in the Hispaniola region (includes offshore, south-dipping interplate thrust fault and the Septentrional fault system). Note cluster of events beginning in 1842 and apparent absence of great earthquakes between 1564 and 1842. (B) Occurrence of large earthquakes in the southern deformation belt of the NCPBZ in the Hispaniola region (includes the left-lateral Enriquillo-Plantain Garden strike-slip fault system [Mann et al., 1984, this volume] and offshore thrust faults of the western Los Muertos deformed belt). Note cluster of large to great earthquakes during 17th and 18th centuries, as well as absence of large earthquakes since 1860. This cluster appears to be anticorrelated with the 19th and 20th century cluster of events in the northern deformation belt. (C) Occurrence of large recorded earthquakes along the northern deformation belt of the NCPBZ in the Puerto Rico–Virgin Islands region (includes offshore, south-dipping interplate thrust fault and left-lateral strike-slip faults of the eastern Septentrional and northern Puerto Rico slope fault systems). In general, Puerto Rico appears to have experienced far fewer large to great earthquakes than Hispaniola (Kelleher et al., 1973). This does not appear to be a result of better record keeping in Hispaniola than Puerto Rico, as the historical record of earthquakes in Puerto is actually better preserved than that for Hispaniola (L. Feldman, personal communication, 1995). Rather, it may be a function of the fact that all of the major active plate-boundary faults are offshore in the Puerto Rico region, in contrast to Hispaniola, where the major strike-slip faults are onshore for most of their lengths. In addition to a great earthquake in 1787, the northern deformation zone off Puerto Rico produced a cluster of earthquakes in the first half of the 20th century. The largest of these shocks was the 1943 Mona Passage earthquake. This cluster is broadly contemporaneous with the recent cluster in northern Hispaniola. (D) Occurrence of large earthquakes in the southern deformation belt of the NCPBZ in the Puerto Rico–Virgin Islands area. The only well-recorded, large event to strike this region during the historic period was the great 1867 Anegada Passage earthquake.

the Western Hemisphere (L. Feldman and W. R. McCann, written communication, 1995). Thus, it remains unknown whether it records the final large event in an earlier northern active period.

Far fewer large earthquakes have been recorded in the Puerto Rico–Virgin Islands areas than in the Hispaniola region, despite comparable historical records in both areas (Kelleher et al., 1973; McCann and Pennington, 1990). In the 450-yr-long historic record from the Puerto Rico area, only the poorly recorded 1787 event (McCann and Sykes, 1984), the Mona Passage earthquakes of 1917, 1918, and 1943, and the Anegada Passage earthquake of 1867 have ruptured large parts of the plate-boundary faults (Figs. 2 and 10). Unlike Hispaniola, however, all of the major plate-boundary faults in the Puerto Rico region (northern Puerto Rico slope fault zone, eastern Septentrional fault zone, Mona Passage normal faults, south- and north-dipping plate-interface thrusts north and south of the island) are located offshore. Offshore earthquakes are less likely to be recorded than onshore events, and the catalog for Puerto Rico may be missing large events. Nevertheless, with the possible exception of the 1787 event north of Puerto Rico, no large earthquakes appear to have occurred near San Juan, Puerto Rico, since the mid-16th century (Kelleher et al., 1973).

Because of the rarity of recorded events and the possibility of a significantly incomplete catalog, we cannot determine whether the Puerto Rico–Virgin Islands region has experienced alternating periods of activity on the northern and southern deformation belts of the NCPBZ. We can say, however, that the 1917–1943 sequence of earthquakes in the northern Mona Passage occurred within the active period along the northern deformation zone in Hispaniola (Fig. 10). As the Mona Passage is located adjacent to Hispaniola, this is perhaps not a surprise. It does, however, suggest that whatever mechanism is controlling the temporal and geographic clusters of major earthquakes operates over an area encompassing most of the northern belt of deformation, from northwestern Hispaniola to the Mona Passage, a distance of 750 km (Fig. 2).

Although it is difficult to generalize from only one cycle of "deformation switching," the striking temporal and geographic separation of the "active" and "quiet" earthquake periods suggests that active deformation alternates between fault systems along the northern and southern edges of the NCPBZ for time periods on the order of hundreds of years. We suggest that it is likely that within each of the deformation zones, an active sequence merely records a stress perturbation that propagates throughout large parts of the fault network. In other words, all but the first earthquake in each active sequence may be triggered by static stress changes (an increase in Coulomb failure stress) within the fault network caused by an earlier earthquake in that deformation belt. Although the mechanics of this stress triggering are not yet fully understood, this idea has recently been successfully used to explain much of the earthquake distribution in California during the past 185 yr (Harris and Simpson, 1992, 1996; Stein et al., 1992, 1994; Harris et al., 1995; Deng and Sykes, 1997) and along the North Anatolian fault during the 1939–1967 rupture sequence (Stein et al., 1997). Alternatively, time-dependent loading caused by viscous relaxation of the lower crust after a large earthquake may provide another mechanism for generating clusters of earthquakes (Ben-Zion et al., 1993).

Although the idea of static stress triggering provides a reasonable, and intuitively understandable, explanation for the clustered earthquake behavior within each of the deformation belts, it does not readily explain the apparent limitation of active deformation to one belt of deformation at a time. This pattern of earthquake occurrence raises a number of interesting questions: Why does deformation in one belt shut off when deformation begins in the other belt? Or does the locus of active deformation truly switch from one edge of the plate boundary zone to the other? Is the "quiet" edge of the plate boundary zone only quiet with respect to earthquakes? In other words, do aseismic processes dominate during the quiet intervals? More detailed geodetic measurements should be able to resolve the question of whether aseismic deformation is an important contributor to strain accommodation, especially on onshore faults in Hispaniola. The other questions, however, particularly the question of what triggered the 19th and 20th century active period in the northern belt of deformation, can probably best be addressed through numerical modeling, both of static stress changes related to earlier earthquakes and of the effects of viscous relaxation of the lower crust.

It is possible, of course, that the apparent switching of active deformation from the southern to the northern edge of the NCPBZ is merely a temporal and geographic coincidence—an artifact of a historical catalog that is not long enough. It is also possible that the "deformation switching" is an artifact of an incomplete historical record. However, although the possibility of an incomplete catalog cannot be ruled out, particularly for the earlier events, it seems unlikely that any large earthquakes are missing from the catalog since the mid-18th century, at least for onshore events. The possibility of an incomplete catalog needs to be investigated further, with a more complete review of original historical documents.

CONCLUSIONS

Our focal mechanisms show that the 1943 northern Mona Passage earthquake and the 1946 northeastern Hispaniola earthquake were both oblique-thrust events that occurred on the gently south-dipping plate-interface between the underthrust North America (Atlantic) plate and the Hispaniola and Puerto Rico blocks of the northern Caribbean plate boundary zone (NCPBZ). Furthermore, a comparison of the aftershock zones of these two events with marine geophysical data reveals that the earthquakes ruptured strongly coupled asperities on the plate-interface thrust associated with zones of active collisional underthrusting of high-standing carbonate banks of the southeastern Bahamas. These two earthquakes represent two of the largest events to strike the northeastern Hispaniola–northwestern Puerto Rico region during the past 400 yr, leading us to suggest that such large thrust events may typically nucleate only at strongly coupled collisional asperities on the

plate interface. The rakes derived from our focal mechanisms for these events reveal a relatively constant, 030–035° direction of slip (in map view) along the plate interface. The northern deformation belt of the NCPBZ, however, exhibits well-developed strain partitioning, with much of the left-lateral slip along the plate boundary partitioned off the south-dipping plate interface and onto the steeply dipping Septentrional (and related) strike-slip faults. The depth at which the strike-slip fault merges with the south-dipping plate interface is poorly constrained, but it probably lies downdip of the 1943 and 1946 rupture planes. This indicates that the rakes derived from those events will show a plate motion direction that is more contractional than the true vector. Thus, the 030–035° orientation of slip along the south-dipping oblique-thrust plate-interface fault represents the most northerly possible orientation of the relative motion vector. Furthermore, the fact that the oblique-thrust 1943 event occurred along an 080°-trending margin requires that relative motion along the northern edge of the NCPBZ be oriented more northerly than 080°, given that the only major strike-slip faults in the region strike approximately east-west to east-northeast.

This estimate is in sharp contrast to published, preliminary GPS data (Farina et al., 1995), which show the overall motion vector oriented ~090°, as well as earlier studies of global plate models (e.g., NUVEL-1; DeMets et al., 1990; DeMets, 1993), which show predominantly east-west relative plate motion. More recent GPS data suggest that significant left-lateral motion may occur offshore northern Hispaniola (Dixon et al., 1998). The marine geophysical and seismicity data discussed by Dolan et al. (this volume) show that the south-dipping, plate-interface thrust fault is the dominant structure north of the Septentrional fault. Our focal mechanisms show that oblique-slip along this interface accommodates significant left-lateral motion. Thus, we suggest that it is likely that the slip rate on the offshore oblique thrust fault may be higher than previously assumed in models suggesting near-pure, east-west relative plate motion. The only other possible fault that could accommodate left-lateral slip north of the Septentrional fault in Hispaniola is the Camu fault. This fault, however, does not appear to be a continuous feature across the Silver-Navidad bank collision zone, and it may no longer be a major active fault. Any future modeling of GPS data must incorporate realistic slip vectors and geometries for the offshore plate-interface fault.

The south-dipping, plate-interface oblique-thrust fault and the Septentrional strike-slip fault—the two major faults within the northern deformation belt of the NCPBZ—represent only two of the seismic hazards affecting the north-central Caribbean region. Other major seismic sources that must be considered in any comprehensive seismic hazard assessment of the region include the two major faults of the southern deformation belt—the left-lateral Enriquillo-Plantain Garden strike-slip fault and the north-dipping Los Muertos plate-interface thrust fault—as well as normal faults in the Mona Passage and large, offshore normal-fault earthquakes within the underthrust Atlantic slab. Direct displacement of the sea floor during offshore thrust and normal-fault events represents a major hazard to the densely populated coastal regions of Hispaniola and Puerto Rico, as many cities are built close to sea level. Tsunamis may also be generated by underwater landslides triggered by strong shaking from nearby ruptures. Because such tsunamis do not require direct tectonic displacement of the sea floor, they can be generated by ruptures on onshore faults. The seismic risk is tremendously increased by the relatively poor construction techniques common to many parts of the region.

The 1943 and 1946 mainshocks were the most recent large earthquakes in a series of major events that occurred on faults in the northern part of the NCPBZ between 1842 and 1953. The historical record suggests that this earthquake cluster was preceded by more than 250 yr of relative quiescence on faults along the northern edge of the NCPBZ. Ruptures on faults along the southern edge of the NCPBZ (Enriquillo-Plantain Garden fault, Los Muertos thrust fault) exhibit exactly the opposite temporal sequence. An ongoing period of quiescence since 1860 was preceded by a 250-yr-long period of intense activity beginning in the early 1600s. Within each of the two belts of deformation, such on-off clustering of events may be triggered by either static stress changes (e.g., Harris and Simpson, 1992, 1996; Stein et al., 1992, 1994, 1997; Harris et al., 1995; Deng and Sykes, 1997) or by time-dependent loading related to viscous relaxation of the ductile lower crust (Ben-Zion et al., 1993). These mechanisms, however, fail to explain in any obvious way why earthquakes should occur in only one of the belts of deformation at a time. This pattern could, of course, be merely coincidental—the function of an incomplete or too-short historical record. Nevertheless, it represents a potentially fruitful subject for both static stress modeling and models of long-distance, long-term, visco-elastic interactions between widely separated fault networks.

ACKNOWLEDGMENTS

Dolan was supported by a grant from the National Science Foundation (OCE 8812082) and Wald was supported as a postdoctoral research fellow by the U.S. Geological Survey and the National Research Council. We would like to thank Paul Mann, Bill McCann, Eric Calais, and Carol Prentice for helpful discussions and thoughtful reviews. Larry Feldman and Bill McCann kindly shared information from their unpublished compilation of historical earthquakes in the northern Caribbean region.

REFERENCES CITED

Abe, K., 1981, Magnitudes of large shallow earthquakes from 1904–1980: Physics of the Earth and Planetary Interiors, v. 27, p. 72–92.

Ambraseys, N. N., 1970, Some characteristic features of the North Anatolian fault zone: Tectonophysics, v. 9, p. 143–165.

Austin, J. A., 1983, Overthrusting in a deep-water carbonate terrane, *in* Balley, A. W., ed., Seismic expression of structural styles: American Association of Petroleum Geologists Studies in Geology 15, p. 3.4.2-167–3.4.2-172.

Barka, A., 1992, The North Anatolian fault zone: Annales Tectonicae, Special Issue—Supplement to v. VI, p. 164–195.

Ben-Zion, Y., Rice, J. R., and Dmowska, R., 1993, Interaction of the San Andreas fault creeping segment with adjacent great rupture zones and earthquake recurrence at Parkfield: Journal of Geophysical Research, v. 98, p. 2135–2144.

Bracey, D. W., and Vogt, P. R., 1970, Plate tectonics in the Hispaniola area: Geological Society of America Bulletin, v. 81, p. 2855–2860.

Burke, K., 1988, Tectonic evolution of the Caribbean: Annual Review of Earth and Planetary Sciences, v. 16, p. 201–230.

Byrne, D. B., Suarez, G., and McCann, W. R., 1985, Muertos Trough subduction—Microplate tectonics in the northern Caribbean: Nature, v. 317, p. 420–421.

Calais, E., Mercier de Lépinay, B., Renard, V., and Tardy, M., 1989, Geometrie et regime tectonique le long d'une limite de plaques en coulissage: La frontiere nord-Caraibe de Cuba a Hispaniola, Grandes Antilles, (Geometry and tectonic regime along a strike-slip plate boundary: The northern Caribbean plate boundary from Cuba to Hispaniola, Greater Antilles): Comptes Rendus de l'Académie des Sciences Paris, v. 308, p. 131–135.

Calais, E., Bethoux, N., and Mercier de Lépinay, B., 1992, From transcurrent faulting to frontal subduction: A seismotectonic study of the northern Caribbean plate boundary from Cuba to Puerto Rico: Tectonics, v. 11, p. 114–123.

Case, J., and Holcombe, T., 1980, Geologic-tectonic map of the Caribbean region: U.S. Geological Survey Miscellaneous Investigations Map I-1100, scale 1:2,500,000.

Case, J. E., MacDonald, W. D., and Fox, P. J., 1990, Caribbean crustal provinces; seismic and gravity evidence, *in* Dengo, G., and Case, J. E., eds., The Caribbean region: Boulder, Colorado, Geological Society of America, The Geology of North America, v. H, p. 15–36.

Chalas-Jimenez, J. A., 1989, Probabilidad de un sismo catastrofico en la Republica Dominicana: Historia sismica, prediccion, y magnitudes esperadas: Revista Geofisica (Instituto de Geografia e Historia), v. 31, p. 185–193.

DeMets, C., 1993, Earthquake slip vectors and present-day plate motions: Journal of Geophysical Research, v. 98, p. 6703–6714.

DeMets, C., Gordon, R. G., Argus, D. F., and Stein, S., 1990, Current Plate Motions: Geophysical Journal International, v. 101, p. 425–478.

Deng, J., and Sykes, L. R., 1995, Determination of Euler pole for contemporary relative motion of Caribbean and North American plates using slip vectors of interplate earthquakes: Tectonics, v. 14, p. 39–53.

Deng, J., and Sykes, L. R., 1997, Evolution of the stress field in southern California and triggering of moderate-sized earthquakes: A 200-year perspective: Journal of Geophysical Research, v. 102, p. 9859–9886.

Dewey, J. W., and Suarez, G., 1991, Seismotectonics of Middle America, *in* Slemmons, D. B., Engdahl, E. R., Zoback, M. D., and Blackwell, D., eds., Neotectonics of North America: Boulder, Colorado, Geological Society of America Decade Map Volume 1, p. 309–321.

de Zoeten, R., Draper, G., and Mann, P., 1991, Geologic map of the northern Dominican Republic, scale 1:100,000, *in* Geologic and Tectonic development of the North America–Caribbean plate boundary in Hispaniola, Mann, P., Draper, G., and Lewis, J., eds., Geological Society of America Special Paper 262, Plate 1.

Dillon, W. P., Austin, J. A., Scanlon, K. M., Edgar, N. T., and Parson, L. M., 1992, Structure and development of the insular margin north of western Hispaniola: A tectonic accretionary wedge on the Caribbean plate boundary: Marine and Petroleum Geology, v. 9, p. 70–88.

Dillon, W. P., Edgar, N. T., Scanlon, K. M., and Coleman, D. F., 1994, A review of the tectonic problems of the strike-slip northern boundary of the Caribbean Plate and examination by GLORIA, *in* Gardner, J. V., Field, M. E., and Twichell, D. C., eds., Geology of the United States' Seafloor: The View from Gloria: United Kingdom, Cambridge University Press, p. 135–164.

Dixon, T. H., 1993, GPS measurement of relative motion of the Cocos and Caribbean plates and strain accumulation across the Middle American Trench: Geophysical Research Letters, v. 20, p. 2167–2170.

Dixon, T. H., and Mao, A., 1997, A GPS estimate of relative motion between North and South America: Geophysical Research Letters, v. 24, p. 535–538.

Dixon, T., Farina, F., DeMets, C., Jansma, P., Mann, P., and Calais, E., 1998, Relative motion between the Caribbean and North American plates and associated boundary zone deformation based on a decade of GPS observations: Journal of Geophysical Research (in press).

Edgar, N. T., 1991, Structure and geologic development of the Cibao Valley, *in* Mann, P., Draper, G., and Lewis, J. F., eds., Geologic and tectonic development of the North America–Caribbean plate boundary in Hispaniola: Geological Society of America Special Paper 262, p. 281–299.

Edgar, N. T., Ewing, J. I., and Hennion, J., 1971, Seismic refraction and reflection in the Caribbean Sea: American Association of Petroleum Geologists Bulletin, v. 55, p. 833–870.

Farina, F., Calais, E., DeMets, C., Dixon, T., Jansma, P., and Mann, P., 1995, GPS measurements across the northern Caribbean plate boundary zone: Preliminary results: Eos (Transactions of the American Geophysical Union), v. 76, p. S94.

Fischer, K. M., and McCann, W. R., 1984, Velocity modeling and earthquake relocation in the North East Caribbean: Seismological Society of America Bulletin, v. 74, p. 1249–1262.

Frankel, A., 1982, A composite focal mechanism for microearthquakes along the northeastern border of the Caribbean plate: Geophysical Research Letters, v. 9, p. 511–514.

Harris, R., A., and Simpson, R. W., 1992, Changes in static stress on southern California faults after the 1992 Landers earthquake: Nature, v. 360, p. 251–254.

Harris, R. A., and Simpson, R. W., 1996, In the shadow of 1857—Effect of the great Ft. Tejon earthquake on subsequent earthquakes in southern California: Geophysical Research Letters, v. 23, p. 229–232.

Harris, R. A., Simpson, R. W., and Reasonberg, P. A., 1995, Influence of static stress changes on earthquake locations in southern California: Nature, v. 375, p. 221–224.

Harvard Centroid Moment Tensor Catalog, 1993 (http://www.seismology.harvard.edu): Harvard University, Department of Earth and Planetary Sciences, Cambridge, Massachusetts.

International Seismological Centre Catalog of Earthquakes, 1994 (http://www.isc.ac.uk): Cambridge, U.K., International Seismological Centre.

International Seismological Summary of 1953, 1961, prepared and edited by the International Union of Geodesy and Geophysics, The British Association Seismological Committee: Richmond, Surrey, U.K., Kew Observatory, 823 p.

Jany, I., Scanlon, K. M., and Mauffret, A., 1990, Geological interpretation of combined SEABEAM, GLORIA, and seismic data from Anegada Passage (Virgin Islands, North Caribbean): Marine Geophysical Research, v. 12, p. 173–196.

Jordan, T. H., 1975, The present-day motions of the Caribbean plate: Journal of Geophysical Research, v. 80, p. 4433–4449.

Kafka, A. L., and Weidner, T. J., 1979, The focal mechanisms and depths of small earthquakes as determined from Rayleigh wave radiation patterns: Bulletin of the Seismological Society of America, v. 69, p. 1379–1390.

Kelleher, J., Sykes, L., and Oliver, J., 1973, Possible criteria for predicting earthquake locations and their application for major plate boundaries of the Pacific and the Caribbean: Journal of Geophysical Research, v. 78, p. 2547–2585.

Kikuchi, M., and Kanamori, H., 1991, Inversion of complex Body Waves-III: Bulletin of the Seismological Society of America, v. 81, p. 2335–2350.

Ladd, J. W., and Watkins, J. S., 1978, Tectonic development of trench-arc complexes on the northern and southern margins of the Venezuela Basin, *in* Watkins, J. S., Montadert, L., and Dickerson, P., eds., Geophysical and geological invetigations of continental margins: American Association of Petroleum Geologists Memoir 29, p. 363–372.

Ladd, J. W., Holcombe, T. L., Westbrook, G. K., and Edgar, N. T., 1990, Caribbean marine geology; Active margins of the plate boundary, *in* Dengo, G., and Case, J. E., eds., The Caribbean region: Boulder, Colorado, Geological Society of America, The Geology of North America, v. H., p. 261–290.

Larue, D., and Ryan, H., 1990, Extensional tectonism in the Mona Passage, Puerto Rico and Hispaniola: A preliminary study: Transactions of the 12th Caribbean Geological Conference, St. Croix, Virgin Islands: Miami,

Florida, Miami Geological Society, p. 223–230.
Larue, D. K., and Ryan, H. F., 1998, Seismic reflection profiles of the Puerto Rico Trench: Shortening between the North American and Caribbean plates, *in* Lidiak, E. G., and Larue, D. K., eds.: Boulder, Colorado, Geological Society of America Special Paper 322, p. 193–210.
Larue, D. K., Joyce, J., and Ryan, H. F., 1990, Neotectonics of the Puerto Rico Trench: Extensional tectonism and forearc subsidence: Transactions of the 12th Caribbean Geological Conference, St. Croix, Virgin Islands: Miami, Florida, Miami Geological Society, p. 231–247.
Lynch, J. J., and Bodle, R. R., 1948, The Dominican earthquakes of August, 1946: Bulletin of the Seismological Society of America, v. 38, p. 1–17.
MacDonald, K. C., and Holcombe, T. L., 1978, Inversion of magnetic anomalies and sea-floor spreading in the Cayman Trough: Earth and Planetary Science Letters, v. 40, p. 407–414.
Mann, P., and Burke, K., 1984, Neotectonics of the Caribbean: Reviews of Geophysics and Space Physics, v. 22, p. 309–362.
Mann, P., Burke, K., and Matumoto, T., 1984, Neotectonics of Hispaniola: Plate motion, sedimentation, and seismicity at a restraining bend: Earth and Planetary Science Letters, v. 70, p. 311–324.
Mann, P., Schubert, C., and Burke, K., 1990, Review of Caribbean neotectonics, *in* Dengo, G., and Case, J. E., eds., The Caribbean region: Boulder, Colorado, Geological Society of America, The Geology of North America, v. H., p. 405–432.
Mann, P., Taylor, F., Edwards, R. L., and Ku, T., 1995, Actively evolving microplate formation by oblique collision and sideways motion along strike-slip faults: An example from the northeastern margin of the Caribbean plate: Tectonophysics, v. 246, p. 1–69.
Masson, D. G., and Scanlon, K. M., 1991, The neotectonic setting of Puerto Rico: Geological Society of America Bulletin, v. 103, p. 144–154.
McCann, W. R., and Pennington, W. D., 1990, Seismicity, large earthquakes, and the margin of the Caribbean Plate, *in* Dengo, G., and Case, J. E., eds., The Caribbean Region: Boulder, Colorado, Geological Society of America, The Geology of North America, v. H, p. 291–306.
McCann, W. R., and Sykes, L. R., 1984, Subduction of aseismic ridges beneath the Caribbean Plate: Implications for the tectonics and seismic potential of the northeastern Caribbean: Journal of Geophysical Research, v. 89, p. 4493–4519.
Minster, J. B., and Jordan, T. H., 1978, Present-day plate motions: Journal of Geophysical Research, v. 83, p. 5331–5354.
Molnar, P., and Sykes, L. R., 1969, Tectonics of the Caribbean and Middle America regions from focal mechanisms and seismicity: Geological Society of America Bulletin, v. 80, p. 1639–1684.
Mullins, H. T., and Lynts, G. W., 1977, Origin of northwestern Bahama Platform: Review and reinterpretation: Geological Society of America Bulletin, v. 88, p. 1447–1461.
Mullins, H. T., Dolan, J., Breen, N., Andersen, B., Gaylord, M., Petruccione, J. L., Wellner, R. W., Melillo, A. J., and Jurgens, A. D., 1991, Retreat of carbonate platforms: Response to tectonic processes: Geology, v. 19, p. 1089–1092.
Mullins, H. T., Breen, N., Dolan, J., Wellner, R. W., Petruccione, J. L., Gaylord, M., Anderses, B., Melillo, A. J., Jurgens, A. D., and Orange, D., 1992, Carbonate platforms along the southeast Bahamas-Hispaniola collision zone: Marine Geology, v. 105, p. 169–209.
Murphy, A. J., and McCann, W. R., 1979, Preliminary results from a new seismic network in the northeastern Caribbean: Bulletin of the Seismological Society of America, v. 69, p. 1497–1513.
National Earthquake Center Catalog of Earthquakes, 1994 (http://wwwneic.cr.usgs.gov): Golden, Colorado, U.S. Geological Survey.
Pacheco, J. F., and Sykes, L. R., 1992, Seismic moment catalog of large, shallow earthquakes, 1900–1989: Bulletin of the Seismological Society of America, v. 82, p. 1306–1349.
Pindell, J. L., and Barrett, S. F., 1990, Geologic evolution of the Caribbean region; a plate-tectonic perspective, *in* Dengo, G., and Case, J. E., eds., The Caribbean region: Boulder, Colorado, Geological Society of America, The Geology of North America, v. H., p. 405–432.
Prentice, C. S., Mann, P., Taylor, F. W., Burr, G., and Valastro, S., 1993, Paleoseismicity of the North American–Caribbean plate boundary (Septentrional fault), Dominican Republic: Geology, v. 21, p. 49–52.
Reid, H., and Taber, S., 1919, The Puerto Rico earthquakes of October–November 1918: Bulletin of the Seismological Society of America, v. 9, p. 95–127.
Reid, H., and Taber, S., 1920, The Virgin Islands earthquakes of 1867–1868: Bulletin of the Seismological Society of America, v. 10, p. 9–30.
Reid, J. A., Plumley, P. W., and Schellekens, J. H., 1991, Paleomagnetic evidence for late Miocene counterclockwise rotation of north coast carbonate sequence, Puerto Rico: Geophysical Research Letters, v. 18, p. 565–568.
Rosencrantz, E., 1995, Opening of the Cayman Trough and evolution of the northern Caribbean plate boundary: Geological Society of America Abstracts with Programs, v. 27, no. 6, p. A–153.
Rosencrantz, E., and Mann, P., 1991, SeaMARC II mapping of transform faults in the Cayman Trough, Caribbean Sea: Geology, v. 19, p. 690–693.
Rosencrantz, E., Ross, M., and Sclater, J. G., 1988, Age and spreading history of the Cayman Trough as determined from depth, heat flow, and magnetic anomalies: Journal of Geophysical Research, v. 93, p. 2141–2157.
Russo, R. M., and Villaseñor, A., 1995, The 1946 Hispaniola earthquake and the tectonics of the North America–Caribbean plate boundary zone, northeastern Hispaniola: Journal of Geophysical Research, v. 100, p. 6265–6280.
Russo, R. M., and Villaseñor, A., 1997, The 1946 Hispaniola earthquake and the tectonics of the North America–Caribbean plate boundary zone, northeastern Hispaniola: Reply: Journal of Geophysical Research, v. 102, p. 793–802.
Schell, B. A., and Tarr, A. C., 1978, Plate tectonics of the northeastern Caribbean Sea region: Geologie En Mijnbouw, v. 57, p. 319–324.
Scherer, J., 1912, Great earthquakes in the island of Haiti: Bulletin of the Seismological Society of America, v. 2, p. 161–180.
Seismological Notes, 1946, Bulletin of the Seismological Society of America, v. 36, p. 373–383.
Small, W. M., 1948, A short description of the general geology of the Dominican Republic, with notes on the earthquake of August 4, 1946: Bulletin of the Seismological Society of America, v. 38, p. 19–32.
Speed, R. C., and Larue, D. K., 1991, Extension and transtension in the plate boundary zone of the northeastern Caribbean: Geophysical Research Letters, v. 18, p. 573–576.
Stein, R. S., King, G. C. P., and Lin, J., 1992, Change in failure stress on the southern San Andreas fault system caused by the 1992 Magnitude M=7.4 Landers earthquake: Science, v. 258, p. 1328–1332.
Stein, R. S., King, G. C. P., and Lin, J., 1994, Stress triggering of the 1994 M=6.7 Northridge, California, earthquake by its predecessors: Science, v. 265, p. 1432–1435.
Stein, R. S., Barka, A., and Dieterich, J. H., 1997, Progressive failure on the North Anatolian fault since 1939 by earthquake stress triggering: Geophysical Journal International, v. 128, p. 594–604.
Stein, S., Englen, J., Wiens, D., Speed, R., and Fujita, K., 1982, Subduction seismicity and tectonics in the Lesser Antilles arc: Journal of Geophysical Research, v. 87, p. 8642–8664.
Stein, S., Engeln, J. F., Wiens, D. A., Speed, R. C., and Fujita, K., 1983, Slow subduction of old lithosphere in the Lesser Antilles: Tectonophysics, v. 99, p. 139–148.
Stein, S., DeMets, C., Gordon, R. G., Brodholt, J., Argus, D., Engeln, J. F., Lundgren, P., Stein, C., Wiens, D. A., and Woods, D. F., 1988, A test of alternative Caribbean Plate relative motion models: Journal of Geophysical Research, v. 93, p. 3041–3050.
Sykes, L. R., and Ewing, M., 1965, The seismicity of the Caribbean region: Journal of Geophysical Research, v. 70, p. 5065–5074.
Sykes, L. R., and McCann, W. R., and Kafka, A. L., 1982, Motion of the Caribbean plate during the last 7 million years and implications for earlier Cenozoic movements: Journal of Geophysical Research, v. 87, p. 10656–10676.

MANUSCRIPT ACCEPTED BY THE SOCIETY JANUARY 9, 1998

Printed in the U.S.A.